MAGNETIC NANOPARTICLES MODIFIED WITH MORINGA SEED PROTEINS FOR WATER TREATMENT AND RECOVERY OF PRECIOUS METAL IONS

A RESEARCH SUBMITTED IN FULFILMENT

OF THE REQUIREMENTS FOR THE DEGREE OF

MASTER OF SCIENCE (CHEMISTRY)

OF

THE UNIVERSITY OF NAMIBIA

BY

MARTA OMBILI NDAKOLA AMUANYENA

9815236

20 MAY 2019

MAIN SUPERVISOR: PROF MARTHA KANDAWA-SCHULZ (UNIVERSITY OF NAMIBIA)

CO-SUPERVISOR: PROF HABAUKA M. KWAAMBWA (NAMIBIA UNIVERSITY OF SCIENCE AND TECHNOLOGY)

ABSTRACT

Access to clean and safe water for everyday use is needed for a healthy society. Water treatment and recovery of precious metals is a serious challenge particularly for developing countries since the current technologies are not attractive because they are often expensive and not environmentally friendly. Precious metals such as gold, palladium, and platinum are valuable and hence crucial for any economy. Coagulants used in the treatment and recovery of precious metals have setbacks such as cost and health concerns associated with them. The study was aimed at addressing both the problem of water treatment and recovery of metal ions using magnetic magnetite nanoparticles modified with Moringa seed proteins. The proteins extracted from Moringa seeds are known to have water treatment properties. Magnetic iron oxide nanoparticles were synthesized by chemical co-precipitation of Fe^{3+} and Fe^{2+} in a 2:1 ratio and complete precipitation was achieved at approximately pH 12.0. The study further prepared aqueous protein solution (1%) extracted from *M. oleifera* seeds that were utilized to obtain the chemical co-precipitation of modified magnetic magnetite nanoparticles. Characterization techniques used were FTIR, SEM, TGA and Zeta potential. They were utilized to identify different functional groups responsible for adsorption, morphology, thermal stability, and surface charges of the nanoparticles. Synthetic turbid water was prepared using kaolin whereas chloride salts of gold, palladium, and platinum were spiked in distilled water to obtain the required concentrations of the respective metal ions. UV-Vis spectrometry was used to measure turbidity, and metal ions percentage recovery was measured using ICP-OES. The effect of pH and modified magnetic iron oxide nanoparticles dosage was studied for turbidity removal and yielded an optimal pH of 2.5 with maximal removal of 97.3% at approximately 0.005 g.The same optimal pH was obtained for the recovery of gold, palladium, and platinum precious metal ions. Gold yielded a maximal recovery of 99.8%, followed by platinum with 87.7% then palladium with 72.7% at 0.065 g optimal dosage of modified magnetic iron oxide nanoparticles. The equilibrium was reached within 120 minutes of agitation. The initial concentration was maximal at 10 mg/L.The data fitted Langmuir model better than the Freundlich one. The maximum adsorption capacities were 34.48 mg/g, 28.90 mg/g and 5.27 mg/g for Au, Pt and Pd respectively. These results demonstrated that modified iron oxide nanoparticles were effective in water treatment and recovery of the precious metal ions.

TABLE OF CONTENTS

List of Tables

List of Figures

List of Abbreviations and Acronyms

APTES	aminopropyl triethoxy silane
BSA	Bovine serum albumin
CMS	Carboxymethyl cellulose
DDASS	dodecyl di-acid sodium salt
DI	Deionized water
DLS	Dynamic Light Scattering
DNA	deoxyribonucleic acid
DSC	Differental Scanning Calorimeter
EDS	Energy Dispersive Spectroscope
ICP-OES	Inductively Coupled Plasma – Optical Emission Spectrometer
IR	Infrared Spectroscopy
FTIR	Fourier Transform Infrared Spectroscopy
$MoFe_3O_4$	Iron oxide modified with Moringa seed proteins extract
MoP	Moringa seed proteins extract
MoPP	Moringa seed purified proteins extract powder
MoUP	Moringa seed unpurified proteins extract powder
MNPs	Magnetic iron oxide nanoparticles
NTU	Nephelometric Turbidity Unit
NUST	Namibia University of Science and Technology
PAA	Polyacrylic acid
PAC	polyaluminium chloride
PEI	Polyethylenimine
PGMs	Platinum Group Metals
pH	potential Hydrogen

PVDF	Polyvinylidene fluoride
QC	Quality control
ROS	Reactive oxygen species
RPC	Research and Publication Committee
RSD	Relative Standard Deviation
SEM	Scanning Electron Microscopy
SDS	Sodium dodecyl sulfate
TEM	Transmission Electron Microscopy
TSC	tri-Sodium citrate
TX-100	Triton X-100
UATR	Universal attenuated total reflectance
UNAM	University of Namibia
UNISA	The University of South Africa
UV-Vis	Ultraviolet – Visible Spectroscopy
VSM	Vibrating Sample Magnetometer
WITS	The University of the Witwatersrand
XRD	X-ray powder diffraction

Acknowledgements

First and foremost, I would like to thank the almighty for the strength and guidance through my studies. I would also like to express my gratitude to my supervisors, Prof Martha Kandawa–Schulz and Prof Habauka Kwaambwa for their support and guidance throughout this work. I am indebted to Prof Luke Chimuka; Prof Titus Msagati and their teams for the assistance granted in the analysis of some of my samples. My sincere gratitude goes to my colleagues, family, and friends for their encouragement, assistance and understanding during my studies. Lastly, I would like to thank the four institutions namely NUST, UNAM, UNISA and WITS for the opportunity I had to use the necessary equipment and materials for this research.

Dedication

I would like to dedicate this thesis to my family and supervisors for their support throughout my study. Thank you for the encouragement and believing in me.

Declarations

I, Marta O.N. Amuanyena, hereby declare that this study is my own work and is a true reflection of my research, and that this work, or any part thereof has not been submitted for a degree at any other institution.

……..	……	…….
Name	Signature	Date

CHAPTER 1: INTRODUCTION

1.1 Orientation of the study

The primary requirement for society is health and an unpolluted environment that include having access to clean and safe water for drinking, washing and other domestic purposes. Wastewater needs to be treated to reduce human and environmental threats [1,2,3]. This is a major concern in developing countries such as Namibia. There are several challenges in meeting the rising demands for safe and clean water supply. The main ones are lack of environmentally friendly as well as cheap technologies for both contaminated water treatment and recovery of precious metals from industrial effluents [4]. The provision of safe and clean water from most raw water and wastewater involves the use of coagulants introduced during the coagulation/flocculation step to remove turbidity in the form of dissolved or suspended materials [5,6].

Conventional chemical coagulants such as aluminium sulphate ($Al_2 (SO_4)_3$), organic polyaluminium chloride (PAC) and ferric chloride ($FeCl_3$) are currently used to enhance coagulation and flocculation [5]. However, the use of these chemicals as coagulants in the production of clean water has several drawbacks associated with costs, health risks, and complexity in sludge management [5,6]. For instance, aluminium residues have been implicated as causative agents in neurological as well as carcinogenic diseases such as pre-senile dementia and Alzheimer [6]. The usage of low-cost and waste materials of natural products has shown to give economic solutions through the reduction of excessive costs of chemicals and is regarded as a sustainable technology for water treatment [7].

The mining industry faces new challenges as economic value for precious metals such as gold (Au) as well as Platinum Group Metals (PGMs) for instance palladium (Pd) and platinum (Pt) rise resulting in high demand [4,8-11]. Platinum and palladium are some of the few abundant elements in the earth's crust. These two elements together with rhodium (Rh), iridium (Ir), ruthenium (Ru) and osmium (Os) make up the PGM family [9]. Precious metals are rare high economic value naturally occurring metals [12]. Various fields such as jewelry, ornament, automobile, pharmaceuticals, medicine, electronics, and dental industries use these metals [4,10,12,13]. Their peculiar physical and chemical characteristics make them useful. Many state-of-the-art technologies require these gold (Au) as well as Platinum Group Metals (PGMs) for instance palladium (Pd) and platinum (Pt) thus increases the need to investigate processes which recover precious metals from industrial wastes and electronic used products (e-waste).

There are some environmental effects associated with precious metal ions, for instance, bioaccumulation of platinum complexes is known to have toxic effects on plants and animals including humans [13]. Palladium is reported to be carcinogenetic in humans and penetrate plant roots thus harming the food chain [12,14]. On the other hand, gold is known to negatively affect the molecular structures of human and animal cells [12]. Another danger associated with consumption of food contaminated with these metal ions waste could be diseases such as kidney failure, liver damage among others [15]. It is, therefore, critical to recovering these metal ions from industrial effluent not only because of the high demand but also to mitigate the environmental effects associated with them. Environmentally friendly recycling techniques with high selectivity and high yield are still essential despite that recycling of precious metals

from waste is currently carried out in industries. Several techniques applied in precious metals recovery are such as chemical precipitation, cementation, liquid-liquid extraction, membrane filtration, photocatalytic degradation, ion–exchange and solid phase extraction [11,15,16]. However, there are several setbacks in applying some of them including the incomplete recovery of precious metal ions as well as introducing other contaminants other than the ones in the first waste [16]. Of these techniques employed, adsorption of metal ions which is a solid phase extraction is still one of the greatest cost-efficient and effective methods for recycling low concentrated precious metal ions in hydrometallurgy [17-19]. The bonds formed between metal ions and the adsorbents utilized are usually strong and compact [20]. Adsorption is, therefore, defined as physical and chemical interactions between adsorbate and adsorbent [19]. Adsorbate is a molecule (pollutant) that attaches to the solid surface which is the adsorbent [2]. The most popular technique is the magnetic solid phase extraction whereby magnetic adsorbents aid in the removal of analytes from solutions [12].

The study attempts to address both the treatment of water and recovery of metal ions. To the best knowledge of the researcher, this approach has not been reported in literature. The Moringa tree, or "miracle tree" as it is sometimes called, could be the solution to the challenges of water quality and recovery of precious metals.

There are 13 known Moringa species in the world [21]. *Moringa oleifera* can be found in Namibia and is cultivated by individuals especially in Zambezi, Kavango and Khomas region. It is the most famous and widely studied. The seed extract of this tropical plant is known to consist of an active coagulating compound which is also antimicrobial that is reported to have water treatment properties by removing colloidal

materials and reducing bacteria [5,22]. Since this can be locally produced, it could be a substitute for imported water treatment chemicals and thus would decrease costs [3]. Furthermore, the protein, unlike aluminium sulphate generally used for water purification, is entirely biodegradable and non-toxic [23,24].

Magnetic iron oxides nanoparticles (MNPs) also called magnetite (Fe_3O_4) nanoparticles are widely available compounds in nature and can easily be synthesized in the laboratory, physically and chemically stable, biocompatible and environmentally safe [25, 26]. These unique physical and chemical properties are due to their minimal size, large specific surface area, large surface area-to-volume ratio and easy separation under applied external magnetic fields [13,25,27,28]. The study was aimed at applying MNPs modified with *M. oleifera* seed proteins in water treatment and the recovery of precious metal ions. Studies conducted by Okoli [24] and Santos *et al.* [29] on the use of *M. oleifera* protein functionalized supermagnetic iron oxide nanoparticles revealed promising results for water treatment. The same principle would, therefore, apply for water treatment and recovery of precious metals ions for use mainly in developing countries.

1.2 Statement of the problem

In developing countries, such as Namibia, the quality of drinking water is often dangerous to health and could be an essential vehicle for spreading diseases. This is due to a lack of environmentally friendly and cheap technologies for water and wastewater treatment and recovery of precious metals [4]. Currently, aluminium salts, iron salts, and synthetic polymers are the widely used coagulants in the treatment, but the cost, health issues and environmental side effects of these compounds are their

fundamental shortcomings [5]. Therefore, it is imperative to develop other cost-effective and more environmentally acceptable materials and technologies for water treatment as well as recovery of precious metals ions [7]. The utilization of a natural coagulant/flocculant from *M. oleifera* modified with MNPs offers several advantages such as fast separation, enhanced efficiency as well as significant reduction in sludge volume and this could be an alternative to synthetic chemical coagulants [24]. The study addressed both the treatment of water and recovery of metal ions using MPNs modified with Moringa proteins.

1.3 Aim and Objectives of the Study

The study was aimed at preparing, characterizing and determining the effectiveness of MNPs modified with *M. oleifera* seed proteins in the water treatment and recovery of precious metals. To achieve this aim, the following were the specific objectives:

a) To synthesize magnetic iron oxide nanoparticles;
b) To modify magnetic iron oxide nanoparticles with protein extract of *M. oleifera* seeds;
c) To characterize magnetic iron oxide nanoparticles modified and unmodified with *M. oleifera* seed proteins using different techniques to evaluate their physicochemical properties;
d) To test the nanocomposite materials (MNPs) prepared in water treatment and recovery of precious metals.

1.4 Significance of the Study

The study intends to use MNPs modified with *M. oleifera* seed proteins extract which is a cheap natural resource with the potential to be a substitute to the conventional

chemicals currently used in both water treatment and recovery of precious metal ions. This substitute is also more environmentally friendly and has no known health concerns associated with it [23,24]. Therefore, the research findings could be used to treat water for possible human use. Also, the system could also be used to recover precious metals ions and hence find application in the dental, jewelry and electronic industries.

1.5 Limitation of the Study

The study intended to use the following additional techniques to characterize the magnetic iron oxide nanoparticles modified and unmodified with *M. oleifera* seed proteins: The X-ray powder diffraction (XRD) to determine the crystal structure and Vibrating Sample Magnetometer (VSM) for magnetic properties of the nanoparticles. The challenge was therefore that, the University of Namibia (UNAM), as well as Namibia University of Science and Technology (NUST), are not technically equipped regarding instruments to allow all these additional analyses for the study to be carried out at the institutions. The samples were therefore sent to other institutions (WITS and UNISA) in South Africa, but due to unforeseen technical hiccups, they could not be analyzed.

CHAPTER 2: LITERATURE REVIEW

2.1 Overview

Presently, sustainable initiatives that use green chemistry to improve and protect our global environment are focal concerns in numerous areas of research. The advances in low-cost and environmentally friendly approaches of synthesis of nanomaterials remains a scientific challenge. Magnetic metal nanoparticles are of use in several catalytic applications, with regard to electronics, biology, and biomedical applications, material science, physics, and environmental remediation fields [30]. Studies of nanoparticles modified with natural coagulants in water treatment and recovery of precious metal ions seem to be rare. The following is an overview of some relevant research findings related to the study.

2.2 Moringa and water treatment

The usage of the *M. oleifera* seeds for domestic household water treatment was used first by rural women to decrease water turbidity in the countries along the Nile River, especially Sudan [31]. In the study by Narasiah *et al*. [31], *M. oleifera* solutions (5% w/w in water) were prepared using both shelled and non-shelled seeds. A significant amount of turbidity removal was shown with shelled compared to non-shelled seeds. Another benefit of the seed proteins extract is that the volume of sludge produced is minimal compared to other coagulants such as alum as observed by Narasiah et al. [31].

The study carried out by Yarahmadi *et al*. [5] compared the efficiency of turbidity removal between *M. oleifera* seed extract and polyaluminum chloride using synthetic

kaolinite. This study revealed that extract of *Moringa* seed is more efficient in removing water turbidities unusually high turbidities compared to low turbidities and had a minimal effect on the pH of water. It further showed that the synthetic coagulant (polyaluminium chloride) required lower pH to remove turbidities in water effectively. Studies by Shan et al. [3] and Ndabigengesere et al. [32] using *Moringa* protein showed similar results that pH and conductivity of water after treatment are reported not to be affected significantly.

Ndabigengesere *et al*. [32] identified the active component as a protein although entire seed crude extract, can all also be used as a flocculant/adsorbent. This active protein in Moringa extracts is identified as a cationic dimer with a molecular weight of 13 kDa and an isoelectric point of between 10 to 11. According to this study, the purified Moringa proteins are more effective in water treatment in comparison to alum, which presently is the widely used coagulant. A study by Arreola *et al.* [33] determined the molecular weights as well as the total content of proteins in Moringa crude extracts. The extraction was carried out in distilled water, 1M NaCl as well as sea water. The molecular weights ranged from 5 kDa to 32 kDa whereas total proteins content ranged from 3160-3400 mg BSA/L. Another study conducted by Hendrawati et al. [34] on the characterization of the physicochemical properties of *M. oleifera* seed powder found out that the major component of the seed is the total protein of approximately 44.5% composition. The rest of the components are oil/fat, water, and ash with averages of 27.0%, 10.1%, and 3.7%, respectively. It is therefore due to this high cationic protein content in the seeds that this can be used as an effective coagulant in water treatment as well as a recovery of precious metal ions.

According to Kwaambwa and Rennie [35], the amino acid residues in *M. oleifera* seeds proteins form negative and positive ions. These are either classified as anionic or cationic depending on amino acid groups dominating. The water-soluble cationic peptides with molecular masses between 6 to 16 kDa and an isoelectric point of approximately pH 10 could be the active components responsible for coagulation. Other results mentioned in the study are that of a peptide that is purified and sequenced. This peptide consists of arginine and histidine, both with positively charged R-groups and aspartic acid negatively charged R-group residue. The study further characterized the protein charges through interactions with four surfactants, namely, anionic sodium dodecyl sulfate (SDS), anionic dodecyl di-acid sodium salt (DDASS), nonionic Triton X-100 (TX-100) as well as zwitterionic N-dodecyl-N, N-dimethyl-3-ammonio-1-propane sulfonate (DDAPS) by zeta potential, turbidity measurements and dynamic light scattering (DLS). The study found out that interactions between SDS and the protein were more compared to the other surfactants studied, i.e. the order of interaction with cation protein was anionic > cationic > zwitterionic and non-ionic and hence providing further support of specific adsorption of surfactant and counter ions to the protein. At low concentrations of SDS, the zeta potential was unusually high but eventually decreased due to adsorption of the surfactant anions onto the protein. The study further established that the type of surfactant determines the interactions with the protein. The study of the interactions of the different surfactants contributed to the understanding of nature and mechanism of water treatment using *M. oleifera* proteins.

Nermark [36] studied the bioremediation of copper and lead-contaminated soil by utilizing defatted *M. oleifera* seeds crude water extract as a washing fluid to remediate

the soil. Comparisons were also made between extraction efficiency of defatted *M. oleifera* seeds and deionized water in removing copper and lead from soil. Defatted *M. oleifera* crude water extract showed a higher removal percentage as a washing fluid of lead and copper contaminated soil compared to deionized water. This was attributed to the presence of glutamic and aspartic acids found in *M. oleifera* protein as being responsible in the binding to the metals. The isoelectric point for these acids with a carboxyl group (-COOH) was found to be around pH 3. Above this pH value, the amino acids net charges are negative, and that could explain why the seeds proteins could remediate the soil contaminated by the cationic lead and copper metals. The same principle would, therefore, apply for water treatment and recovery of precious metals ions.

Neutron scattering and reflection studies have shown that the proteins adsorb strongly on different surfaces such as silica (SiO_2), sapphire (Al_2O_3) and polystyrene [37-38]. This suggests that Moringa seed proteins can adsorb on the ordinary sand, which is mainly SiO_2. Therefore, the principle behind plant-based coagulants/flocculants such as *M. oleifera* seeds in water and wastewater treatment is based on adsorption mechanism followed by charge neutralization or polymeric bridging effect leading to the aggregation of the impurities [5,22]. Furthermore, it has been revealed that the resulting aggregates (flocs) formed with the *M. oleifera* seed proteins are much more strongly packed, i.e., larger floc dimensions, $d_f \rightarrow 3$ (limiting value), than those produced with conventional flocculating agents [40]. In other words, the seed proteins adsorb to the impurities and cause flocculation as dense aggregates. This is advantageous in water treatment as such flocs are more easily separated. The

application of this natural product would decrease the necessity for costly synthetic chemicals.

A study by Sanchez - Martin *et al.* [41] further revealed that *M. oleifera* seed extract could be an alternative to the industrial coagulants/flocculants such as $FeCl_3$, $Al_2(SO_4)_3$) and synthetic polyelectrolytes applied in water treatment. Water treated using this natural resource presents a competitive advantage in turbidity removal efficiency compared to the coagulants/flocculants utilized currently. Another benefit of the technology of using the *M. oleifera* seed extract is that it is less complex and cheaper than the traditional coagulation/flocculation process. Since *M. oleifera* is a natural product, it is also environmentally friendly compared to the utilization of chemicals that could be of health concern. Furthermore, this natural product is easily stored and widely accessible. Other studies by Shan *et al.* [3] and Araujo *et al.* [42] further confirmed that *M. oleifera* seeds biomass is a good biosorbent for heavy metal ions. These studies also reinforce the fact that the biosorbent is cheaper, effective and yields minimal environmental impact. It is therefore against this background that the current study explored Moringa seed proteins for water treatment and selective recovery of precious metal ions.

2.3 Magnetic iron oxide nanoparticles and water treatment

Nanomaterial studies have nowadays gained popularity [43]. Magnetic separation is a technique mainly applied in mining whereby magnetic force is utilized to extract magnetically susceptible material from a mixture [44]. There are several magnetic nanoparticles that can be manipulated with a magnetic field. These are particles consisting of magnetic elements such as iron, nickel, cobalt as well as their chemical

compounds. On the other hand, nanoparticles are generally defined as materials with structural components ranging between 1 to 100 nm [2,45,46]. As a result of their small size and thus enormous surface areas, they tend to have strong reactivity as well as adsorption capacities. The regularly applied magnetic nanoparticles are iron oxides of which superparamagnetic Fe_3O_4 nanoparticles are the most predominant because of their low toxicity and good biocompatibility [24] in addition to their high surface area and adsorption capacity [1,27,28,45,47].

A study by Dave and Chopda [48] on the application of iron oxide nanomaterials for the removal of heavy metals revealed different methods for synthesizing iron oxide nanomaterials. They are categorized as physical, chemical as well as biological. Types of physical methods are gas phase deposition, electron beam lithography, pulsed laser ablation, laser - induced pyrolysis, powder ball milling, and aerosol. On the other hand, co-precipitation, micro-emulsion, hydrothermal, electrochemical deposition, sonochemical and thermal decomposition fall under chemical methods. Lastly under biological methods are fungi, bacteria as well as protein - mediated methods. Similar methods were discussed by Xu *et al.* [27]. Of these methods, chemical co-precipitation is popular because it is a cost-effective standard method that allows the preparation of large quantities of nanoparticles in a single batch [49]. Also, it is regarded as a simplest and efficient method that results in magnetic nanoparticles [50]. These magnetic nanoparticles are popular in heavy materials removal from wastewater mainly due to the external magnetic fields that are applied.

Magnetic nanoparticles (MNPs) prepared using the co-precipitation method have been used for the removal of heavy metal ions from wastewaters [17]. The study applied

this method and the iron oxide nanoparticles produced had an average size of 8 nm. The metal ions of interest in the study were Pb(II), Cu(II), Zn(II) and Mn(II) and Pb(II) showed the maximum adsorption capacity and Mn(II) the minimum. This was attributed to the differences in the electrostatic attraction between the negatively charged adsorption sites with the positively charged heavy metals ions. The metal ions differ in their atomic radii, and this could also account for the differences in the adsorption capacities. Another study conducted by Rajput *et al.* [51] utilized magnetic magnetite (Fe_3O_4) synthesized by co-precipitation successfully remediated Cr(VI) and Pb(II) from wastewater. The study further revealed that the heavy metals ions removal from wastewater is a physicochemical process resulting from electrostatic attractions.

Velez *et al.* [52] used magnetic iron oxide nanoparticles prepared by co-precipitation method and stabilized in aloe vera to remove mercury from wastewater. The size of the nanoparticles was approximately 100 nm. Satisfactory percentage removal of mercury from wastewater was reported as 70% on average. Gui *et al.* [53] synthesized iron oxide nanoparticles stabilized in materials such as carboxymethyl cellulose (CMC) and polyacrylic acid (PAA) functionalized polyvinylidene fluoride (PVDF) microfiltration membranes for removing trichloro ethylene from groundwater. PAA/PVDF membrane was also reported to be effective in controlling the sizes of the nanoparticles as well as preventing their agglomeration.

A study by Al-Sand *et al.* [18] used iron oxide nanoparticles of size 25-55 nm to treat synthetic aqueous solutions contaminated with Al(III), As(III), Cd(II), Co(II), Cu(II), and Ni(II). The metal ions that showed the maximum percentage removal of more than 95% were Cu(II) and As(III) whereas the other metal ions in the study depicted the

percentage removal ranging from 35% to 65%. Similar results were obtained by Giraldo *et al.* [17] and Rajput *et al.* [51] in the removal of heavy metals ions removal from wastewater by a physicochemical process resulting from electrostatic attractions.

Xu *et al.* [54] also used magnetic nanoparticles synthesized by chemical co-precipitation method for water purification. Pathogenic bacteria such as *Escherichia, Acinetobacter, Pseudomonas,* and *Bacillus* were effectively removed from drinking water. The study further reported that no significant toxicity was shown when magnetic nanoparticles were utilized. A study by Meng *et al.* [55] confirmed the antimicrobial property of iron oxide nanoparticles in the treatment of bacteria such as *Escherichia coli*. Another study by Patil [56] on wastewater treatment using nanoparticles revealed that magnetic nanoparticles are useful in the removal of toxic heavy metals, natural organic matter, biological contaminants, organic pollutants, nitrates, fluoride as well as arsenic from wastewater. The study also stated that of the available techniques, adsorption by magnetic nanoparticles is the most convenient due to its easy handling, minimal cost as well as effectiveness.

Khiadani *et al.* [57] demonstrated that a column with stainless steel wool with iron oxide nanoparticles in the presence of a magnetic field could be utilized in improving urban runoff quality. Runoff from roads surface is considered as the primary source of environmental pollution. Synthesized runoff in the study consisted of Pb, Zn, Cd, PO_4^{3-} and NO_3^- ions as well as turbidity of 60 NTU. Significant removal efficiency was attained for lead, zinc, cadmium and phosphate ions with percentages of 93.9%, 96.4%, 88.4%, and 87.4%, respectively. However, the turbidity average removal efficiency was not very satisfactory as it was only 45.1%. The column used in the study

could also not remove nitrate ions as physical, or adsorption mechanisms are likely not to be suitable methods for nitrates removals [57].

A good comparison by Hassan and Malidi [58] was conducted between nanoparticles synthesized from copper and iron to remove lead from aqueous solution. The study found that removal efficiency was higher, about 88%, using iron oxide nanoparticles compared to 84% with copper oxides. The electrostatic attraction was mainly responsible for metal ions removal. Lead ions were also reported to adsorb onto the nanoparticles very quickly thus equilibrium could be reached within a short period of approximately 30 minutes. A system that attains equilibrium in a short period is significant for wastewater treatment plant.

2.4 Magnetic iron oxide nanoparticles modified with *Moringa* seed proteins and water treatment

According to Wu *et al.* [26], the MNPs must have combined properties of high magnetic saturation, stability, biocompatibility and interactive functions at the surface. However, the surface could be modified by organic or inorganic materials such as polymers, biomolecules, silica, alumina, zirconium, ferrites, metals, iminodiacetic acid, thiols, amines and so on [12]. Of these, silica and alumina are popular for the recovery of precious metals. It is vital for superparamagnetic iron oxide to be coated before or after synthesis. This does not only provide stability but also prevents corrosion, oxidation and positively contributes to their functionality as well as biological fate [43]. On the other hand, naked iron oxide nanoparticles might not optimize their use due to agglomeration as well as flocculation properties [59].

Several studies have demonstrated that turbidity removal and recovery of metal ions from contaminated water is mainly pH dependent [5,45,47,60-62]. Generally, the isoelectric point (pI) of Moringa seed proteins is 10-11 [32,35,63]. However, some amino acids have additional -COOH functional groups and acidic amino acids, aspartic and glutamic acids have pI values of about 3 [35,36]. Since the pI of magnetite nanoparticles is known to be close to neutral pH range of 6-7 [12,59], it implies that above pH 3, these amino acid groups are negatively charged and adsorb onto iron oxide nanoparticles which are positively charged at pH below neutral range thus forming a nano-composite for recovery of precious metal ions. On the other hand, the proteins from Moringa seeds overall tend to be positively charged at pH below 10-11 and adsorb onto iron oxide which is negatively charged at pH above neutral range again forming a nanocomposite for water turbidity removal.

A study by Okoli [24] revealed that *M. oleifera* modified with MNPs enhanced the performance coagulating/flocculating properties in contaminated water samples. This agrees with the study conducted by Santos *et al.* [29] on the evaluation of the effectiveness of the coagulation/flocculation using *M. oleifera* seed extract functionalized with magnetic iron oxide nanoparticles for water treatment. The study found out that more than 90% turbidity could be removed from surface water under the effect of an exterior magnetic field in 30 minutes.

A promising approach is the use of magnetic iron oxide nanoparticles prepared from microemulsion for the purification or immobilization of proteins [24]. Magnetic iron oxide nanoparticles which are silica-coated have been synthesized for rapid and selective magnetic field-based separation of mixed proteins. A key consideration

during protein separation process is to control the driving force of the sorbent surface behind the adsorption of proteins that involves hydrophobic and electrostatic interactions [64]. Therefore, the successful adsorption of proteins onto MNPs depends on the proper surface modification.

An interesting study by Hussein *et al.* [65] utilized iron oxide nanoparticles modified with polyurethane for arsenic removal. The two different nanoparticles size ranges tested 15-20 nm and 50-100 nm. A smaller size range (15-20 nm) attained a higher maximum removal capacity compared to the bigger one (50-100 nm). Dewi et al. [66] demonstrated the formation of magnetic photocatalyst $Fe_3O_4/SiO_2/TiO_2$ composite with the size of 20 nm that was tested on the removal of methylene blue (MB) in water. A slightly similar study by Zemtsova et al. [67] synthesized Fe_3O_4/SiO_2 with particles sized between 30-50 nm for targeted drug delivery.

Another study was conducted by Ehrampoush *et al.* [68] on the use of co-precipitated iron oxide nanoparticles prepared in tangerine peel extracts as an adsorbent for cadmium ions removal from contaminated solution. This extract was utilized as a stabilizer agent and the nanoparticles produced were reported to be free of harmful contaminants. The average size of nanoparticles produced also decreased from 200 nm to 50 nm when the peel extract was increased from 2 to 6%. However, when the concentration was increased up to 10%, the nanoparticles size also increased due to the strong bonding of nanoparticles.

Lakshmanam [69] conducted a study on the treatment of wastewater using iron oxide nanoparticles by synthesizing the nanomaterials using both co-precipitation as well as

microemulsion methods. The dimensions of the nanomaterials ranged from 8 to 40 nm. In the study, the nanomaterials were functionalized with tri-sodium citrate (TSC), 3-aminopropyl triethoxysilane (APTES), polyethylenimine (PEI) and chitosan. Functionalization of nanoparticles is believed to play a significant role in stabilization as well as enhancing the removal efficiency of contaminants in wastewater. The findings of the study were such that process time, complexity, sludge production as well as the use of additional chemicals in wastewater treatments could be reduced when both coated and uncoated magnetic iron oxide nanoparticles are employed. This approach was further identified as simple, robust as well as environmentally friendly. Another benefit revealed by the study is the toxicity of the magnetic nanoparticles utilizing human keratinocytes (HaCaT) and endothelial (HMEC-1) cells that yielded very satisfactory results. This was performed for the viability of the cell, strand damage of DNA as well as reactive oxygen species (ROS) generation.

Another study conducted by Gill *et al.* [70] utilized a co-precipitation method to synthesize superparamagnetic iron oxide nanoparticles and coated them with chitosan. The nanocomposite materials prepared were then applied in removing metals from wastewater. The study also showed that coating nanomaterials with suitable materials such as silica or chitosan could also minimize the health concern associated with the application of nanoparticles in water treatment. These results concur with a study conducted by Remya *et al.* [71] that suggested that metal and metal oxide nanoparticles potential harm could be minimized by coating their surfaces with stabilizers such as dextran. However, characteristics such as particle size, surface properties, chemical composition play a vital role in the toxicity of nanoparticles [72].

Vasylkiv *et al.* [73] demonstrated that addition of chitosan in the synthesis of iron oxide nanoparticles results in nanoparticles with various morphologies. An example is polycrystalline mesoporous structures sized between 60-105 nm obtained from the cubo-octahedral morphology of Fe_3O_4 nanoparticles sized between 50-125 nm.

According to Gutierrez *et al.* [74], chitosan is a natural material with active sites on its polymeric chain because of $-NH_2$ groups. It is, therefore, a popular biosorbent when modified with iron oxide nanoparticles for water and wastewater treatment for contaminants that are negatively charged. Moringa proteins also depict similar properties to chitosan thus could be modified with iron oxide nanoparticles for water treatment as well as selective recovery of precious metal ions. The study further mentioned that the future for iron oxide nanoparticles composite adsorbents looks good. This is for both organic pollutants from water and wastewater as well as other contaminants in contaminated areas.

CHAPTER 3: METHODOLOGY

3.1 Research design

The study conducted at a laboratory scale was quantitative in nature. MNPs were prepared using the co-precipitation method. The characterization of the nanoparticles was done as well as modification of magnetic iron oxide nanoparticles with protein extract of *M. oleifera* seeds. The purposive sampling was used to sample the seed pods. During the synthesis of modified MNPs variables controlled were the stirring rate, pH and temperature because these contribute to the size as well as the morphology of the nanocomposite obtained. The effectiveness of magnetic iron oxide modified with *M. oleifera* seed proteins was tested using synthetic kaolin (clay) turbid water and precious metals spiked water for recovery studies.

3.2 Samples

The study used only the *M. oleifera* seeds. Samples of *M. oleifera* mature dry pods were collected from a tree grown in Cimbesbasia, a residential area in Windhoek in the Khomas region. They were collected in paper bags and carried to the laboratory where they were prepared for the experiment.

3.3 Instrumentation

The research was based on laboratory experiments, and several techniques were used to characterize the MNPs. The characterization techniques included the following: Perkin Elmer Fourier Transform Infrared (FTIR) Spectroscopy for functional groups determination; Q600 V20.9 Build 20 Thermogravimetric Analyser (TGA) and Differential Scanning Calorimeter (DSC) for decomposition and thermal stability; Jeol JSM-IT300A Scanning Electron Microscope (SEM) for morphology and a Zeta

potential with a nano Zetasizer for surface charge determinations. A permanent magnet was used to test whether the nanoparticles synthesized were magnetic. The Perkin Elmer Lambda 35 Ultra Violet-Visible (UV-Vis) spectrometry was used for turbidity measurements. FTIR was also used to confirm the adsorption and immobilization of MNPs/Moringa seed proteins composite. Quantitative determination of metals was done using the Perkin Elmer Inductively Coupled Plasma-Optical Emission Spectrometer (ICP-OES).

3.4 Experimental Procedure

3.4.1 Reagents and materials

Reagents used throughout the study were either chemically pure or of analytical grade. Deionized water was obtained from a Rios - DI system supplied by Merck. Whatman no. 1 filter papers with a diameter of 90 mm manufactured by GE Healthcare company were used. Ferric chloride ($FeCl_3.6H_2O$) and hydrochloric acid (HCl) were supplied by Merck, petroleum ether (40-60°C) by Skychem, whereas ferrous chloride ($FeCl_2.4H_2O$), acetone and ammonium sulphate were obtained from Promark Chemicals. Sodium hydroxide (NaOH) was supplied by Skylabs, kaolin and sodium chloride by LD didactic in Germany, gold *(*III) chloride by Sigma-Aldrich, and platinum (IV) chloride and palladium *(*II) chloride by Alfa aesar. Preswollen Carboxymethyl cellulose was supplied by Biophoretics (USA.) Multielement precious metals standard was supplied by Perkin Elmer.

3.4.2 Preparation of *Moringa oleifera* seed extract

The extraction of the soluble cationic protein was carried out using the method by Maikokera and Kwaambwa [39]. Briefly, the seeds obtained from the dry *M. oleifera*

mature pods were deshelled skinned and the kernels crushed using a pestle and mortar to obtain a powder. The seeds powder (75-80 g) was defatted by mixing with 40-60°C petroleum ether (200 mL) using hot plate magnetic stirrer at 1100 rpm for two hours followed by suction filtration. The removal of oil is necessary as its presence is known to reduce the effectiveness of water treatment [3]. The powder obtained was dried in open air on a paper towel. This powder was then stirred in 1M potassium chloride (200 mL) at 1100 rpm for an hour followed by suction filtration to remove the bigger solid particles, and then lastly by gravity filtration until a clear solution was obtained. Studies have shown that coagulating component extracted from *M. oleifera* seed is more efficient using salt solution than tap water [39,75]. The active ingredient (proteins) in the extract was precipitated by adding ammonium sulphate salt to saturation that results in a sticky paste due to 'salting out' effect. The precipitated active ingredient was filtered using suction filtration. It was then re-dissolved in distilled water (200 mL) and dialyzed using Sigma-Aldrich dialysis tubing cellulose membrane of 43 mm width. The protein solution was purified with the carboxymethyl cellulose (CMC) resin, eluted with 1M sodium chloride (NaCl) solution then finally dialyzed. The resulting solution was frozen at -80°C and freeze-dried using the Chris Alpha 1-2 LD plus freeze drier. The resulting powder was kept in an airtight container until ready for use.

3.4.3 Preparation of magnetic iron oxide (Fe_3O_4) and modification of nanoparticles

Magnetic iron oxide (Fe_3O_4) nanoparticles were prepared by chemical co-precipitation of Fe^{3+} and Fe^{2+} ions [17,26,76]. This is a cost effective standard method that allows the preparation of large quantities of nanoparticles in a single batch [49]. According to

this method, the iron salts solution was prepared by mixing 3.24 g (0.02 moles) of ferric ($FeCl_3.6H_2O$) and 1.99 g (0.01 moles) of ferrous chloride ($FeCl_2.4H_2O$) in 20 mL distilled water at 20-23ºC and stirring at a rate of 300 rpm for 20 minutes. Sodium hydroxide (8 M) solution was prepared by dissolving 4.58 g in 14 mL distilled water and stirred at 300 rpm for 30 minutes at 20-25ºC. The magnetite (Fe_3O_4) nanoparticles were precipitated by dropping the iron salts solution into the NaOH solution at 20-30ºC while stirring at 600 rpm for an hour. Sodium hydroxide is preferred since magnetite nanoparticles with this base as a precipitant proved to have better magnetic properties [59]. The resulting black nanoparticles were separated with the help of a permanent magnet before decanting the supernatant. Lastly, nanoparticles were washed with deionized water and acetone. The obtained fine Fe_3O_4 nanoparticles (approximately 4 g) were finally freeze-dried for 24 hours and stored in a vial that is airtight until use. For the protein modified magnetic nanoparticles, the co-precipitation was carried out in 1% aqueous protein solution instead of distilled water.

The formation of Fe_3O_4 is represented by the following overall equation [26]:

$$Fe^{2+}(aq) + 2Fe^{3+}(aq) + 8OH^{-}(aq) \rightarrow Fe_3O_4\downarrow (s) + 4H_2O \quad (l)$$

3.4.4 Characterisation of magnetic iron oxide nanoparticles modified and unmodified with *M. oleifera* seed proteins

The characterization was done as briefly described below [42,47]. The Perkin Elmer UATR spectrum two system Fourier transform Infrared (FTIR) spectroscopy was used to assess the main functional groups present that are responsible for adsorption in the magnetic iron oxide nanoparticles modified and unmodified with *M. oleifera* seed proteins. Sufficient sample to cover the prism of the instrument was placed. The range

of the spectra recorded in transmittance band mode was between 4000 to 400 cm^{-1} with four scans. The decomposition, as well as thermal stability, was characterized using a Q600 V20.9 Build 20 Thermogravimetric Analyser (TGA) and Differential Scanning Calorimeter (DSC). This was done by heating approximately 10 mg of a sample from 30°C to 900°C at a constant rate of 10°C per minute under nitrogen gas, at a flow rate of 20 mL per minute. The sample lost mass over the specified rate and temperature thus the decomposition, as well as thermal stability, could be deduced. The morphology of the synthesized nanoparticles was characterized with the Jeol JSM-6010PLUS/LA Scanning Electron Microscope (SEM) equipped with the Oxford X-ray energy dispersive spectroscope (EDS). The characterization of the surface charge of the nanoparticles was measured with a nano Zetasizer (Nano Zs model) between pH 2-12.

3.4.5 Preparation of synthetic turbid water

Turbid water was prepared using kaolin powder as briefly described below [5]. Kaolin powder was dried in an oven at 105^{o}C for three hours and cooled off in a desiccator for about half an hour. A suspension of kaolin with distilled water was prepared and kept for 24 hours. This is to allow coarse particles to settle and the cloudy supernatant decanted for use.

3.4.6 Preparation of aqueous precious metal ions solutions

Precious metal chloride salts of gold, palladium, and platinum were used for this study. Precious metal ions solutions were prepared as briefly described by Witek-Krowiak [7] and Obuseng *et al.* [63] as follows: Predefined quantities of respective metal chloride salts were dissolved in distilled water to get stock solutions of 100 mgL^{-1}. The

stock solutions were diluted further to get the desired working concentrations. The pH of solutions was adjusted using 0.1 M HCl and 0.1 M NaOH to create acidic and basic environments, respectively.

3.4.7 Turbidity removal and selective recovery of precious metal ions using modified and unmodified nanoparticles

The modified, as well as unmodified nanoparticles, were tested for turbidity removal and recovery of precious metals using the method described by Okoli [24]. The nanoparticles were added to turbid water, shaken for two hours and then allowed to settle overnight before filtration using gravity filtration (Whatmann filter paper No.1).

Turbidity reveals information regarding the formation of insoluble complexes. Turbidity measurements were carried out with a Perkin Elmer Lambda 365 UV/Vis-spectrophotometer to detect aggregates formed by the modified as well as unmodified MNPs powder with kaolin particles. The turbidity of the modified, as well as unmodified MNPs powder-kaolin, suspensions were monitored by the transmittance at wavelengths 360, 450, 540, and 600 nm [35]. The turbidity is therefore plotted as 100 - %T, whereby T refers to transmittance.

The precious metals recovery was studied using batch experiments. To the water spiked with precious metals, known amounts of modified MNPs powder was added, shaken for two hours and allowed to settle overnight before filtration using gravity filtration (Whatmann filter paper No. 1). Analysis of metal ions was carried out with a Perkin Elmer Optima 8000 ICP-OES.

The recovery efficiency (R) was calculated using the equation [77]:

$$\%R = \frac{C_i - C_f}{C_i} x100 \quad (2)$$

where, C_i is the initial concentration, C_f is the final concentration of the analyte, and %R is the extraction percentage.

The adsorption process of precious metal ions on unmodified and modified iron oxide nanoparticles was tested using the Langmuir and Freundlich isotherm models. Linear forms of these models are shown in the following equations [47,78, 79]:

Langmuir: $$\frac{C_e}{q_e} = \frac{1}{q_m b} + \frac{1}{q_m C_e} \quad (3)$$

Freundlich: $$\ln q_e = \ln K_f + \frac{1}{n} \ln C_e \quad (4)$$

The adsorption capacity of the modified and unmodified iron oxide nanoparticles for each concentration of precious metal ions at equilibrium, q_e is calculated using the following equation [47,78, 79]:

$$q_e\,(mg/g) = \frac{V(C_o - C_f)}{m} \quad (5)$$

where, C_0 is initial precious metal ions concentration, C_f is final concentration after adsorption, V is the volume of solution (L) and m is the mass of adsorbent (modified and unmodified iron oxide nanoparticles).

In equations 3 and 4 for Langmuir and Freundlich, C_e (mg/L) is the equilibrium concentration of adsorbate (precious metal ions); q_e (g) is the amount of precious metal ions per gram of unmodified / modified iron oxide nanoparticles at equilibrium; q_m (mg/g) and b (L/mg) are Langmuir constants for adsorption capacity and rate of adsorption. These are obtained from the slope and intercept of the linear Langmuir

plot. K_f and n are adsorption capacity and intensity constants in the Freundlich linear plot calculated from the intercept and slope, respectively.

R_L is a dimensionless separation factor from the Langmuir isotherm that is calculated using the following equation [47,78, 79]:

$$R_L = \frac{1}{1+bC_o} \quad (6)$$

where, C_o (mg/L) is the initial precious metal ion concentration, and b (slope/intercept) is obtained from the Langmuir plot.

3.5 Data Analysis

The study utilizes quantitative data analysis. All the measurements of turbidity and precious metal ions recoveries were represented graphically. The averages are reported. For turbidity studies, the shortest wavelength of 360 nm was more sensitive since its peak in absorbance is higher at the dosage used compared to the other wavelengths hence it was utilized. Whereas for precious metal ions recoveries, the Quality Control (QC) standards calibration units such as Relative Standard Deviation (RSD) percentage, percentage recovery as well as the R^2 (the coefficient of determination value) determined the suitable wavelength.

CHAPTER 4: ETHICAL CONSIDERATIONS

Seeds of *M. oleifera* were collected from a tree grown in Cimbebasia in Windhoek, Khomas region. The research was done with the ethical clearance from the UNAM Research and Publication Committee (RPC).

CHAPTER 5: RESULTS

5.1 Characterisation of magnetic iron oxide nanoparticles modified and unmodified with *M. oleifera* seed proteins

5.1.1 Fourier Transform Infrared (FTIR) Spectrometry

The FTIR was used to assess the main functional groups responsible for adsorption present in the magnetic iron oxide nanoparticles modified and unmodified with *M. oleifera* seed proteins extract. The FTIR spectra were recorded in transmittance band mode in the wavelength range from 4000 cm^{-1} to 400 cm^{-1} as shown in Figures 5.1-5.7. The magnetic iron oxide nanoparticles modified with *M. oleifera* seed proteins extract were studied in acidic, basic and neutral media and are shown in Figures 5.5-5.7. Tables 5.1-5.6 show the analysis of the IR spectra for Moringa protein powder (purified and unpurified), magnetic iron oxide nanoparticles, and magnetic iron oxide nanoparticles modified with Moringa proteins extract in acidic, basic and neutral medium, respectively.

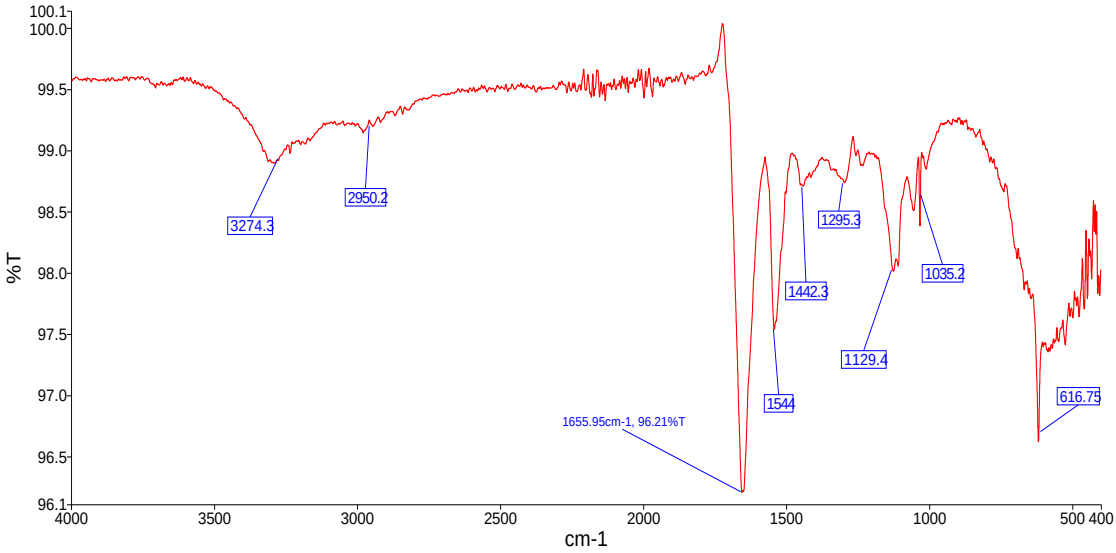

Figure 5.1: FTIR spectrum of Moringa seed unpurified proteins extract powder

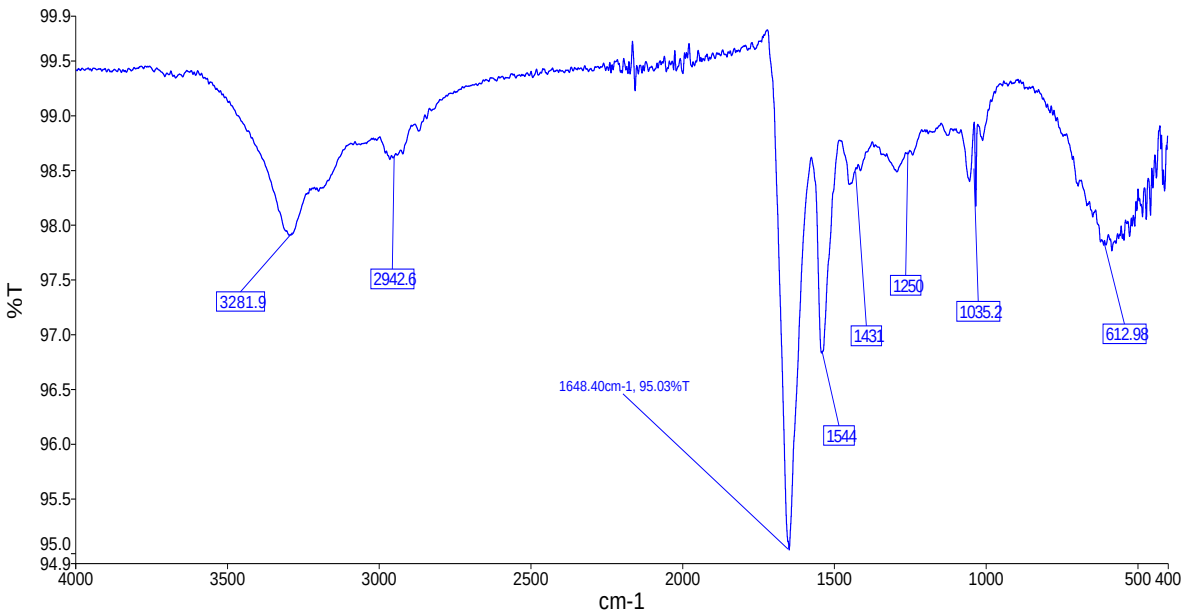

Figure 5.2: FTIR spectrum of Moringa seed purified proteins extract powder

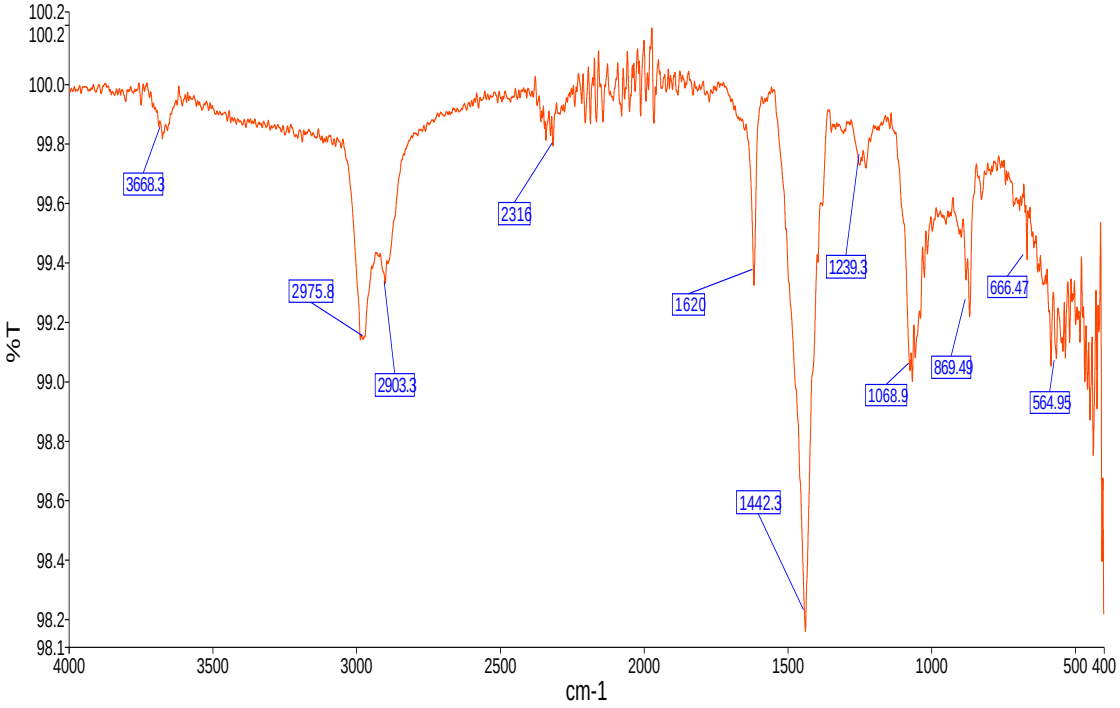

Figure 5.3: FTIR spectrum of magnetic iron oxide

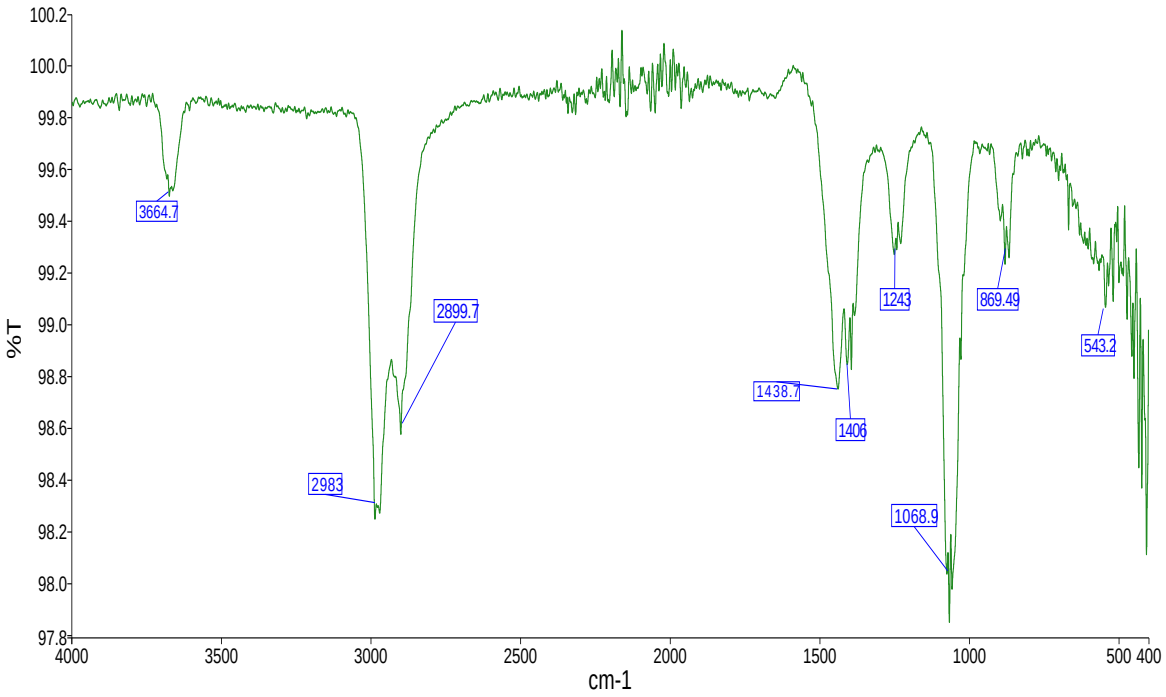

Figure 5.4: FTIR spectrum of iron oxide modified with Moringa seed proteins extract

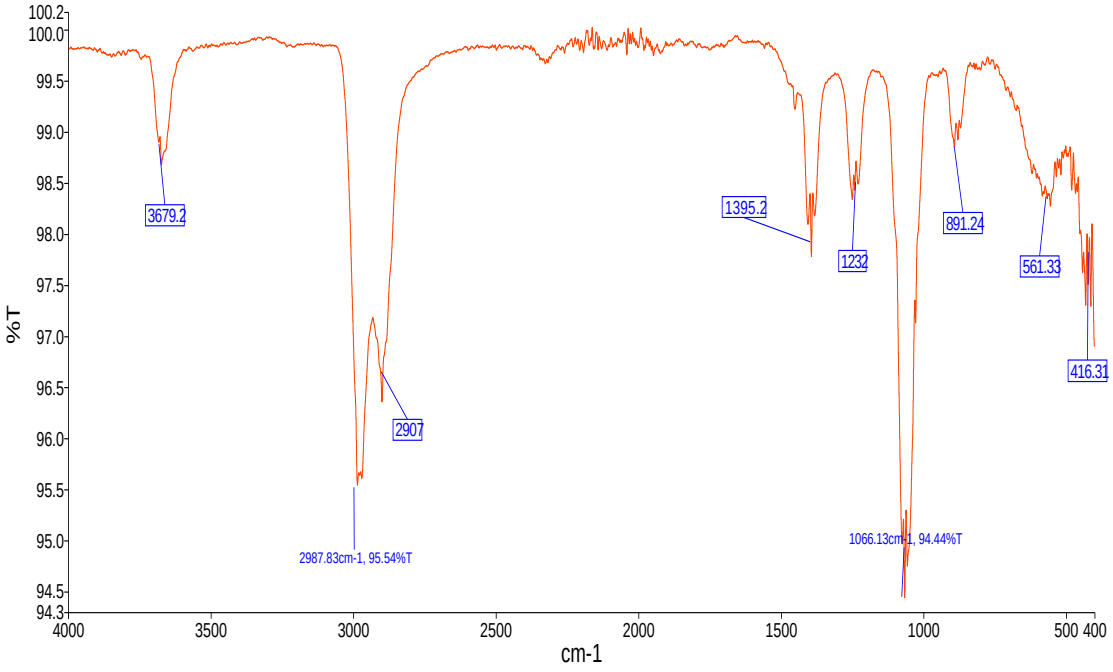

Figure 5.5: FTIR of iron oxide modified with Moringa seed proteins extract in acidic medium

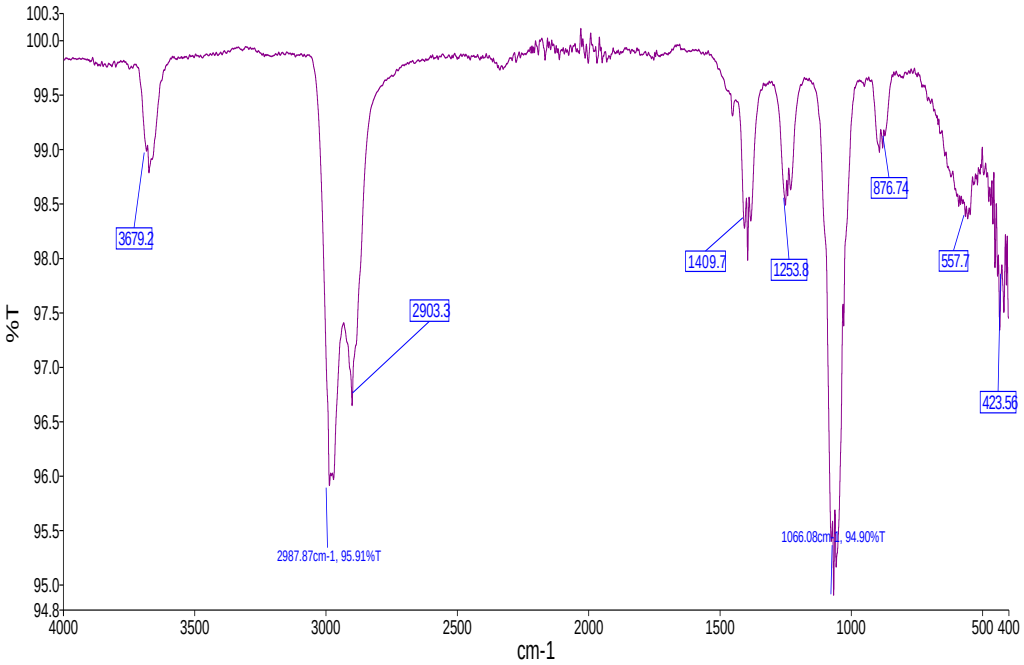

Figure 5.6: FTIR of iron oxide modified with Moringa proteins extract in basic medium

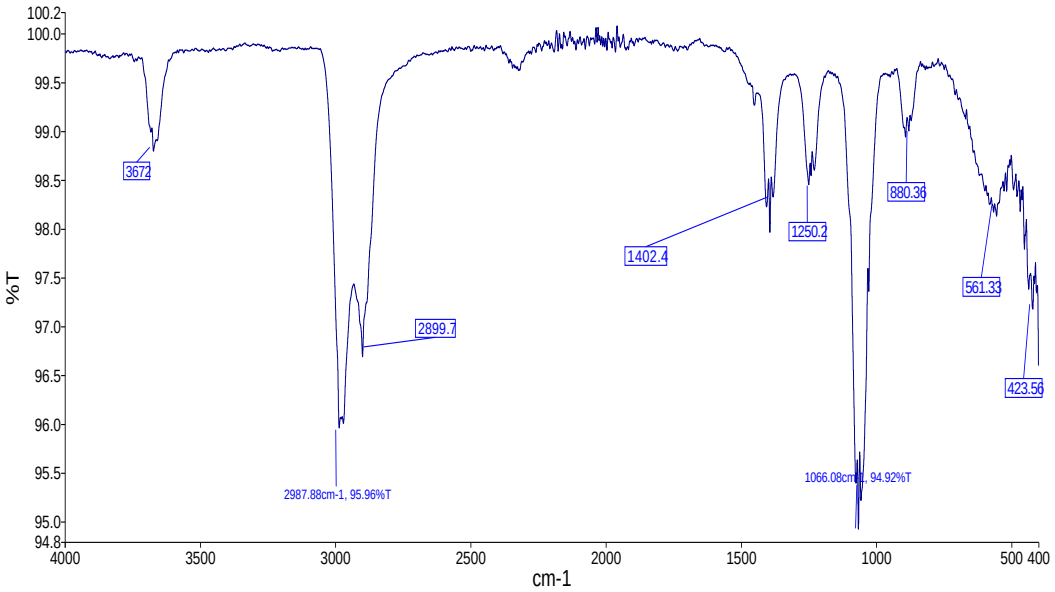

Figure 5.7: FTIR of iron oxide modified with Moringa seed proteins extract in neutral medium

Table 5.1: Analysis of the IR spectra for Moringa seed unpurified (MoUP) and purified (MoPP) proteins extract powder

Functional group	**Reference frequency range (cm^{-1}) [42,47,51, 77,80,81]**	**Observed IR frequency (cm^{-1}) for MoUP**	**Observed IR frequency (cm^{-1}) for MoPP**	**Peak shift (cm^{-1})**
Amides stretch (C=O)	1680-1640	1656.95	1648.40	8.55
Carbonyl and Amides (C=O and N-H)	2000-1500	1544	1544	0
OH (Alcohol; Carboxylic acid);	3400-2400	3274.3 2950.2	3281.9 2942.6	-7.6 7.6
OH bend (Carboxylic acid)	1440-1400	1442.3	1431	11.3
CO stretching (Carboxylic acid)	1320-1210	1295.3	1250	45.3
CO stretching (Alcohol)	1260-1000	1129.4 1035.2	 1035.2	- 0
Alkynes (acetylenic CH bend)	650-600	616.75	612.98	3.77

Table 5.2: Analysis of the IR spectra for unmodified magnetic iron oxide nanoparticles and iron oxide modified with Moringa seed proteins extract ($MoFe_3O_4$)

Functional group	**Reference frequency range (cm^{-1}) [42,47,49,51, 77,78,80,82]**	**Observed IR frequency (cm^{-1}) for iron oxide**	**IR frequency (cm^{-1}) for $MoFe_3O_4$**	**Peak shift (cm^{-1})**
OH stretching	3700-3500	3668.3	3664.7	3.6
OH (Alcohol)	3400-2400	2903.3 2975.8	2899.7 2983.3	3.6 -7.5
OH bend (Carboxylic acid)	1440-1400	-	1438.7 1406	-
H-O-H (Adsorbed water)	1652-1429	1442.3; 1620	1438.7 -	3.6
CO stretching (Carboxylic acid)	1320-1210	-	1243	-
OH stretching vibration	1092-1060	1068.9	1068.9	0
CO stretching (Alcohol)	1260-1000	1239.3	1243	-3.7
Alkenes (CH bend)	~890	889.49	869.49	20
Aromatics (CH bend)	~880	889.49	869.49	20
Fe-O	588-535	564.95	543.2	21.75

Table 5.3: Analysis of the IR spectra for Moringa seed proteins extract powder (MoP); magnetic iron oxide nanoparticles; magnetic iron oxide nanoparticles modified with Moringa seed proteins extract ($MoFe_3O_4$)

Functional group	**Reference frequency range (cm^{-1}) [42,47,49,51,77, 80,81,82]**	**Observed IR frequency (cm^{-1}) for MoP powder (1)**	**Observed IR frequency (cm^{-1}) for iron oxide (2)**	**Observed IR frequency (cm^{-1}) for $MoFe_3O_4$ (3)**	**Peak shift (1-3) and (2-3) (cm^{-1})**
NH (Amine / Amide) stretching; OH stretching Amides stretch (C=O)	3700-3500 1680-1640	- 1648.40	3668.3 -	3664.7 -	(1-3): - (2-3): 3.6 -
Carbonyl and Amides (C=O and N-H)	2000-1500	1544	-	-	-
OH (Alcohol; Carboxylic acid);	3400-2400	3281.9 2942.6 -	- 2975.8 2903.3	- 2983.3 2899.7	- (1-3): -40.7 (2-3): -7.5; 3.6
OH bend (Carboxylic acid)	1440-1400	1431	-	1406 1438.7	(1-3): 25; -7.7
OH stretching vibration	1092-1060	1035.2	1068.9	1068.9	(1-3): -33.7 (2-3): 0
H-O-H (Adsorbed water)	1652-1429	1431	1442.3; 1620	1438.7	(1-3): -7.7 (2-3): 3.6
CO stretching (Carboxylic Acid)	1320-1210	1250	-	1243	(1-3): - (2-3): 7
CO stretching (Alcohol)	1260-1000	1250	1239.3	1243	(1-3): 7 (2-3): -3.7
Alkenes (CH bend)	~890	-	889.49	869.49	(1-3): - (2-3): 20
Aromatics (CH bend)	~880	-	889.49	869.49	(1-3): - (2-3): 20
Alkynes (acetylenic CH bend)	650-600	612.98	-	-	-
Fe-O	588-535	-	564.95	543.2	(1-3): - (2-3): 21.75

Table 5.4: Analysis of the IR spectra for Moringa seed proteins extract powder; magnetic iron oxide nanoparticles; magnetic iron oxide nanoparticles modified with Moringa seed proteins extract in acidic media

Functional group	**Reference frequency range (cm^{-1}) [42,47,49,51,77, 80,81,82]**	**Observed IR frequency (cm^{-1}) for MoP powder (1)**	**Observed IR frequency (cm^{-1}) for iron oxide (2)**	**Observed IR frequency (cm^{-1}) for $MoFe_3O_4$ in acidic media (3)**	**Peak Shift (1-3) and (2-3) (cm^{-1})**
NH (Amine / Amide) stretching; OH stretching	3700-3500	-	3668.3	3679.2	(1-3): - (2-3): -10.9
Amides stretch (C=O)	1680-1640	1648.40	-	-	-
Carbonyl and Amides (C=O and N-H)	2000-1500	1544	-	-	-
OH (Alcohol; Carboxylic Acid);	3400-2400	3281.9 2942.6 -	- 2975.8 2903.3	- 2987.83 2907	- (1-3): -45.23; (2-3): -5.8 -3.7
OH bend (Carboxylic Acid)	1440-1400	1431	-	1395.2	(1-3): 35.8 (2-3): -
OH stretching vibration	1092-1060	1035.2	1068.9	1066.13	(1-3): -30.93 (2-3): 2.77
H-O-H (Adsorbed water)	1652-1429	1431	1442.3; 1620	-	-
CO stretching (Carboxylic Acid)	1320-1210	1250	-	1232	(1-3): 18 (2-3): -
CO stretching (Alcohol)	1260-1000	1250	1239.3	1232	(1-3): 18 (2-3): 7.3
Alkenes (CH bend)	~890	-	889.49	891.24	(1-3): - (2-3): -1.8
Aromatics (CH bend)	~880	-	889.49	891.24	(1-3): - (2-3): -1.8
Alkynes (acetylenic CH bend)	650-600	612.98	-	-	-
Fe-O	588-535	-	564.95	561.33; 557.7; 561.33	(1-3): - (2-3): 3.6

Table 5.5 : Analysis of the IR spectra for Moringa seed proteins extract powder; magnetic iron oxide nanoparticles; magnetic iron oxide nanoparticles modified with Moringa seed proteins extract in basic media

Functional group	**Reference frequency range (cm^{-1}) [42,47,49,51 ,77, 80,81,82]**	**Observed IR frequency (cm^{-1}) for MoP powder (1)**	**Observed IR frequency (cm^{-1}) for iron oxide (2)**	**Observed IR frequency (cm^{-1}) for $MoFe_3O_4$ in basic media (3)**	**Peak Shift (1-3) and (2-3) (cm^{-1})**
NH (Amine / Amide) stretching; OH stretching	3700-3500	-	3668.3	3679.2	(1-3): - (2-3): -3.7
Amides stretch (C=O)	1680-1640	1648.40	-	-	-
Carbonyl and Amides (C=O and N-H)	2000-1500	1544	-	-	-
OH (Alcohol; Carboxylic Acid);	3400-2400	3281.9 2942.6 -	- 2975.8 2903.3	- 2987.83 2903.3	- (1-3): -45.23; (2-3): -2.1; 0
OH bend (Carboxylic acid)	1440-1400	1431	-	1409.7	(1-3): 21.3 (2-3): -
OH stretching vibration	1092-1060	1035.2	1068.9	1066.13; 1066.08; 1066.08	(1-3): -30.88 (2-2): 2.82
H-O-H (Adsorbed water)	1652-1429	1431	1442.3; 1620	-	-
CO stretching (Carboxylic acid)	1320-1210	1250	-	1253.8	(1-3): -3.8 (2-3): -
CO stretching (Alcohol)	1260-1000	1250	1239.3	1253.8	(1-3): -3.8 (2-3): -14.5
Alkenes (CH bend)	~890	-	889.49	876.74	(1-3): - (2-3): 12.8
Aromatics (CH bend)	~880	-	889.49	876.74	(1-3): - (2-3): 12.8
Alkynes (acetylenic CH bend)	650-600	612.98	-	-	-
Fe-O	588-535	-	564.95	557.7	(1:3) - (2-3): 7.3

Table 5.6: Analysis of the IR spectra for Moringa seed proteins extract powder; magnetic iron oxide nanoparticles; magnetic iron oxide nanoparticles modified with Moringa seed proteins extract in neutral media

Functional group	**Reference frequency range (cm^{-1}) [42,47,49,51,77, 80,81,82]**	**Observed IR frequency (cm^{-1}) for MoP powder (1)**	**Observed IR frequency (cm^{-1}) for iron oxide (2)**	**Observed IR frequency (cm^{-1}) for $MoFe_3O_4$ in neutral media (3)**	**Peak Shift (1-3) and (2-3) (cm^{-1})**
NH (Amine / Amide) stretching; OH stretching	3700-3500	-	3668.3	3672	(1-3): - (2-3): -3.7
Amides stretch (C=O)	1680-1640	1648.40	-	-	-
Carbonyl and Amides (C=O and N-H)	2000-1500	1544	-	-	-
OH (Alcohol; Carboxylic acid);	3400-2400	3281.9 2942.6 -	- 2975.8 2903.3	- 2987.88 2899.7	- (1-3): -45.28 (2-3): 1.5; 3.6
OH bend (Carboxylic acid)	1440-1400	1431	-	1395.2; 1409.7; 1402.4	35.8; 21.3; 28.6 -
OH stretching vibration	1092-1060	1035.2	1068.9	1066.08	(1-3): -30.88 (2-3): 2.82
H-O-H (Adsorbed water)	1652-1429	1431	1442.3; 1620	-	-
CO stretching (Carboxylic acid)	1320-1210	1250	-	1250.2	(1-3): -0.2 (2-3): -
CO stretching (Alcohol)	1260-1000	1250	1239.3	1250.2	(1-3): -0.2 (2-3): -10.5
Alkenes (CH bend)	~890	-	889.49	880.36	(1-3): - (2-3): 9.1
Aromatics (CH bend)	~880	-	889.49	880.36	(1-3): - (2-3): 9.1
Alkynes (acetylenic CH bend)	650-600	612.98	-	-	-
Fe-O	588-535	-	564.95	561.33	(1-3): - (2-3): 3.6

5.1.2 Thermogravimetric Analyzer (TGA)

Thermal stability of unmodified and modified magnetic iron oxide nanoparticles was studied with Perkin Elmer Thermogravimetric analyzer as shown in Figures 5.8-5.10.

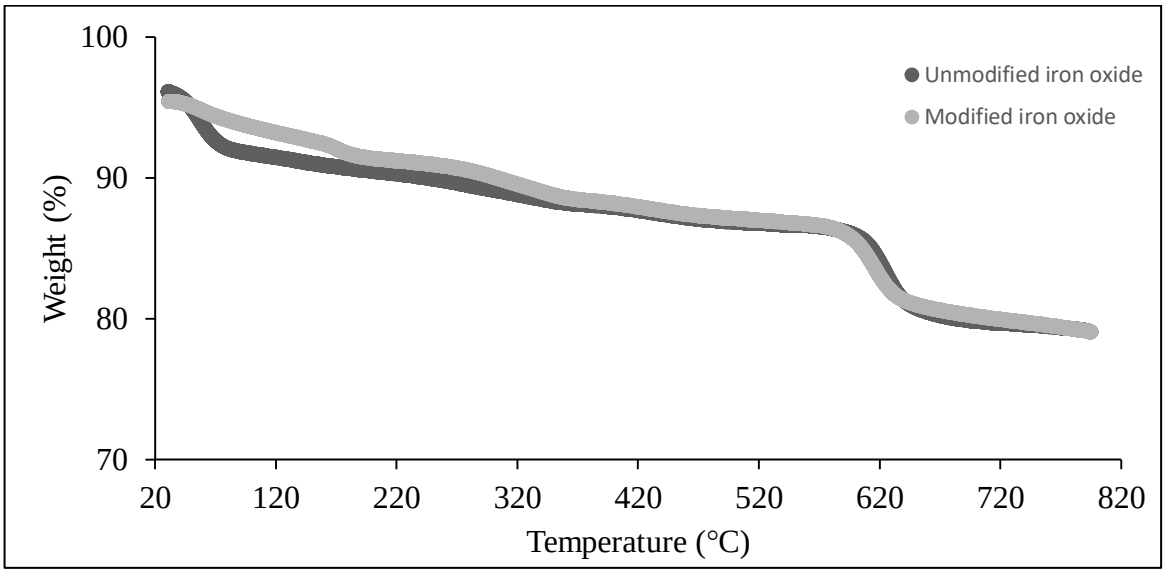

Figure 5.8: TGA curve for unmodified and modified magnetic iron oxide nanoparticles with weight loss

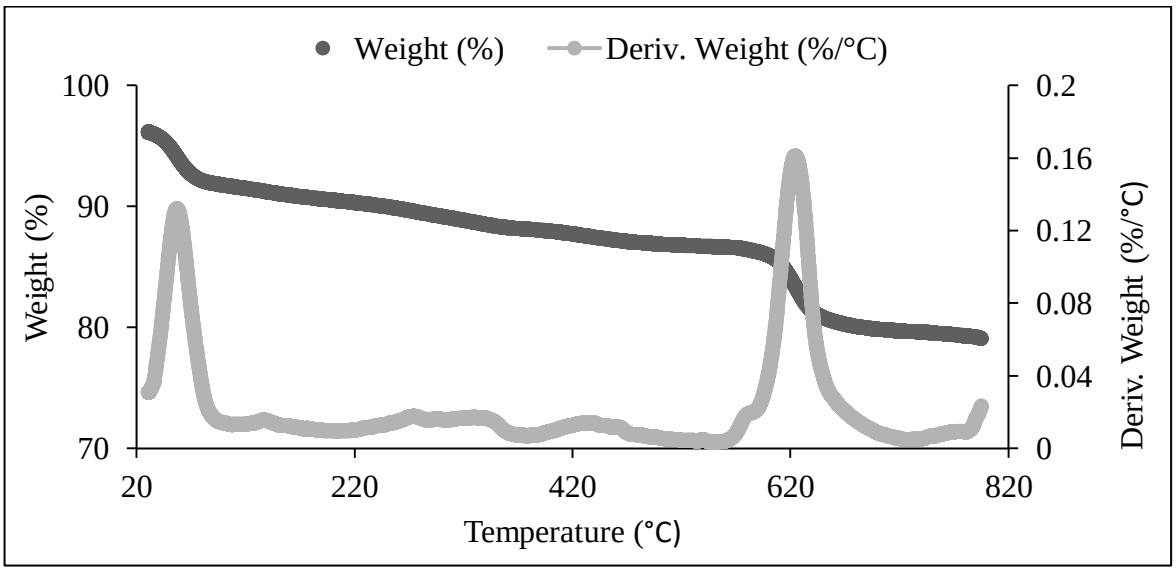

Figure 5.9: TGA curve for unmodified magnetic iron oxide nanoparticles with weight loss and derivative weight loss

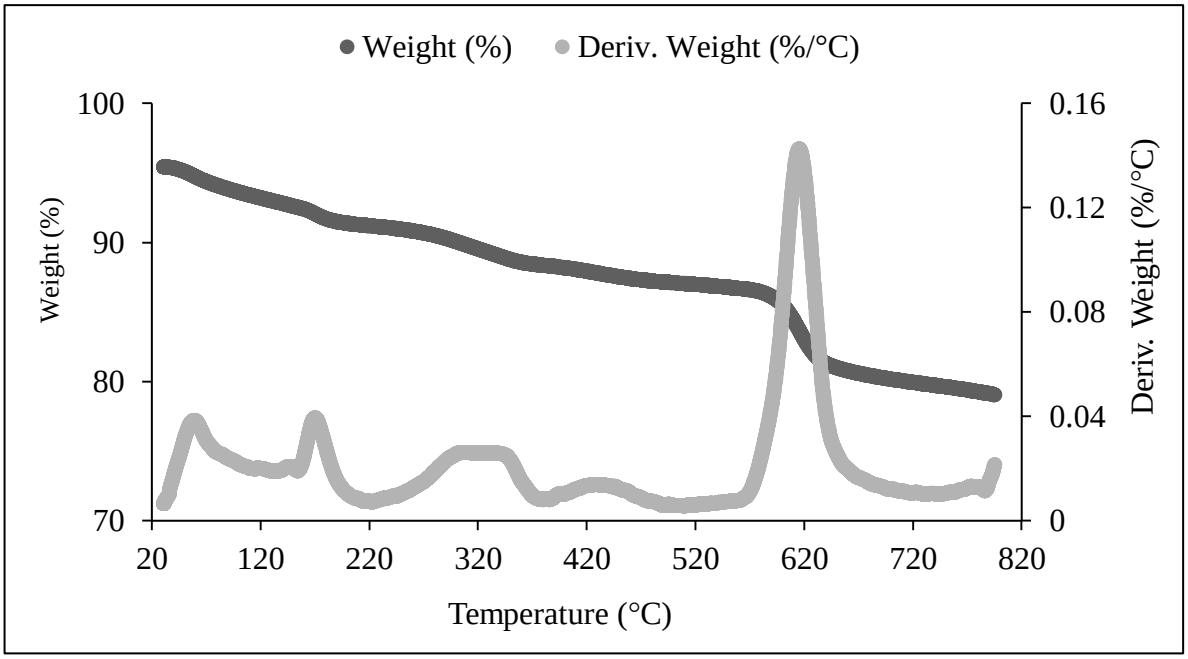

Figure 5.10: TGA curve for modified magnetic iron oxide nanoparticles with weight loss and derivative weight loss

5.1.3 Scanning Electron Microscope (SEM)

The Scanning Electron Microscope (SEM) was utilized to study the morphology of the synthesized unmodified (left) and modified (right) magnetic iron oxide nanoparticles as shown in Figure 5.11.

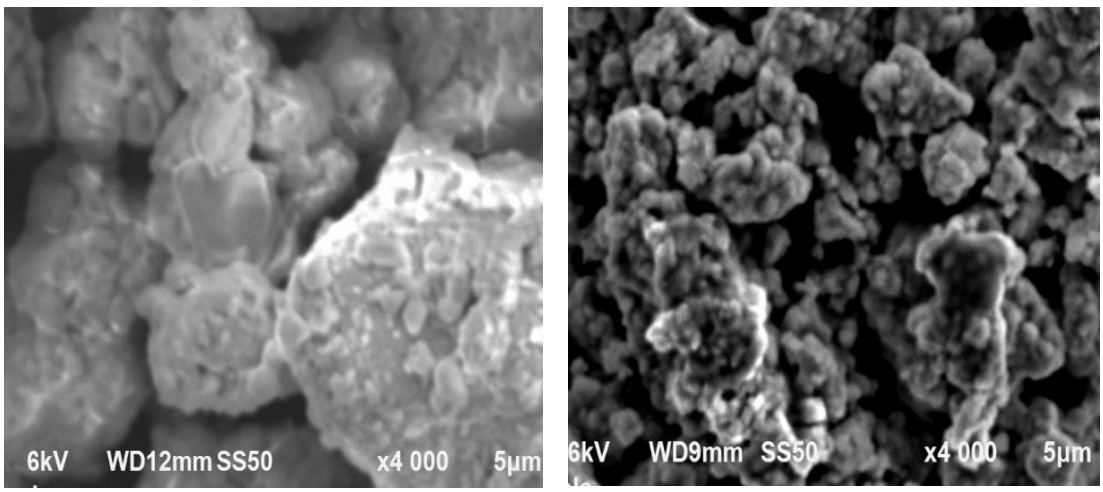

Figure 5.11: SEM for unmodified and modified magnetic iron oxide nanoparticles

5.1.4 Zeta potential

The surface charge of the unmodified and modified iron oxide nanoparticles was analysed by zeta potential measurements with a nano Zetasizer as shown in Figure 5.12.

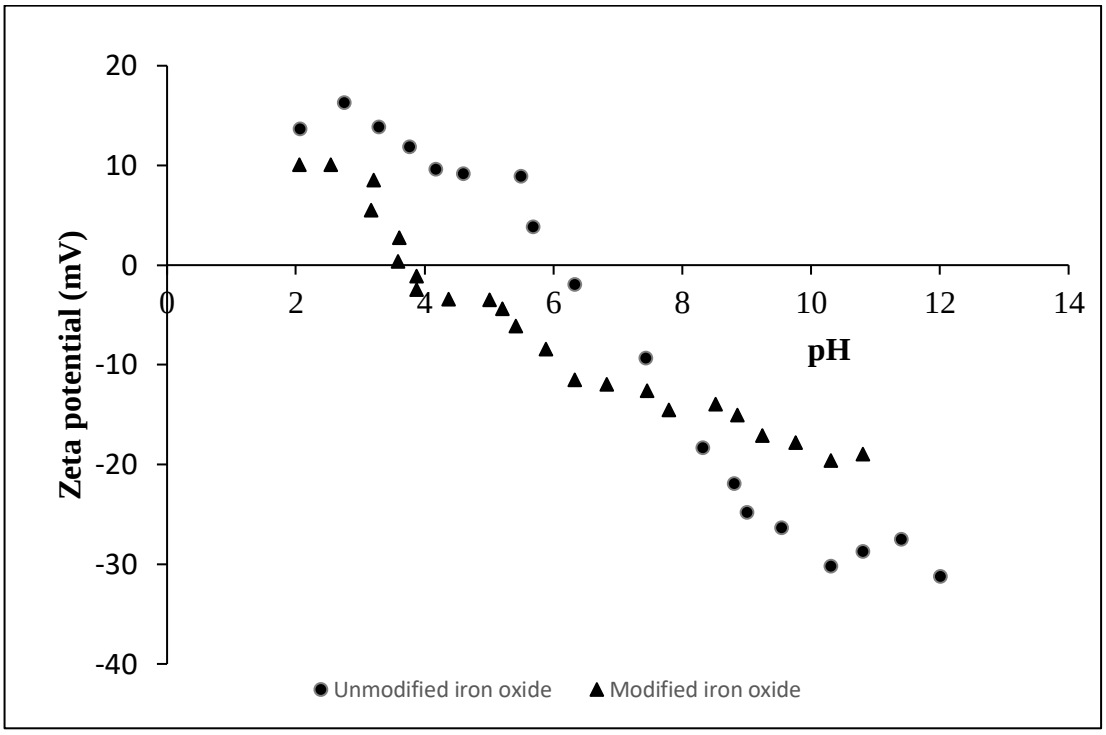

Figure 5.12: Zeta potential trends for unmodified and modified magnetic iron oxide nanoparticles

5.2 Turbidity removal using unmodified as well as modified nanoparticles

The turbidity of the modified MNPs powder-kaolin suspensions was monitored by the transmittance (T) at wavelengths 360, 450, 540, and 600 nm using the UV-Vis spectrophotometer as shown in Figure 5.13. The wavelength of 360 nm was more sensitive since its peak in absorbance is higher compared to the other wavelengths (450, 540 and 600 nm) and was therefore used for the rest of the turbidity measurements as shown in Figure 5.14. The results in Figure 5.14 as well as Tables 5.7 and 5.8 show the effect of dosage in the range of 0.0054 g to 0.1067 g for

unmodified and modified magnetic iron oxide nanoparticles used for turbidity removal measurements from synthetic kaolin turbid water at 360 nm wavelength. Effect of pH on turbidity removal using 0.005 g of unmodified and modified magnetic iron oxide nanoparticles was analysed as shownn in Figure 5.15.

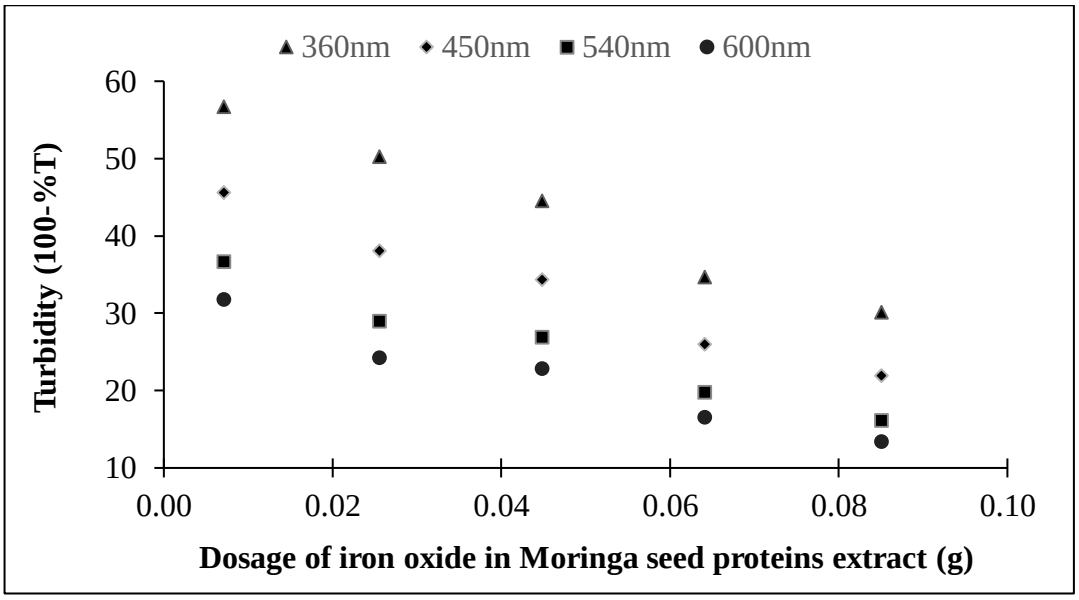

Figure 5.13: Turbidity (100-%T) using magnetic iron oxide nanoparticles modified with Moringa seed proteins extract at wavelengths 360, 450, 540 and 600 nm

Table 5.7: Turbidity removal using magnetic iron oxide nanoparticles modified with *M. oleifera* seed proteins extract at wavelength 360 nm

Dosage (g)	**Turbidity (100-%T) 360 nm**	**%Turbidity removal**
0.0	72.3	0
0.0055	48.2	33.3
0.0238	28.6	60.4
0.0491	27.0	62.7
0.0647	17.4	75.9
0.0854	29.5	59.2
0.1067	27.0	62.7

Table 5.8: Turbidity removal using magnetic iron oxide nanoparticles unmodified with *M. oleifera* seed proteins extract at wavelength 360 nm

Dosage (g)	Turbidity (100-%T) 360nm	%Turbidity removal
0.0	72.3	0
0.0054	39.3	45.6
0.0261	38.4	46.9
0.0419	26.5	63.3
0.0652	28.7	60.3
0.0889	26.2	63.8
0.1053	25.1	65.3

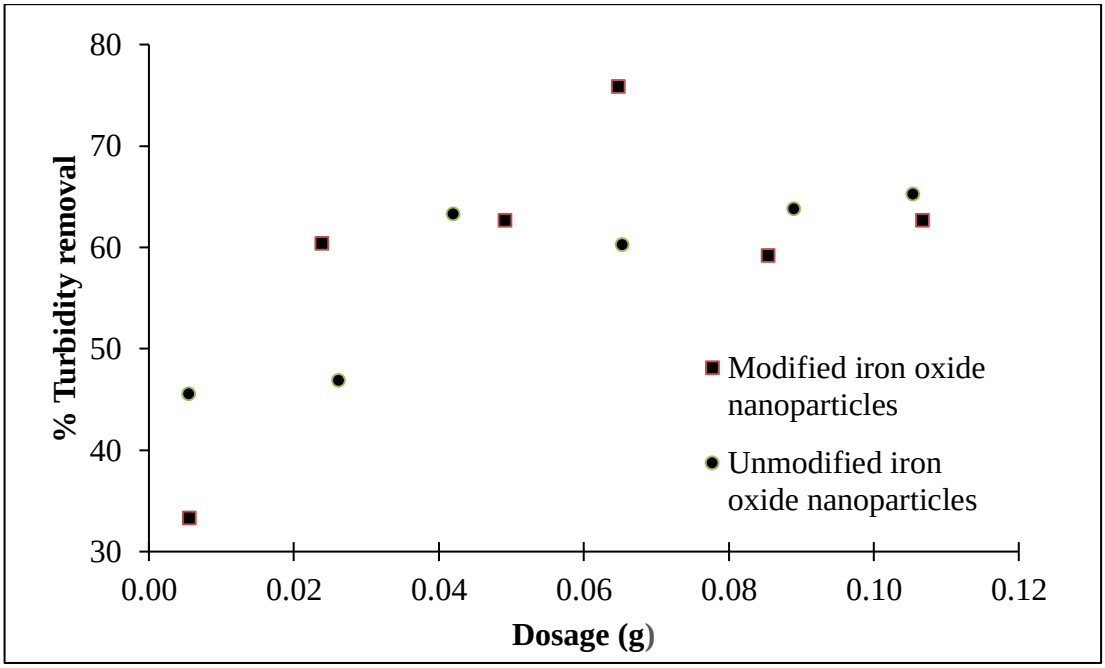

Figure 5.14: Graph showing the effect of dosage on turbidity removal using magnetic iron oxide nanoparticles modified and unmodified with Moringa seed proteins extract at wavelength 360 nm

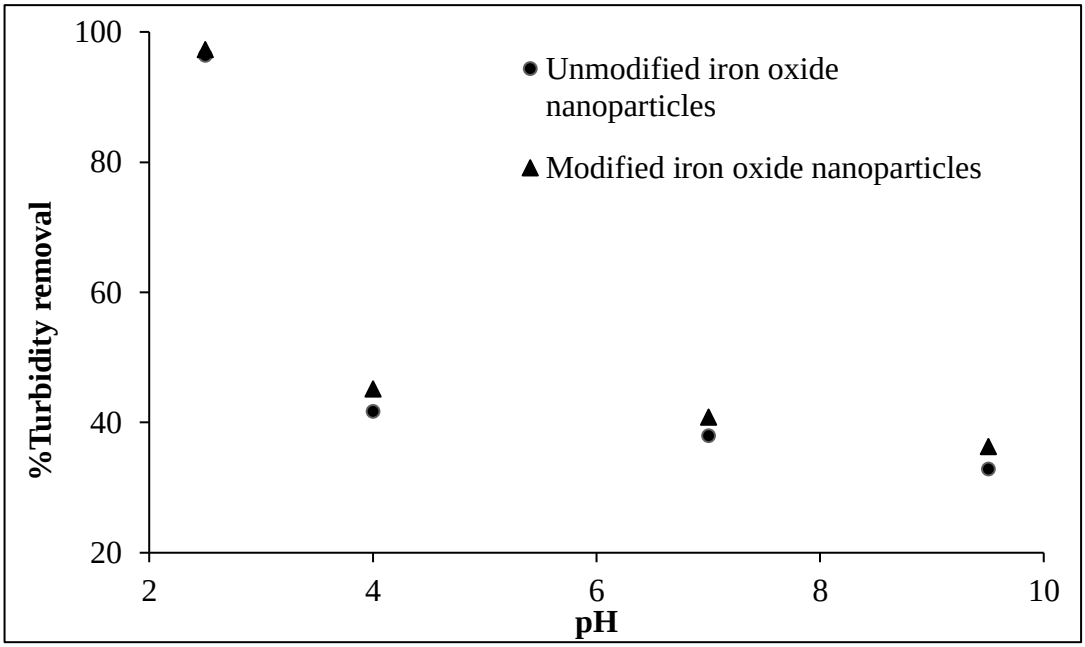

Figure 5.15: Effect of pH on turbidity removal using 0.005 g of unmodified and modified magnetic iron oxide nanoparticles

5.3 Recovery of precious metal ions using modified and unmodified nanoparticles

5.3.1 Recovery using modified and unmodified nanoparticles at different pH values

The percentage recovery of palladium, platinum and gold, precious metal ions using modified and unmodified nanoparticles were measured using ICP-OES as summarized in Figures 5.16-5.18. This was conducted at several pH values.

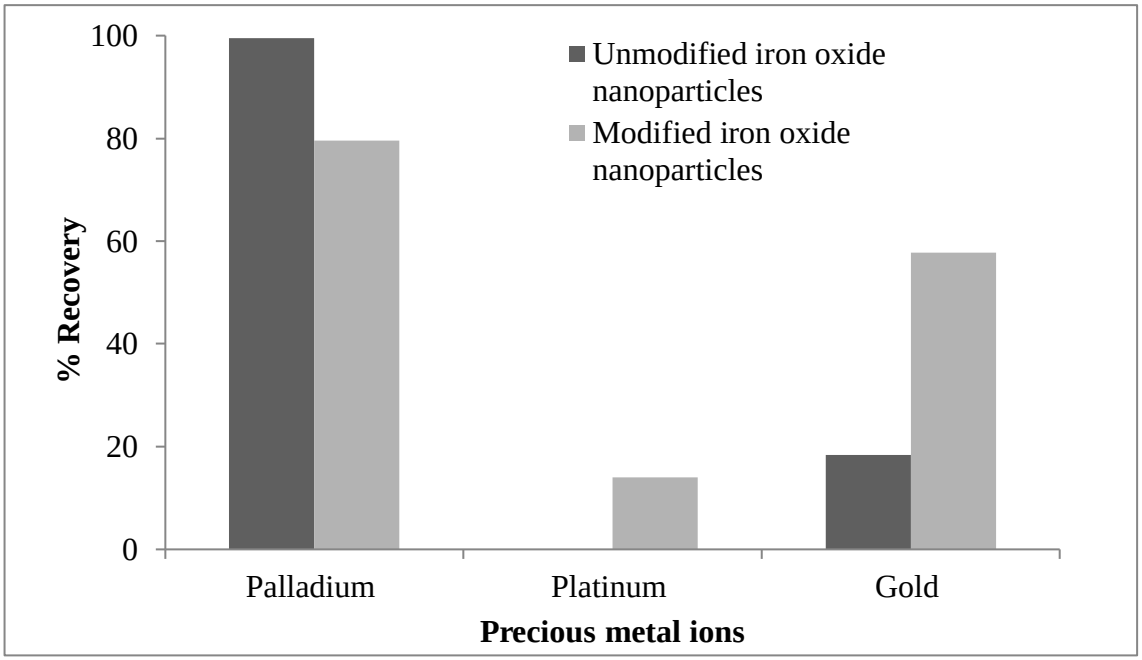

Figure 5.16: Recovery of precious metal ions at 100 mg/L using 0.065 g of unmodified and modified iron oxide nanoparticles at pH 2.0 for palladium and 3.0 for both gold and platinum

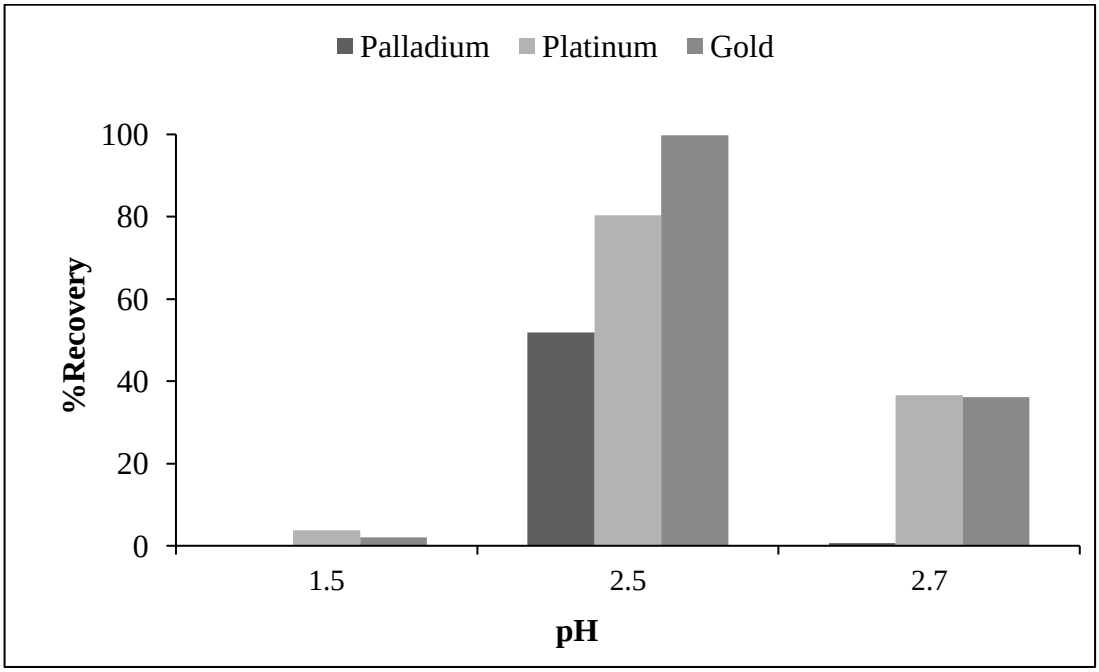

Figure 5.17: Recovery of precious metal ions at 10 mg/L using 0.065 g unmodified iron oxide nanoparticles at different pH values

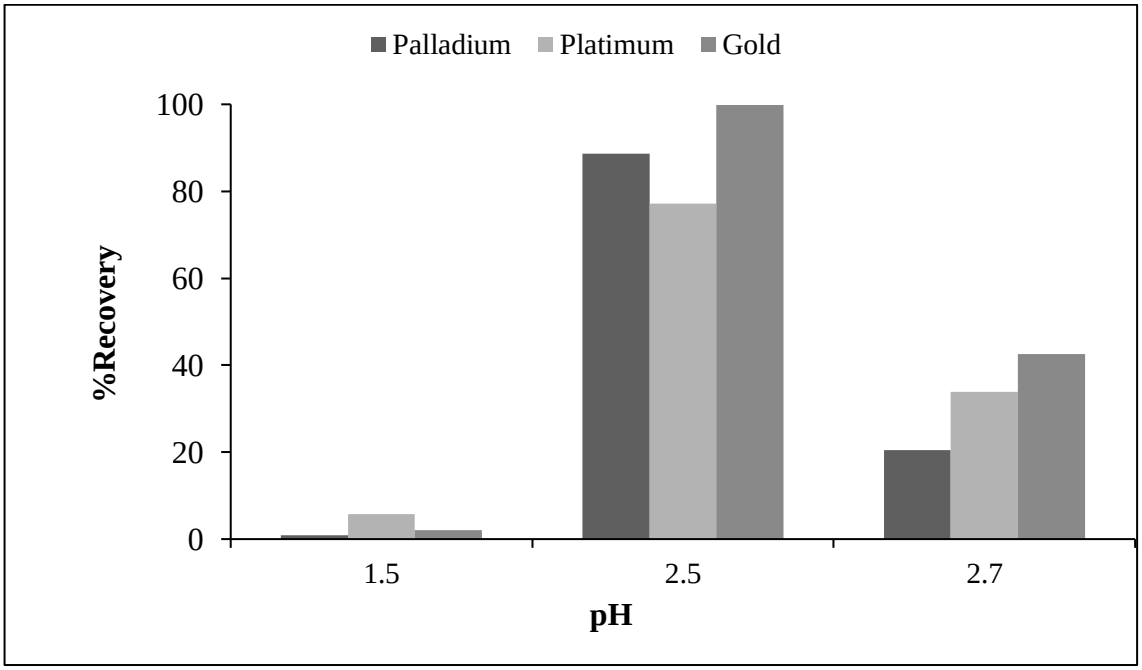

Figure 5.18: Recovery of precious metal ions at 10 mg/L using 0.065 g modified iron oxide nanoparticles at different pH values

5.3.2 Recovery of precious metal ions using modified and unmodified nanoparticles at different dosages

The percentage recoveries of palladium, platinum, and gold, precious metal ions with modified and unmodified nanoparticles at 10 g/mL using different dosages in the range of 0.005 g to 0.0085 g are summarized in Figures 5.19 and 5.20. Characterization of precious metals ions loaded unmodified magnetic iron oxide and modified magnetic iron oxide nanoparticles were observed in the wavelength range 4000 - 400 cm^{-1} as summarized in Tables 5.9 and 5.10. These confirm the functional groups responsible for recovery of precious metal ions.

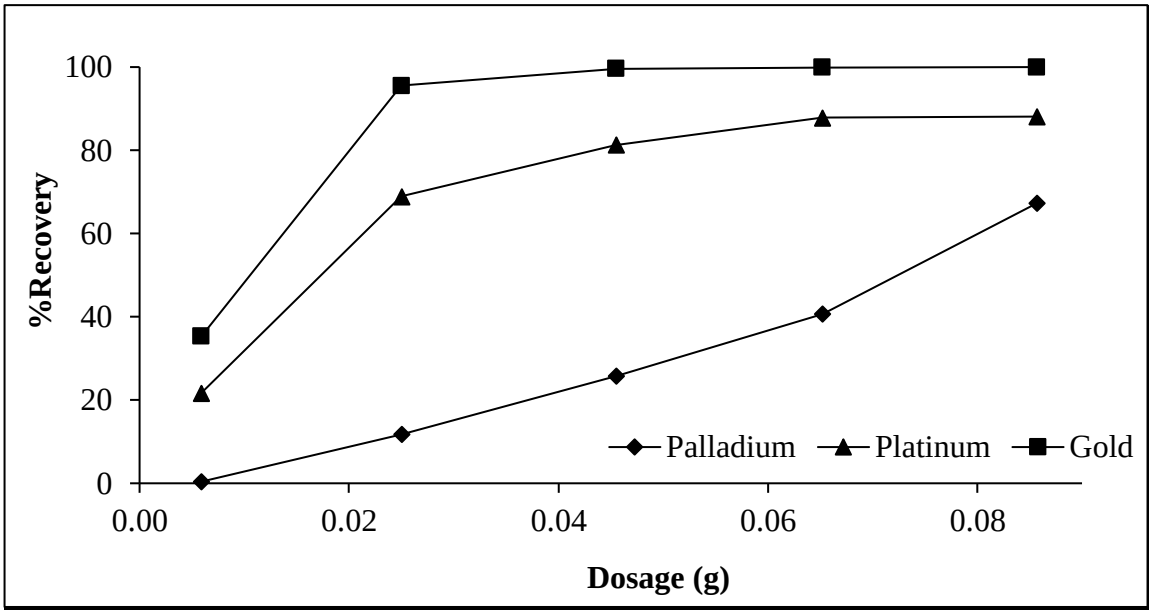

Figure 5.19: Recovery of precious metal ions at 10 mg/L using different dosages of unmodified nanoparticles

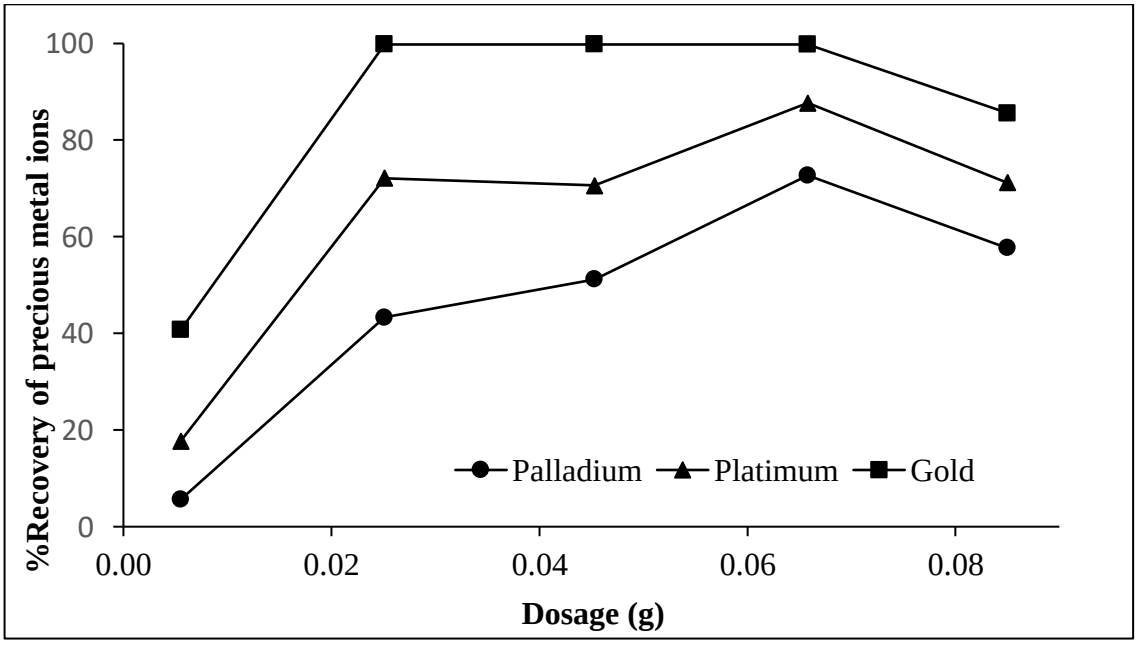

Figure 5.20: Recovery of precious metal ions at 10 mg/L using different dosages of modified nanoparticles

Table 5.9: Analysis of the IR spectra for unmodified magnetic iron oxide nanoparticles and precious metals ions loaded unmodified magnetic iron oxide nanoparticles

Functional group	**Reference frequency range (cm^{-1})[42,47,49, 51,78,81,82,83]**	**Observed IR frequency (cm^{-1}) for iron oxide**	**Observed IR frequency (cm^{-1}) for precious metals ions loaded iron oxide**	**Peak shift (cm^{-1})**
OH stretching	3700-3500	3676.9	3692	-15.1
OH (Alcohol)	3400-2400	2983; 2824.4	2987; 2828.4	-4
OH stretching vibration	1092-1060	1033.04	1033	0.04
CO stretching (Alcohol)	1260-1000	1033.04	1033	0.04
Fe-O	588-535	560.57	552.64	7.93

Table 5.10: Analysis of the IR spectra for magnetic iron oxide nanoparticles modified with Moringa seed proteins extract and precious metals loaded magnetic iron oxide nanoparticles modified with Moringa seed proteins

Functional group	**Reference frequency range (cm^{-1}) [42,47,49,51, 78,81,82,83]**	**Observed IR frequency (cm^{-1}) for $MoFe_3O_4$**	**Observed IR frequency (cm^{-1}) for precious metals ions loaded $MoFe_3O_4$**	**Peak shift (cm^{-1})**
NH (Amine / Amide) stretching; OH stretching	3700-3500	3684.8	3680.8	4
Carbonyl and Amides (C=O and N-H)	2000-1500	1567.6	1516	51.6
OH (Alcohol; Carboxylic acid)	3400-2400	2983; 2880	2987; 2876	-4; 4
OH stretching vibration	1092-1060	1033.04	1033	0.04
CO stretching (Carboxylic acid)	1320-1210	1349.6	1341.6	8
CO stretching (Alcohol)	1260-1000	1033.04	1033	0.04
Fe-O	588-535	580.57	552.64	27.93

5.3.3 Effect of agitation time on recovery of precious metal ions using modified and unmodified nanoparticles

The effect of agitation time between 30 – 240 minutes on percentage recoveries of palladium, platinum, and gold, precious metal ions with modified and unmodified are summarized in Figures 5.21 and 5.22.

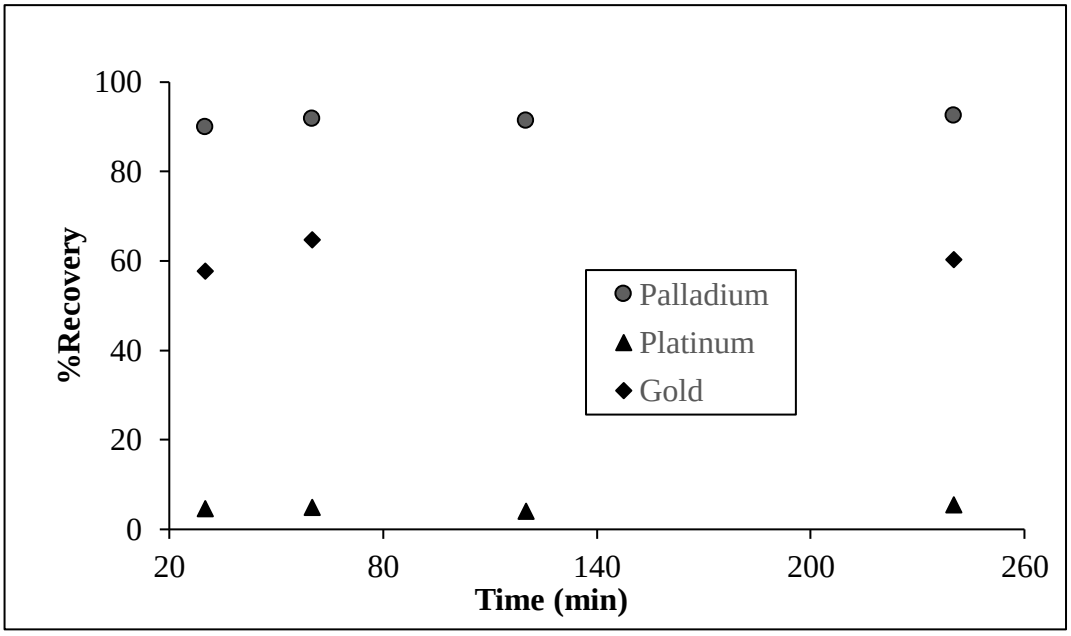

Figure 5.21: Effect of agitation time on recovery of precious metal ions using unmodified nanoparticles between 30 – 240 minutes

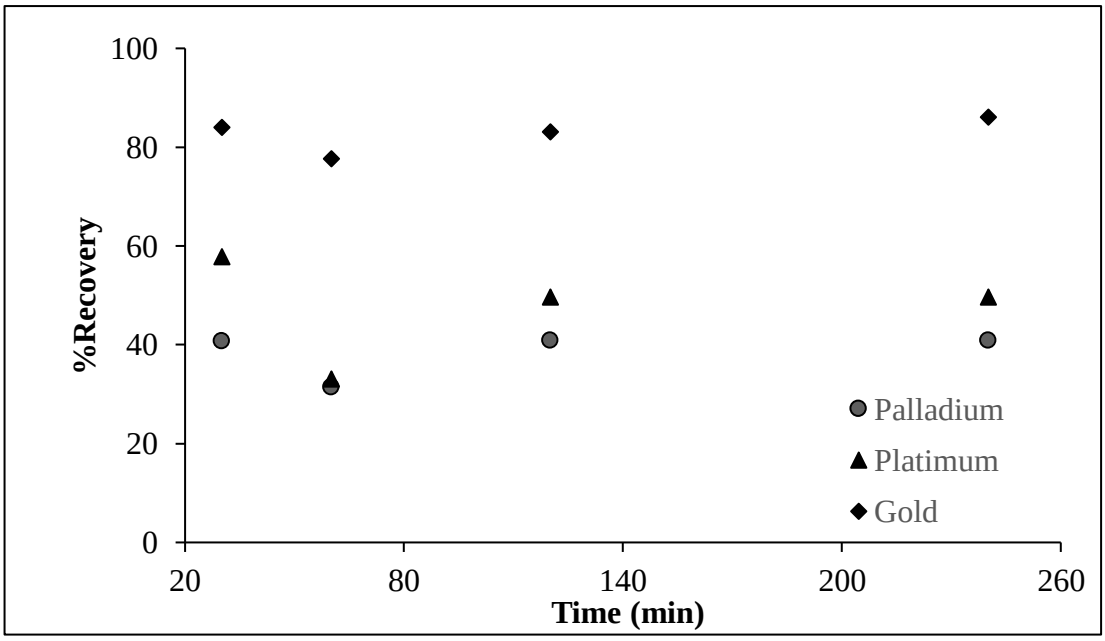

Figure 5.22: Effect of agitation time on recovery of precious metal ions using modified nanoparticles between 30– 240 minutes

5.3.4 Effect of initial concentration on recovery of precious metal ions using modified and unmodified nanoparticles

Figures 5.23 and 5.24 summarizes the effect of initial concentration in the range 10 – 100 mg/L on percentage recoveries of palladium, platinum, and gold, precious metal ions with modified and unmodified nanoparticles.

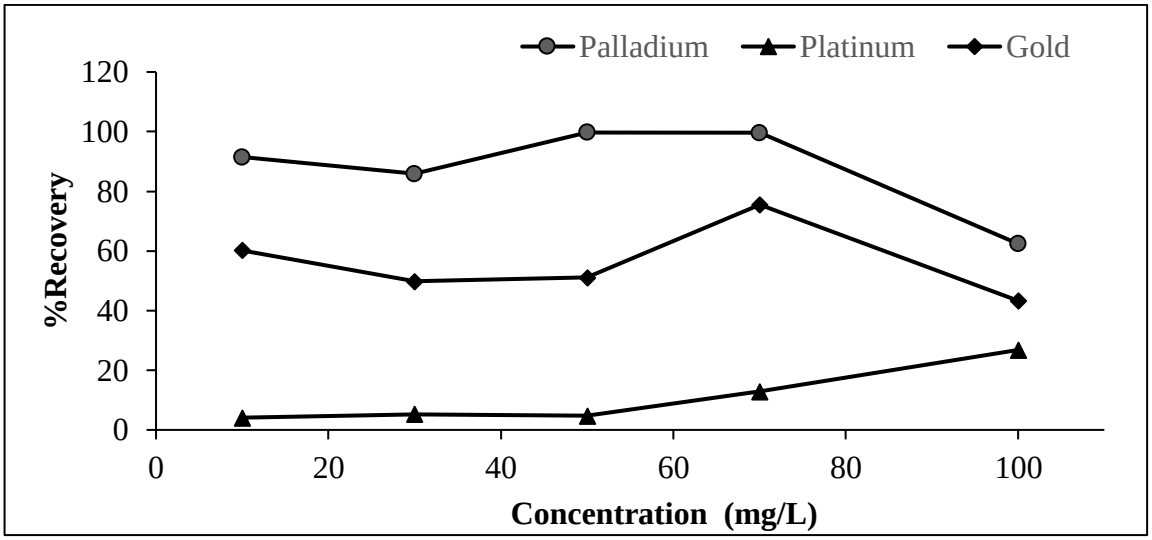

Figure 5.23: Effect of initial concentration on the recovery of precious metal ions using unmodified nanoparticles at 10 – 100 mg/L

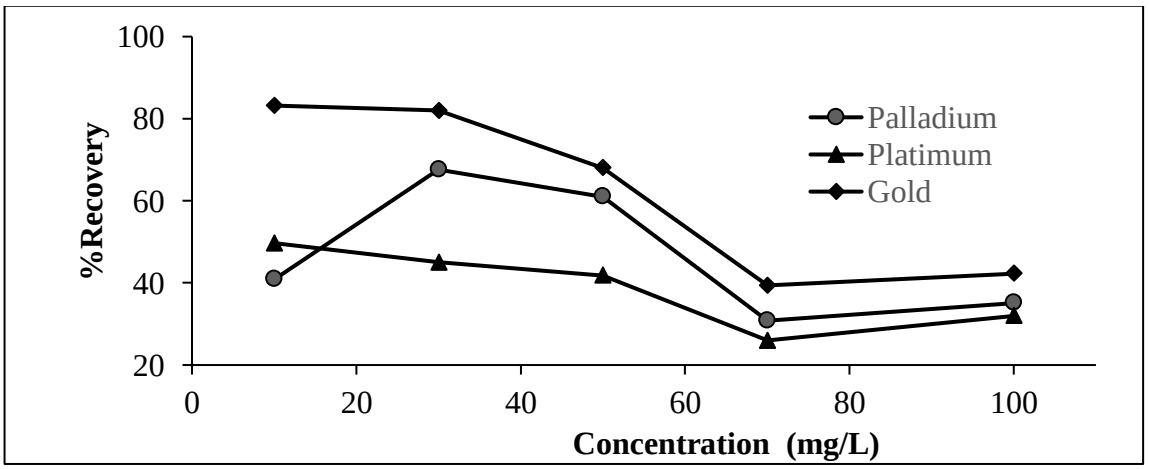

Figure 5.24: Effect of initial concentration on the recovery of precious metal ions using modified nanoparticles at 10 – 100 mg/L

5.4 Langmuir and Freundlich adsorption isotherms

The data were fitted to the Langmuir and Fleundlich models as indicated in Figures 5.25-5.26 and Tables 5.11-5.14. Langmuir model is a theoretical treatment representing nonlinear adsorption involving monolayer adsorption whereas Fleundlich is an empirical treatment that involves a multilayer adsorption [47,78,79].

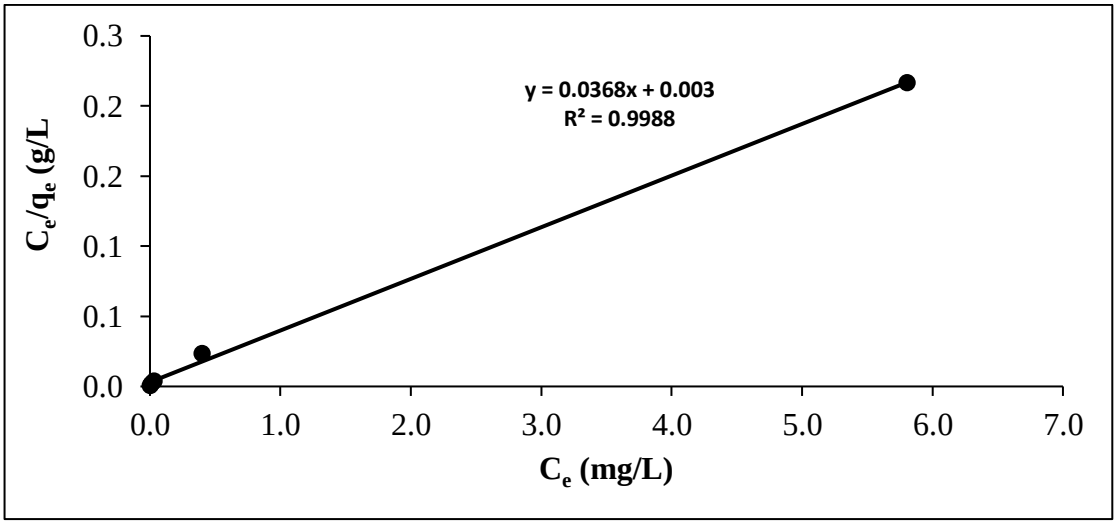

Figure 5.25: A typical linear Langmuir isotherm for adsorption of gold (III) on unmodified iron oxide nanoparticles

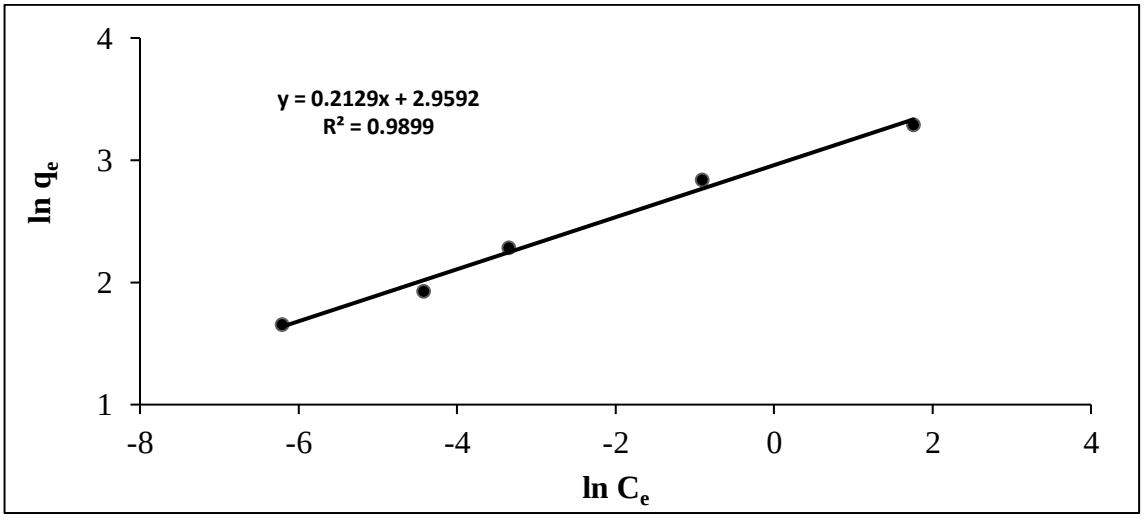

Figure 5.26: A typical linear Freundlich isotherm for adsorption of gold (III) on unmodified iron oxide nanoparticles

Table 5.11: Langmuir isotherm constants for the adsorption of precious metal ions on unmodified iron oxide nanoparticles

Precious metal ion	**Platinum (IV)**	**Palladium (II)**	**Gold (III)**
Slope ($1/q_m$) g/mg	0.0336	3.2564	0.0368
Intercept ($1/q_mb$) g/L	0.1523	-14.333	0.003
R^2	0.9253	0.4668	0.9988
q_m (mg/g)	29.76	0.307	27.17
b (L/mg)	0.221	-0.227	12.27
R_L	0.310	-0.867	0.0090

Table 5.12: Langmuir isotherm constants for the adsorption of precious metal ions on modified iron oxide nanoparticles

Precious metal ion	**Platinum (IV)**	**Palladium (II)**	**Gold (III)**
Slope ($1/q_m$), g/mg	0.0346	0.1896	0.0293
Intercept ($1/q_mb$), g/L	0.2651	0.0553	0.0511
R^2	0.1883	0.6826	0.2737
q_m (mg/g)	28.90	5.27	34.48
b (L/mg)	0.131	3.43	0.573
R_L	0.432	0.298	0.660

Table 5.13: Freundlich isotherm constants for the adsorption of precious metal ions on unmodified iron oxide nanoparticles

Precious metal ion	**Platinum (IV)**	**Palladium (II)**	**Gold (III)**
Slope (1/n)	0.6304	-1.4912	0.2129
Intercept ($\ln K_f$)	1.7259	3.3547	2.9592
R^2	0.9128	0.4464	0.9899
K_f (mg/mg)	5.62	28.64	19.28
n (L/mg)	1.59	-0.671	4.70

Table 5.14: Freundlich isotherm constants for the adsorption of precious metal ions on modified iron oxide nanoparticles

Precious metal ion	**Platinum (IV)**	**Palladium (II)**	**Gold (III)**
Slope (1/n)	0.4704	0.0997	0.0777
Intercept ($\ln K_f$)	1.6521	1.481	2.5736
R^2	0.3225	0.0184	0.0724
K_f (mg/mg)	5.22	4.40	13.11
n (L/mg)	2.13	10.03	12.87

CHAPTER 6: DISCUSSION

6.1 Characterisation of magnetic iron oxide nanoparticles modified and unmodified with Moringa seed proteins extracts

6.1.1 Fourier transform infrared (FTIR) spectrometry

The infrared spectra shown in Figures 5.1-5.2 and summarized in Table 5.1 are typical for *M. oleifera* seed protein extract. As reflected, there seems to be no significant difference between the unpurified and purified Moringa seed proteins extract. However, minimal intensities differences at various wavenumber could be observed.

According to a study by Araujo et al. [42] and the results shown in Figure 5.2, a band at 3281.9 cm^{-1} representing the OH might be due to proteins and fatty acids structures in Moringa seeds. The study further indicates that both the symmetrical as well as asymmetrical stretching of C-H bond from the -CH_2 group as well as OH (alcohol, carboxylic acid) occur at 2942.6 cm^{-1} wavenumber. Also, the frequencies 1648.4 cm^{-1} for Amide I and 1544 cm^{-1} for Amide II are also among the characteristics bands depicted in the spectrum. Another study by Nermark [36] reveals that these amides mainly come from the amide bonds connecting amino acids. The study further confirms that absorption at amide I and II result in C=O bond stretching vibrations and N-H bond bending vibrations respectively, and they are mainly assigned to the α-helix of the secondary structure in a protein. This is a further confirmation of the protein structure in the Moringa seeds.

As shown in Figure 5.3 as well as the corresponding Table 5.2, the infrared spectrum obtained with the FTIR is typical of iron oxide nanoparticles. The absorption band at

3668.3 cm^{-1} corresponds to the hydroxyl functional group; the one at 1442.3 cm^{-1} is assigned to H-O-H and the Fe-O group at 564.95 cm^{-1} [49]. Figures 5.3-5.4 and the summary in Tables 5.2-5.3 show the IR spectra with functional groups responsible for adsorption in magnetic iron oxide nanoparticles modified and unmodified with Moringa seed proteins extract. They occur at the peak ranges of 3700-3500 cm^{-1}, 3400-2400 cm^{-1}, 1320-1210 cm^{-1}, 1260-1000 cm^{-1}, ~890 cm^{-1} and 588-535 cm^{-1} that correspond to NH (amine /amide) groups, OH (alcohol/carboxylic) groups, CO (carboxylic) groups, CO (alcohol) groups, alkenes (CH) groups and Fe-O (iron oxide) groups [42,47,49,51,77,80,81,82]. Most of these groups were also obtained for *Plantago ovata* seeds [83], *M. oleifera* seed pods and *Sclerocarya birrea* [77]. The functional groups identified may, therefore, be responsible for turbidity removal from water and the recovery of precious metal ions.

FTIR spectra in Figures 5.5-5.7 and Tables 5.4-5.6 further confirm that *M. oleifera* seed protein is effective in a wide range of pH values. According to Obuseng e*t al.* [63], the isoelectric point of the Moringa seed proteins is about pH 10-11. This implies that below 10-11 the proteins are positively charged and interact with magnetic iron oxide nanoparticles that are negatively charged at pH above neutral range forming a nanocomposite for water turbidity removal. However, amino acids functional groups -COOH in for instance aspartic and glutamic acids, found in Moringa seed proteins have pI values of 3 or less [35]. This means that above pH 3, the groups are negatively charged and can interact with magnetic iron oxide nanoparticles which are positively charged at pH below neutral range therefore forming a nano-composite for selectively recovery of precious metal ions [12,59]. It is therefore against this background that

iron oxide nanoparticles modified with Moringa seed proteins functional groups are still able to have active peaks in acidic, neutral and basic environments.

6.1.2 Thermogravimetric Analyzer (TGA)

Thermal stability of unmodified and modified magnetic iron oxide nanoparticles was studied with Perkin Elmer Thermogravimetric analyzer as shown in Figures 5.8-5.10. The percentage weight loss and their respective derivatives weight loss percentage per °C (Figures 5.9-5.10) were obtained when the unmodified and modified magnetic iron oxide nanoparticles were heated from 30.81ºC to 794.77ºC and 30.86ºC to 794.80ºC, respectively. In both cases, the weight loss decreased at a slow rate with overall weight loss of 17.7% and 17.2% for unmodified and modified magnetic iron oxide nanoparticles, respectively. This suggest that modified magnetic iron oxide nanoparticles might be slightly stable than unmodified magnetic iron oxide nanoparticles since the curve for the modified magnetic iron oxide nanoparticles appears slightly on top and the weight loss percentage is slightlty lower (Figure 5.8). However, the inconsistency in the percentages loss values between 100-350°C for modified magnetic iron oxide nanoparticles might be associated with the proteins amino acid residues with various functional groups [42]. A study by Sneha and Sundaram [84] attained a similar weight loss of approximately 17% on uncoated Fe_3O_4 which is very close to 17.7% obtained for unmodified magnetic iron oxide nanoparticles in the current study. This study prepared and characterized iron oxide – hydroxyapatite nanocomposite for potential bone cancer therapy.

Padmavathy et al. [47] on the effect of pH on efficiency and Cr(IV) ion uptake from wastewater using iron oxide nanoparticles obtained a similar curve for magnetite

nanoparticles as in the current study. Another study by Araujo *et al.* [42] on characterization and use of *M. oleifera* seeds as a biosorbent for removing metal ions from aqueous effluents also obtained a similar mass loss curve. This study describes the mass loss in several stages depending on temperature ranges as follows: The first stage referred to as the water desorption or water loss process occurs during the initial stage of decomposition (30ºC to 128ºC); the second stage is organic matter loss (128ºC to 268ºC), and the last stage is decomposition of compounds with higher boiling points (268ºC to 898ºC). At the end of the decomposition stage (898ºC), total residue mainly made up of ash as well as inorganic oxides compounds is obtained. Figures 5.9 and 5.10 in the current study also show similar mass loss stages in the following temperature ranges: Stage one of water loss (30ºC to 100ºC); stage two of organic matter loss (100ºC to 350ºC); stage three that decomposes compounds with higher boiling points (350ºC to 795ºC). Total residue was therefore obtained at the end of decomposition stage (795ºC).

6.1.3 Scanning Electron Microscope (SEM)

Scanning Electron Microscope was used to study the morphological characteristics of the synthesized unmodified (left) and modified (right) magnetic iron oxide nanoparticles. This, in turn, assesses the profile of the nanoparticles responsible for turbidity removal and adsorption of the precious metal ions. As shown in Figure 5.9, the scanning electron micrographs are porous with varying pore sizes thus able to remove turbidity from waste water and adsorb the precious metal ions [42,77]. The porosity for the modified magnetic iron oxide nanoparticles has improved compared to the unmodified magnetic iron oxide nanoparticles. This may therefore explain the difference in the adsorption capacity as well as recovery of precious metal ions using

these adsorbents. As also shown, the nanoparticles seems to have agglomerated and this could be attributed to strong bonding of nanoparticles, magnetic dipoles as well as Van der Wall forces [51,68].

6.1.4 Zeta potential

As shown in Figure 5.12, zeta potential of unmodified and modified iron oxide nanoparticles was studied at pH range between 2 to 12 to measure the surface charge. The curves show that the surface charges are highly dependent on pH. The point of zero charges (isoelectric points) are around pH 6.12 and 3.69 for unmodified and modified magnetic iron oxide nanoparticles respectively. The surfaces are positively charged at lower pH range below the isoelectric points of the nanoparticles and negatively charged at higher pH range above the isoelectric points of the nanoparticles. Similar studies on the characterization of magnetic iron oxide by Aghaei *et al.* [12] and Yang *et al*. [59] obtained isoelectric points in the pH range of 6-7 as well. In the current study, the surface charge values obtained therefore explain the dependency of adsorption on pH and also the difference in turbidity removal as well as recovery of precious metal ions using these adsorbents.

6.2 Turbidity removal using modified and unmodified nanoparticles

Dosages range of 0.0071 g to 0.0850 g for unmodified and modified magnetic iron oxide nanoparticles were used for turbidity removal measurements from synthetic kaolin turbid water at wavelengths 360, 450, 540 and 600 nm. The turbidity measurements in this visible spectrum shown in Figure 5.13 show similar trends at every wavelength used. However, the shortest wavelength of 360 nm was more sensitive since its peak in absorbance is higher at the dosages used compared to the

other wavelengths. Similar results were obtained for protein/surfactants turbidity measurements by Kwaambwa and Rennie [35].

The results in Figure 5.14 as well as Tables 5.7-5.8 show the effect of dosage in the range of 0.0054 g to 0.1067 g for unmodified and modified magnetic iron oxide nanoparticles used for turbidity removal measurements from synthetic kaolin turbid water at 360 nm wavelength. The initial turbidity (100-%T) was 72.3 (Tables 5.7-5.8). For unmodified magnetic iron oxide nanoparticles, the turbidity level decreased as the dosage increased whereas turbidity removal, expressed as a percentage, increased with values of 45.6, 46.9, 63.3, 60.3, 63.8 and 65.3 with the increase in dosage. Similarly, for modified magnetic iron oxide nanoparticles, turbidity level decreased when dosage increased but reached the optimum level at the dosage of approximately 0.0647 g and then started slightly increasing again then decreasing when dosage increased. The same trend but in the opposite direction was followed for the turbidity removal whereby turbidity removal increased when dosage increased with percentages of 33.3, 60.4 and 62.7 reached the optimum level (75.9%) at the same dosage and then started slightly decreasing (59.2%) then increasing again (62.7%) when dosage increased.

A similar study conducted by Santos *et al.* [29] reported that coagulant combination of Moringa seed extract and an inorganic compound (iron oxide nanoparticles) yielded better physicochemical parameter (turbidity, colour, and compounds with UV254 absorption) removal efficiency thus a good option for water treatment. According to this study, coagulant combination under the influence of the magnetic field could effectively remove 90%, 85% and 50% of the surface water turbidity, colour as well as compounds with UV254 absorption, respectively. Therefore, the results obtained in

the current study have demonstrated that modified magnetic iron oxide was more efficient in turbidity removal compared to unmodified magnetic iron oxide since 75.9% highest turbidity removal at 0.0647 g for modified magnetic iron oxide was greater than 60.3% turbidity removal at almost the same mass of 0.0652 g for unmodified magnetic iron oxide.

A study on the treatment of waste water by coagulation and flocculation using biomaterials by Muruganandam *et al.* [85] reported that adsorption followed by neutralization are responsible for turbid removal. According to the study, at the optimal pH value, turbidity removal increase with an increase in dosage until an optimal dosage is reached. Afterwards, an increase in dosage simply increases turbidity as adsorbents get added since no neutralization between the adsorbent and colloidal particles in turbid water takes place anymore to form into new flocs. Similar results were obtained in the current study (Figure 14 and Tables 5.7-5.8).

Figure 5.15 shows the effect of pH in the range of 2.5 to 9.5 on turbidity removal using modified and unmodified magnetic iron oxide nanoparticles at a dosage of 0.005g. Modified magnetic iron oxide nanoparticles yielded the highest percentage removal of 97.3% at pH 2.5 compared to 96.4% obtained with unmodified magnetic iron oxide nanoparticles at the same pH. This pH was also optimal since the percentage turbidity removal obtained was higher compared to pH 4.0, 7.0 and 9.5 for both unmodified and modified iron oxide nanoparticles. The current study, therefore, agrees with a study by Muruganandam *et al.* [85] that demonstrated that turbidity removal is pH dependent.

6.3 Recovery of precious metal ions using modified and unmodified nanoparticles

6.3.1 Recovery of precious metal ions using modified and unmodified nanoparticles at different pH values

Recovery of precious metals ions from contaminated water is mainly pH dependent [5,45,47,60,61,62]. Therefore, adsorption studies in the current study were conducted at various pH values. In the present study, chloride salts of the precious metals palladium and platinum were used and palladium (II) chloride ($PdCl_2$) could hardly dissolve in water thus acidifying the solution with HCl was suitable due to the metal's affinity for acid and hence make it soluble.

In Figure 5.16, the efficiency of using unmodified magnetic iron oxide nanoparticles has shown to be better than using modified magnetic iron oxide nanoparticles for palladium ion. This was different for platinum and gold ions that showed the opposite results. Unmodified magnetic iron oxide nanoparticles recovered 99.5% Pd, 18.4% Pt and hardly anything for Au ions whereas modified magnetic iron oxide nanoparticles recovered 79.6% Pd, 57.7% Au and 18.1% Pt ions. The pH for palladium solution was 2.0 compared to platinum and gold solutions with pH 3.0 each. The difference in the percentage recovery obtained could, therefore, be attributed to the difference in the initial solution pH values.

Figures 5.17 and 5.18 show the effect of pH in the range of 1.5 to 2.7 on recovery of precious metal ions at 10 mg/L using 0.065g unmodified and modified magnetic iron oxide nanoparticle. This range was utilized since a study on the effect of pH on efficiency and Cr(IV) ion uptake from wastewater using iron oxide nanoparticles by Padmavathy *et al.* [47] reported that removal efficiency increased with a decrease in

pH. This is because the iron oxide nanoparticles surface tends to become highly negatively charged with higher pH. This, in turn, results in higher repulsions between iron oxide nanoparticles and the metal ion and thus preventing the interaction between the nanoparticles and the metal ion. Similar results were obtained on adsorptive removal of Cr(IV) by green Moringa tea leaves biomass from aqueous solution [79]. Also, a study on adsorption of platinum and palladium from aqueous solution using grape stalk waste reported that pH 1.5 was optimal [61]. According to this study, the adsorption capacity decreases as the pH rises. This might be because at a high pH; the metal ions tend to be less absorbable because of declining chloride anions from the metal salts.

Furthermore, another study by Ilankoon [45] confirmed that optimum pH for Cr(IV) ions removal from aqueous solutions range between 2-3. The reason behind this is mainly that at a higher pH range, the Cr(IV) is in the form of CrO_2^{4-}, highly negatively charged whereas at the low pH the ions are in the form of $HCrO_4^-$. According to this study, the mechanisms playing a role are mainly electrostatic attractions, redox, ion exchange, and surface complexation, respectively.

At pH 2.7, modified magnetic iron oxide nanoparticles have shown to be efficient than unmodified magnetic iron oxide nanoparticles in recovering Pd and Au ions. The recovery was, however, the same for Pt ion. Modified magnetic iron oxide nanoparticles recovered 42.5% Au, 33.9% Pt and 20.5% Pd. On the other hand, percentage recovery for Au, Pt and Pd were 36.2%, 33.9% and 0.7%, respectively, using unmodified magnetic iron oxide nanoparticles. Almost a similar trend was obtained at pH 1.5, but the recovery was almost the same for the gold ion. Modified

magnetic iron oxide nanoparticles recovered 2.1% Au, 5.7% Pt and 0.9% Pd. Percentage recovery for Au, Pt and Pd were 2.1%, 3.8% and 0%, respectively, using unmodified magnetic iron oxide nanoparticles. At pH 2.5, a similar trend was again obtained using modified magnetic iron oxide nanoparticles whereby the percentage recoveries were 99.8, 88.6 and 77.2 for Au, Pt and Pd, respectively. This is different for unmodified magnetic iron oxide nanoparticles whereby 99.8% Au, 51.8% Pd and 80.4% Pt were recovered. However, the lower recovery at pH 1.5 which is below the optimal pH of 2.5 might be due to the competition between positively charged hydrogen and precious metal ions [63].

As shown in Figures 5.17 and 5.18, precious metals ions (gold, palladium and platinum) in the present study were recovered with high efficiency at pH 2.5. The same precious metals as in the present study were recovered with high efficiency at pH 2.5 using *Galdieria sulphuraria* [60]. This study agrees with the findings by Silva *et al.* [62] that these precious metals could be selectively recovered at the pH range of 2.5 – 3.0 using sericin/alginate and sericin/alginate/PEG (polyethylene glycol diglycidyl ether) biosorbents. Radius size, as well as electronegativity of precious metals ions under study, may explain differences in percentage recoveries [86]. Ionic radii in picometers (pm) for Au, Pd and Pt are 85.0, 86.0 and 62.5 respectively whereas electronegativity (Pauling) for Au, Pd and Pt are 2.54, 2.20 and 2.28 respectively [87]. This implies that recovery of precious metal ion with a larger ionic radius as well as high electronegativity value might be higher compared to the one with small ionic radius and low electronegativity value. However, at the optimal pH of 2.5 in the present study gold (III) ion showed a higher adsorption capacity onto the modified magnetic iron oxide nanoparticles compared to palladium (II) ion with a slightly larger

ionic radius. On the other hand, palladium (II) ion showed a higher adsorption capacity onto the modified magnetic iron oxide nanoparticles compared to platinum (IV) ion with a slightly higher electronegativity value. Therefore, other factors might play a vital role in the process of adsorption.

6.3.2 Recovery of precious metal ions using modified and unmodified nanoparticles at different dosages

The effects of modified and unmodified iron oxide nanoparticles for gold (III), palladium (II) and platinum (IV) at different dosages are shown in Figures 5.19 and 5.20. The dosages were varied from 0.005 g to 0.085 g, equilibrated for two hours with 10 mg/L.

For unmodified iron oxide nanoparticles (Figure 5.19) metals ions recovery increase with dosage. Gold (III) showed a higher recovery percentage of 100% followed by platinum with 88.1% and then palladium with 67.3%. On the other hand, for modified iron oxide nanoparticles (Figure 5.20) metals ions recovery increase with dosage until an optimal dosage of approximately 0.065g is reached. A similar trend as for unmodified iron oxide nanoparticles was obtained whereby the highest removal of 99.8% was obtained for Au followed by Pt with 87.7% and then Pd with 72.7%. This trend agrees with the study by Oke [87] that demonstrated that recovery of precious metal ions with high electronegativity value might be higher compared to the ones with low electronegativity values. According to the study, the electronegativity (Pauling) for Au (III), Pd (II) and Pt (IV) are 2.54, 2.28 and 2.20, respectively.

A study by Hariani *et al.* [88] revealed that a higher recovery percentage with increase in dosage is obtained as a result of the high availability of vacant active sites on the

surface of the adsorbent. This infers that higher availability of vacant active sites with increase in dosage on the surface of modified and unmodified magnetic iron oxide nanoparticles allow fast penetration of the precious metal ions thus resulting in higher percentage recoveries. This study agrees with the findings by Mavhungu *et al.* [61] that the increase in platinum and palladium recoveries with increase in grape stalk waste dosage is as a result of the increase in vacant active sites on the surface of this adsorbent. However, a study by Maina *et al.* [77] explained that an increase in the metal ions recoveries percentage with increase in the adsorbent dosage occurs only until an optimal adsorption level is reached. If the dosage is increased further beyond this level, the metal ions recoveries percentages are reduced due to the decrease in vacant active sites on the surface of the adsorbent.

On the other hand, Tables 5.9 and 5.10 analyses the IR spectra for precious metals ions loaded unmodified magnetic iron oxide and modified magnetic iron oxide nanoparticles. The peak shifts obtained at various wavenumber confirms functional groups responsible for recovery of precious metal ions. These are hydroxyl, carbonyl, amine/amide, carboxylic as well as iron oxide groups for unmodified magnetic iron oxide and modified magnetic iron oxide respectively [42,47,49,51, 78,80-82].

6.3.3 Effect of agitation time on recovery of precious metal ions using modified and unmodified nanoparticles

Figures 5.21 and 5.22 show the effect of agitation time between 30– 240 minutes on percentage recoveries of palladium, platinum, and gold, precious metal ions with modified and unmodified magnetic iron oxide nanoparticles at constant pH of 2.5, 10 mg/L initial concentration and 0.065 g dosage. As indicated, the percentage recovery

either increased or decreased in the first 120 minutes. After this period, the percentage recovery remains almost constant or just slightly raised. Attainment of equilibrium was, therefore, within 120 minutes. Padmavathy *et al.* [47] obtained a similar trend. Another study by Candice *et al.* [79] using Moringa leaves biomass as adsorbent for Cr(VI) also reached equilibrium within 120 minutes. According to this study, adsorption takes place because of available sites on the surface of the adsorbent. The rate of adsorption therefore depends on the availability of these vacant sites. The current study, therefore, used 120 minutes agitation time.

6.3.4 Effect of initial concentration on recovery of precious metal ions using modified and unmodified nanoparticles

Figures 5.23 and 5.24 show the effect of initial concentration in the range of 10 to 100 mg/L in the recovery of precious metals using unmodified and modified magnetic iron oxide nanoparticles. Other variables such as agitation time of two hours, pH at 2.5 and 0.065g dosage were kept constant. Percentage recovery with unmodified magnetic iron oxide nanoparticles, varied from 91.4 to 62.4% for palladium, 4.1 to 26.8% for platinum and 60.2 to 43.3% for gold. On the other hand, for modified iron oxide percentage recovery varied from 49.7 to 32.0 for platinum, 40.9 to 35.1 for palladium and 83.2 to 42.3 for gold. These results except for platinum with unmodified iron oxide nanoparticles illustrate that percentage recovery tends to decrease with increase in initial concentration.

A study by Padmavathy *et al.* [47] on Cr(IV) removal using magnetite with an initial concentration of 10 to 60 mg/L yielded results in the range of 70 to 66 percentages, and this is a similar trend obtained in the current study. Candice *et al.* [79] using

Moringa leaves biomass as adsorbent for Cr(VI) with an initial concentration of 10 to 150 mg/L yielded a similar trend in the range of 75 to 8%. According to this study, when the initial concentration is lower, the ratio of available sites on the surface of the adsorbent to the concentration of the adsorbate is raised resulting in higher removal percentage. In the contrary, when the initial concentration is higher, the ratio of available sites on the surface of the adsorbent to the concentration of the adsorbate is lowered resulting in lower removal percentage. These findings might, therefore, suggest that initial concentration might affect adsorption. Another study by Hariani *et al.* [88] on the synthesis and properties of Fe_3O_4 nanoparticles by co-precipitation method to removal Procion dye also concurs that initial concentration plays a role in the adsorption process.

However, a study by Obuseng *et al.* [63] on the removal of heavy metals from aqueous solutions by *M. oleifera* seeds and amine-based ligand utilized a lower range of initial concentration between 1-14mg/L. This study showed that as the concentration increases, the recovery percentage of metal ions also increases until the point of biomass saturation or optimal concentration is reached after which a steady decrease is observed when initial concentration is raised. This infers that the availability of the vacant adsorption sites on the surface of the adsorbent determines the rate of adsorption thus the recovery of the metal ions. Similar findings were obtained by Maina *et al.* [77] on the use of Moringa seed pods and Morula nut shells for removal of heavy metals from waste water and borehole water. The results obtained in the current study, therefore, propose that the range of initial concentration studied might have been toward the optimal concentration thus a decrease in recovery percentage of precious metal ions when the initial concentration was raised.

6.4 Langmuir and Freundlich adsorption isotherms

Figures 5.25-5.26 as well as Tables 5.11-5.14 summarize Langmuir and Fleundlich models for monolayer and multilayer adsorption respectively. Maximum adsorption capacities and regression constants (R^2), for Langmuir and Freundlich adsorption isotherms, are obtained [47,78,79]. Table 5.15 compares adsorption capacity of different adsorbents.

The adsorption of Pt (IV), Pd (II), and Au (III) precious metal ions on both modified and unmodified iron oxide nanoparticles yield a better fit for Langmuir isotherm compared to Freundlich isotherm. However, Au (III) yield a good fit of $r^2 = 0.9988$ on unmodified iron oxide nanoparticles since this is very close to 1.

Padmavathy *et al.* [47]; Nethaji *et al.* [78] and Candice *et al.* [79] further state that, from the Langmuir model, the separation factor R_L determines whether the adsorption is favourable or not. In the current study, R_L values for Pt (IV) and Au (III) on unmodified iron oxide nanoparticles are 0.310 and 0.009, respectively, which fall between 0 and 1 thus indicating favourable adsorption. On the contrary, the R_L obtained for Pd (II) on unmodified iron oxide is less than zero thus unfavourable. On the other hand, the R_L value obtained for Pt (IV), Pd (II), and Au (III) on modified iron oxide are 0.432, 0.298 and 0.660, respectively, thus favourable adsorption.

Table 6.1: Comparison of adsorption capacities of different adsorbents

Adsorbent	**Adsorbate adsorption capacity (mg/g)**	**Adsorbate initial concentration (mg/L)**	pH	**Reference**
Magnetite nanoparticles modified with Moringa	Au (III): 34.48 Pt (IV): 28.90 Pd (II): 5.27	10-100	2.5	This study
Grape stalk	Pt: 1.5 Pd: 1.4	10-60	1.5	Mavhungu et al. [61]
Moringa seeds	Ag(I): 23.13	5	6.5	Araujo et al. [42]
Moringa leaves biomass	Cr(VI): 33.9	10-150	2	Candice et al. [79]
Magnetite nanoparticles	Cr(VI): 0.015	10-60	3	Padmavathy et al. [47]

CHAPTER 7: CONCLUSION

The study synthesized magnetic iron oxide nanoparticles by chemical co-precipitation of Fe^{3+} and Fe^{2+} (2:1) whereby complete precipitation was achieved at around pH 12. The study further prepared aqueous protein solution (1%) extracted from *M. oleifera* seeds that were utilized to obtain the chemical co-precipitation of modified magnetic iron oxide nanoparticles. The characterization techniques such as FTIR, TGA, SEM and Zeta potential were utilized to identify different functional groups responsible for adsorption, thermal stability, morphology and surface charge of the nanoparticles.

The infrared spectra obtained with the FTIR confirmed the synthesis of magnetic iron oxide and modified magnetic iron oxide nanoparticles respectively. Possible functional groups that could be responsible for turbidity removal and recovery of precious metal ions obtained in the spectra were hydroxyl, carbonyl, amine/amide, carboxylic and iron oxide groups. The scanning electron micrography of unmodified magnetic iron oxide nanoparticles showed porous morphology with varying pore sizes thus associated with turbidity removal in waste water and adsorption of the precious metal ions. The TGA curves depicted the weight loss that decreased at a slow rate with overall weight loss of 17.2% for modified magnetic iron oxide in comparison to 17.7% obtained for unmodified magnetic iron oxide. These values and also the curve for modified magnetic iron oxide nanoparticles appearing slightly above the one for the unmodified one suggests that the modified nanoparticles are slightly stable compared to the unmodified nanoparticles. On the other hand, there seems to be inconsistency in the percentages loss values between 100-350°C for modified magnetic iron oxide nanoparticles that might be associated with the proteins amino acid residues with various functional groups. The surface charges of unmodified and modified iron oxide

nanoparticles were studied with the zeta potential in the pH range between 2 to 12. The isoelectric point values between 6.12 and 3.69 were obtained for unmodified and modified iron oxide nanoparticles respectively. The dependency of adsorption on pH, the difference in turbidity removal and recovery of precious metal ions using these adsorbents in the current study could therefore be explained by the surface charge values obtained.

The effect of pH and modified magnetic iron oxide nanoparticles dosage was studied for turbidity removal using UV-Vis spectrophotometer at a wavelength of 360nm. An optimal pH of 2.5 with maximal removal of 97.3% at approximately 0.005g was yielded. The removal percentage of 96.4% was obtained with unmodified magnetic iron oxide nanoparticles at the same pH and dosage. The same optimal pH was obtained for the selective recovery of precious metal ions when ICP-OES was used. The highest recovery of 99.8% was obtained for gold , followed by platinum with 87.7% then palladium with 72.7% at 0.065g optimal dosage of modified magnetic iron oxide nanoparticles. However, the recoveries of 99.8%, 51.8% and 80.4% for Au, Pd and Pt respectively, were obtained with unmodified magnetic iron oxide nanoparticles at the same pH. The equilibrium agitation time was reached within 120 minutes. The maximal initial concentration was 10mg/L. The data better fitted Langmuir model than Freundlich. These results, therefore, demonstrated that modified iron oxide nanoparticles were effective in water treatment and recovery of the precious metal ions.

CHAPTER 8: RECOMMENDATIONS

Based on the findings from this work, the following may be recommended for future studies:

- Magnetic iron oxide may be synthesized using other methods such as micro-emulsion, hydrothermal, electrochemical, deposition, sono-chemical and thermal decomposition to compare the nanoparticles produced.
- Modification of the magnetic iron oxide may be conducted at different concentrations of the protein extract to compare the effectiveness.
- Other characterization techniques such as Transmission Electron Microscopy (TEM), Dynamic Light Scattering (DLS), Vibrating Sample Magnetometer (VSM) and X-ray powder diffraction (XRD) may reveal useful information on the nanoparticles.
- The nanocomposite materials of MNPs may be tested on other types of water and other precious metal ions to verify the results obtained in the present study.

CHAPTER 9: REFERENCES

[1] A. Suhada, A.R. Arifin, Ismayadi, Ismail, A. Halim, Abdullah, I. Riati, Ibrahim, F. Nabilah, Shafiee, Magnetite nanoparticles in wastewater treatment, Pert. J. Sch. Res. Rev. 2 (2016) 108-122.

[2] I. Ali, New generation adsorbents for water treatment, Chem. Rev. 112 (2012) 5073-5091.

[3] T.C. Shan, M. Al Matar, E.A. Makky, E.N. Ali, The use of *Moringa oleifera* seed as a natural coagulant for wastewater treatment and heavy metals removal, Appl. Water Sci. 7(2017) 1369-1376.

[4] H. Umeda, A. Sasaki, K. Takahashi, K. Haga, Y. Takasaki, A. Sibayama, Recovery and concentration of precious metals from strong acidic wastewater, Mater. trans. 52 (2011) 1462-1470.

[5] M. Yarahmadi, M. Hossieni, B. Bina, M.H. Mahmoudian, A. Naimabadie, A. Shahsavani, Application of *Moringa Oleifera* seed extract and polyaluminium chloride in water treatment. World Appl. Sci. J. 7 (2009) 962-967.

[6] G. K. Folkard, J.P. Sutherland, R. Shaw, Chemical coagulants, In: R. Shaw (Ed.), Running Water, Intermediate Technology Publications., London, 1999, pp. 109-112.

[7] A. Witek – Krowiak, Application of beech sawdust for removal of heavy metals from water: bisorption and desorption studies, Eur. J. Wood Prod. 71 (2013) 227-236.

[8] X. Ju, K. Igaraschi, S. Miyashita, H. Mitsuhashi, K. Inagaki, S. Fuji, H. Sawada, T. Kuwabara, A. Minoda, Effective and selective recovery of gold and palladium

ions from metal wastewater using a sulfothermophilic red alga, *Galdieria sulphuraria*, Bioresour. Technol. 211 (2016) 759-764

[9] A.N. Nikoloski, K.L. Ang, Review of the application of ion exchange resins for the recovery of platinum-group metals from hydrochloric acid solutions, Miner. Process. Extra. Metall. Rev. 35 (2014) 369-389.

[10] S.J. Kulkarni, Removal and recovery of platinum: an insight into studies and research, Int. J. Res. Rev. 3 (2016) 74-77.

[11] J. He, A. Kappler, Recovery of precious metals from waste streams, Microb. Biotechnol. 10(2017) 1194-1198.

[12] E. Aghaei, R.D. Alorro, A.N. Encila, K. Yoo, Review: Magnetic adsorbents for the recovery of precious metals from leach solutions and wastewater, Met. 7(2017) 1-32.

[13] F. Reith, S.G. Campbell, A.S. Ball, A. Pring, G. Southam, Platinum in Earth Surface environments, Earth Sci.- Reviews. 131 (2014) 1-21.

[14] S. Sharma, A. K. S. Kumar, N. Rajesh, Review: A perspective on diverse adsorbent materials to recover precious palladium and the way forward, R. Soc. Chem. 7 (2017) 52133-52142.

[15] V. Kavitha, Extraction of precious metals from e-waste, J. Chem. Pharm. Sci. 3(2014) 147-149.

[16] V. Yahorava, M. Kotze, Ion exchange technology for the efficient recovery of precious metals from waste and low – grade streams, J. S. Afri. Inst. Min. Metall. 114 (2014) 173-181.

[17] L. Giraldo, A. Erto, J.C. Moreno-Pirajan, Magnetite nanoparticles for removal of heavy metals from aqueous solutions: synthesis and characterization, Adsorp. Sci. Technol. 19 (2013) 465–474.

[18] K.A. Al-Sand, M.A. Amr, D. T. Hadi, R.S. Arar, M.M. AL- Suloiti, T.A. Abdul Malik, N.M. Alsahamary, J.C. Kwak, Iron oxide nanoparticles: applicability for heavy metal removal from contaminated water, Arab J. Nucl. Sci. App. 45 (2012) 335-346.

[19] N. Neyaz, W. A. Siddiqui, K.K. Nair, Application of surface functionalized iron oxide nanomaterials as a nanosorbents in extraction of toxic heavy metals from groundwater: A review, Int. J. Environ. Sci. 4 (2014) 472-483.

[20] K. Simeonidis, S. Mourdikoudis, E. Kaprara, M. Mitrakas, L. Polavarapu, Inorganic engineered nanoparticles in drinking water treatment: A critical review, Environ. Sci. Water. Res. Technol. 2 (2016) 43-70.

[21] S.R. Umaya, Application of *Moringa oleifera* in poultry: a review. World J. Pharm. Res. 3 (2014) 1955-1960.

[22] C. Yin, Emerging usage of plant-based coagulants for water and wastewater treatment: a review. Process Biochem. 45 (2010) 1437-1444.

[23] J. Xu, J. Sun, Y. Wang, J. Sheng, F. Wang, M. Sun, Application of iron magnetic nanoparticles in protein immobilization, Molecules. 19 (2014) 11465-11486.

[24] C.C. Okoli, Development of protein-functionalized magnetic iron oxide nanoparticles; Potential application in water treatment [dissertation]. Stockholm: University service Stockholm, Sweden; 2012

[25] C. N. Tang, I. M. Lo, Magnetic nanoparticles: Essential factors for sustainable environmental applications, Water Res. 47 (2013) 2613-2632.

[26] W. Wu, Z. Wu, T. Yu, C. Jiang, W. Kim, Recent progress on magnetic iron oxide nanoparticles: synthesis, surface functional strategies, and biomedical applications: a review. Sci. Technol. Adv. Mater. 16 (2015) 43.

[27] P. Xu, G.M. Zeng, D.L. Huang, C.L. Feng, S. Hu, M.H. Zhao, C. Lai, Z. Wei, C. Huang, G.X. Xie. Z.F. Liu, Use of iron oxide nanomaterials in wastewater treatment: A review, Sci. Total. Environ. 424 (2012) 1-10.

[28] S. Shaker, S. Zafarian, C.H.S. Chakra, K.V. Rao, Preparation and characterization of magnetite nanoparticles by sol-gel method for water treatment, Int. J. Innovative. Res. Sci. Eng. Technol. 2 (2013) 2969 – 2973.

[29] T.R. Santos, M.F. Silva, L. Nishi, A.M. Vieira, M.R. Faqundes-Klen, M.B. Andrade, M.F. Vieira, R. Berqamasco, Development of a magnetic coagulant based on *Moringa oleifera* seed extract for water treatment, Environ. Sci. Pollut. Res. 23 (2016) 7642-7700.

[30] D. Marcinkowska, Application of magnetic nanoparticles for water treatment, Tech. Iss. 2(2016) 33-38.

[31] K.S. Narasiah, A. Vogel, N.N. Kramadhati, Coagulation of turbid waters using *Moringa oleifera* Seeds from Two Distinct Sources, Water Sci. Technol. 2 (2002) 53-58.

[32] A. Ndabigengesere, K.S. Narasiah, B.G. Talbot, Active agents and mechanism of coagulation of turbid waters using *Moringa oleifera*, Wat. Res. 29 (1995) 703-710.

[33] M.M. S Arreola, J.R.L. Canepa, J.R.H. Barajas, Molecular characterization of crude seed extracts from Moringa oleifera, Interciencia. 41 (2016) 548-551.

[34] Hendrawati, E. Rohaeti, H. Effendi, L.K.Darusman, Characterterization of physicochemical properties of nano-sized *Moringa oleifera* seed powder and its

application as natural coagulation in water purification process, J. Environ. Earth. Sci. 5 (2015) 19-26.

[35] H.M. Kwaambwa, A.R. Rennie, Interaction of surfactants with a water treatment protein from *Moringa oleifera* seeds in solution studied by zeta potential and light scattering measurements, Biopolymers. 97 (2012) 209-218.

[36] F.M. Nermark, Bioremediation of copper and lead contaminated soil using *Moringa oleifera* seeds water extract and physicochemical studies,. MSc Dissertation, University of Botswana, Gaborone; 2014

[37] H.M. Kwaambwa, M.S. Hellsing, A.R. Rennie, R. Barker, Interaction of *Moringa oleifera* seed protein with a mineral surface and the influence of surfactants, J. Collo. Interface Sci. 448 (2015) 339–346.

[38] H.A. Jerri, K.J. Adolfsen, L.R. McCullough, D. Velegol, S.B. Velegol, Antimicrobial sand via adsorption of cationic *Moringa oleifera* protein, Langmuir. 28 (2012) 2262–2268.

[39] R. Maikokera, H.M. Kwaambwa, Interfacial properties and fluorescence of a coagulating protein extracted from *Moringa oleifera* seeds and its interaction with sodium dodecyl sulphate, Colloids Suf, B. 55 (2007) 173-178.

[40] M.S. Hellsing, H.M. Kwaambwa, F.M. Nermark, B.B.M Nkoane, A.J. Jackson, M.J. Wasbrough et al. Structure of flocs of latex particles formed by addition of protein from *Moringa* seeds, Colloids Suf, A: Physicochem. Eng. Aspects. 460 (2014) 460-467.

[41] J. Sanchez – Martin, J. Beltran – Heredia, J.A. Peres, Improvement of the flocculation process in water treatment by using *Moringa oleifera* seeds extract, Braz. J. Chem. Eng. 29 (2012) 495-501.

[42] C.S.T. Araujo, V.N. Alves, H.C. Rezend, I.L.S. Almeida, R.M.N. de Assuncao, C.R.T. Tarley, M.G. Segatelli, N.M.M. Coelho, Characterization and use of *Moringa oleifera* seeds as biosorbent for removing metal ions from aqueous effluents, Wat. Sci. Tech. 62.9 (2010) 2198-2203.

[43] E. Tombacz, K. Farkas, I. Foldesi, M. Szekeres, E. Illes, I.Y. Toth, D. Nesztor, T. Szabo, Polyelectrolyte coating on supermagnetic iron oxide nanoparticles as interface between magnetic core and bio relevant media, Interface focus 6 (2016) 1-8.

[44] X.M. Li, G. Xu, Y. Liu, T. He, Magnetite Fe_3O_4 nanoparticles: Synthesis and application in water treatment, Nano. Sci. Nanotechnol.- Asia, 1 (2011), 14-24.

[45] N. Ilankoon, Use of iron oxide magnetic nanosorbents for Cr (IV) removal from aqueous solutions: A review, J. Eng. Res. Appl. 10 (2014) 55-63.

[46] H. Lu, J. Wang, M. Stoller, T. Wang, J. Bao, H. Hao, An overview of nanomaterials for water treatment and wastewater: Review article, Adv. Mater. Sci. Eng. 4964828 (2016) 1-11.

[47] K.M. Padmavathy, G. Madhu, P.V. Haseena, A study on the effects of pH, adsorbent dosage, time, initial concentration and adsorption isotherm study for the removal of hexavalent chromium (Cr (IV)) from wastewater by magnetite nanoparticles, Proc. Technol. 24 (2016) 585-594.

[48] P.N. Dave, L.V. Chopda, Application of iron oxide nanomaterials for the removal of heavy metals: Review Article, J. Nanotechnol. 398569 (2014) 1-15.

[49] N.D. Kandpal, N. Sah, R. Loshali, R. Joshi, J. Prasad, Co-precipitation method of synthesis and characterization of iron oxide nanoparticles, J. Sci. Ind. Res. 73 (2014) 87-90.

[50] L. Carlos, F.S.G. Einschlag, M.C. Gonzalez, D.O. Martire, Applications of magnetite nanoparticles for heavy materials removal from wastewater, Instit. New. Technol. 54608 (2013) 63-77.

[51] S. Rajput, C.U.Pittman, J.D. Mohan, Magnetic magnetite (Fe_3O_4) nanoparticles synthesis and application for lead (Pb^{2+}) and chromium (Cr^{6+}) removal from water, J. Collo. Interf. Sci. 468 (2016) 334-346.

[52] E. Velez, G.E. Campillo, G. Morales, C. Hincapie, J. Osorio, O. Arnache, J.I. Uribe, F. Jaramillo, Mercury removal in wastewater by iron oxide nanoparticles, J. Phys.: Conf. ser. 87 (2016) 1-5.

[53] M. Gui, V. Smuleac, L.E. Ormsbee, D.L. Sedlak, D. Bhattacharyya, Iron oxide nanoparticles synthesis in aqueous and membrane systems for oxidative degradation of trichloroethylene from water, J. Nanopart. Res. 14 (2012) 1-6.

[54] Y. Xu, C. Li, X. Zhu, W. E. Huang, D. Zhang, Application of magnetic nanoparticles in drinking water purification, Environ. Eng. Manage. J. 13 (2013) 2023-2029.

[55] X. Meng, J. Ryu, B. Kim, S. Ko, Application of iron oxide as a pH-dependent indicator for improving the nutritional quality, Cli. Nutri. Res. 5 (2016) 172-179.

[56] B.B.T. Patil, Wastewater treatment using nanoparticles, J. Adv. Chem. Eng. 5 (2015) 1-2.

[57] M. Khiadani, M.M. Foroughi, M.M. Amin, Improving urban runoff quality using iron oxide nanoparticles with magnetic field, Desalin. Water Treat. 52 (2013) 678-682.

[58] K. H. Hassan, E. R. Malidi, Synthesis, and characterization of Copper, Iron oxide, nanoparticles used to remove Lead from aqueous solution, Asian. J. Appl. Sci. 4 (2016) 730-738.

[59] X.C. Yang., Y.L.Shang. Y.H. Li, J. Zhai, N.R. Foster, Y.X. Li, D. Zou, Y.Pu, Synthesis of monodisperse iron oxide nanoparticles without surfactants, J. Nanomater. (2014) 1-6.

[60] X.Ju, K. Igarashi, S. Miyashita, H. Mitsuhashi, K. Inagaki, S. Fuji, H.Sawada, T. Kuwabara, A. Minoda, Effective and selective recovery of gold and palladium ions from metal wastewater using a sulfothermophilic red alga, *Galdieria sulphuraria*, Bioresour. Technol. 211 (2016) 759-764.

[61] A. Mavhungu, R.K.K. Mbaya, M.L. Moropeng, Recovery of platinum and palladium ions from aqueous solution using grape stalk waste, Inter. J. Chem. Eng. Appl. 4 (2013) 1-5.

[62] T.L. Silva, V.H. Melnerz, J.M.M. Vidart, M.L. Gimenes, M.G.A. Vieira, M.G.C. Silva, Metallic affinity of toxic and noble metals by particles produced sericin, alginate and poly ethylene glycol, Chem. Eng. Trans. 56 (2017).

[63] V. Obuseng, F. Nareetsile, H.M. Kwaambwa, A study of the removal of heavy metals from aqueous solutions by *Moringa oleifera* seeds and amine-based ligand 1,4 – bis [N, N – bis (2- picoyl) amino) butane], Anal. Chim. Acta. 730 (2012) 87-92.

[64] J.H. Chang, J. Lee, Y. Jeong, J.H. Lee, I.J. Kim, S.E. Park, Hydrophobic partitioning approach to efficient protein separation with magnetic nanoparticles, Anal. Biochem. 405 (2010) 135.

[65] F.B. Hussein N.H. Abu-Zahra, Adsorption kinetics and evaluation study of iron oxide nanoparticles impregnated in polyurethane matrix for water filtration application, J. Miner. Mater. Char. Eng. 5 (2017) 298-310.

[66] S.H. Dewi, S.A. Fisli, S. Wardiyati, Synthesis and characterization of magnetized photocatalyst $Fe_3O_4/SiO_2/TiO_2$ by hetero-agglomeration method, J. Phys.: Conf. Ser. 739 (2016) 1-9.

[67] E.G. Zemtsova, A.N. Ponomareva, V.V. Panchuk, L.F. Galiullina, V.M. Smirnov, Synthesis, structure and magnetic properties of Fe3O4 – SiO2, nanocomposites with core-shell structures for targeted drug delivery, Rev. Adv. Mater. Sci. 52 (2017) 82-90.

[68] M. H. Ehrampoush, M. Miria, M.H. Salmani, A.H. Mahvi, Cadmium removal from aqueous solution by green synthesis iron oxide nanoparticles with tangerine peel extract, J. Environ. Health. Sci. Eng. 13 (2015) 1-7.

[69] R. Lakshmanam, Application of magnetic nanoparticles and reactive filter materials for wastewater treatment [dissertation] Stockholm: Royal Institute of technology, Sweden; 2013.

[70] S.K. Gill, G. Singh, M. Khatri, Synthesis and characterization of superparamagnetic iron oxide nanoparticles for water purification applications, Int. J. Eng. Technol. Sci. Res. 4 (2017) 355-359.

[71] N. S. Remya, S. Syama, A. Sabareeswaran, P.V. Mohanan, Safety of iron oxide nanoparticles – a regulatory perspective, Int. J. Pharm (2016) 1-2.

[72] S.Y.R. Paik, J.S. Kim, S.J. Shin, S. Ko, Characterization, quantification and determination of the toxicity of iron oxide nanoparticles to the bone marrow cells, Int. J. Mol. Sci. 16 (2015) 22243-22257.

[73] O. Vasylkiv, O.Bezdorozhev, Y. Sakka, Synthesis of iron oxide nanoparticles with different morphologies by precipitation method with and without chitosan addition, J. Ceram. Soc. Jpn. 124 (2016) 489-494.

[74] A. M. Gutierrez, T. D. Dziubla, J.Z. Hilt, Recent advances on iron oxide magnetic nanoparticles as sorbents of organic pollutants in water and wastewater treatment: Review, Rev. Environ. Health, 32 (2017) 111-117.

[75] M.N. Idris, M.S. Jami, A.M. Hammed, P. Jamal, *Moringa oleifera* seed extract: A review on its environmental applications, Int. J. Inv. Sci. 11 (2016) 1469-1486.

[76] H. Kazemzadeh, A. Ataie, F. Rashchi, Synthesis of magnetic nanoparticles by reverse co-prcipitation, Int. J. Mod. Phys. Conf. Ser. 5 (2012) 160-167.

[77] I.W. Maina, V.Obuseng, F.Nareetsile, Use of *Moringa oleifera* (Moringa) seed pods and *Sclerocarya birrea* (Morula) nut shells for removal of heavy metals from waste water and borehole water, J.Chem. 9312952 (2016) 1-13.

[78] S. Nethaji, A. Sivasamy, A.B. Mandal, Adsorption isotherms, kinetics and mechanism for the adsorption of cationic and anionic dyes onto carbonaceous particles prepared from Juglans regia shell biomass, Int. J. Environ. Sci. Technol. 10 (2013) 231-242.

[79] C.T. Candice, M. Kandawa-Schulz, M. Amuanyena, H.M. Kwaambwa, Adsorptive removal aqueous solution of Cr (IV) by green *Moringa* tea leaves biomass, Journal of encapsulation and adsorption sciences, J. Encap. Ads. Sci. 7 (2017) 108-119.

[80] M. Mahdari, F. Namvar, M.B. Ahmad, R. Mohamad, Green Biosynthesis and characterisation of magnetic iron oxide (Fe_3O_4) nanoparticles using seaweed (*Sargassum muticum*) aqueous extract, Molecules. 18 (2013) 5954-5964.

[81] Z. Shu, S. Wang, Synthesis and characterization of magnetic nanosized Fe_3O_4 / MnO_2 composite particles, J. Nanomater. 340217 (2009) 1-5.

[82] E.N. Ramsden, A-level chemistry detection and analysis, Stanely Thormes publishers Ltd. Great Britain.,1996, pp, 72-73.

[83] B. Ramavandi, S. Hashemi, R.Kafaei, A novel method for extraction of a proteinous coagulant from *Plantago ovata* seeds for water treatment purposes, MethodsX. 2 (2015) 278-282.

[84] M. Sneha, N.M. Sundaram, Preparation and characterization of an iron oxide – hydroxyapatite nanocomposite for potential bone cancer therapy, Int. J. Nanomed. 10 (2015) 99-106.

[85] L. Muruganandam, M.P.S. Kumar, A. Jena, S. Gulla, B. Godhwani, Treatment of waste water by coagulation and flocculation using biomaterials, IOP Conf. Ser. Mater. Sci. Eng. 263 (2017) 1-12.

[86] J. Lim, H.M. Kang, L.H. Kim, S.O. Ko, Removal of heavy metals by sawdust adsorption: Equilibrium and kinetic studies, Environ. Eng. Res. 13 (2008), 79-84.

[87] D. Oke, Purification of platinum group metals process stream using *Saccharomyces cerevisiae* waste yeast biomass [dissertation]. Johannesburg: University of Witwatersrand, South Africa; 2014.

[88] P.L. Hariani, M. Faizal, Ridwan, Marsi, D. Setiabudidaya, Synthesis and properties of Fe_3O_4 nanoparticles by co-precipitation method to removal procion dye, Int. J. Environ. Sci. Dev. 4(2013) 336-340.

CPATER 10: APPENDICES

ETHICAL CLEARANCE CERTIFICATE

UNAM
UNIVERSITY OF NAMIBIA

ETHICAL CLEARANCE CERTIFICATE

Ethical Clearance Reference Number: FOS/168/2017 **Date: 28 March, 2017**

This Ethical Clearance Certificate is issued by the University of Namibia Research Ethics Committee (UREC) in accordance with the University of Namibia's Research Ethics Policy and Guidelines. Ethical approval is given in respect of undertakings contained in the Research Project outlined below. This Certificate is issued on the recommendations of the ethical evaluation done by the Faculty/Centre/Campus Research & Publications Committee sitting with the Postgraduate Studies Committee.

Title of Project: Magnetic Nanoparticles modified with Moringa seed protiens for water treatment and selective recovery of precious metal ions-

Nature/Level of Project: Masters

Researcher: Marta O.N. Amuanyena

Student Number: 9815236

Faculty: Faculty of Science

Supervisors: Dr Martha Kandawa-Schulz (Main) Prof Habauka M. Kwaambwa (Co)
Take note of the following:

(a) Any significant changes in the conditions or undertakings outlined in the approved Proposal must be communicated to the UREC. An application to make amendments may be necessary.
(b) Any breaches of ethical undertakings or practices that have an impact on ethical conduct of the research must be reported to the UREC.
(c) The Principal Researcher must report issues of ethical compliance to the UREC (through the Chairperson of the Faculty/Centre/Campus Research & Publications Committee) at the end of the Project or as may be requested by UREC.
(d) The UREC retains the right to:
(i) Withdraw or amend this Ethical Clearance if any unethical practices (as outlined in the Research Ethics Policy) have been detected or suspected,
(ii) Request for an ethical compliance report at any point during the course of the research.

UREC wishes you the best in your research.

Prof. P. Odonkor: UREC Chairperson

Ms. P. Claassen: UREC Secretary

TABLES: A1-A48

Table A1: TGA curves data for unmodified and modified iron oxide nanoparticles (Figures 5.8-5.10)

Parameter	Unmodified iron oxide nanoparticles	Modified iron oxide nanoparticles
Initial temperature (ºC)	30.81	30.86
Final temperature (ºC)	794.77	794.80
Initial weight %	96.128	95.457
Final weight %	79.068	79.061
Weight loss %	17.7	17.2

Table A2: Zeta potential data for unmodified and modified iron oxide nanoparticles (Figure 5.12)

Unmodified iron oxide nanoparticles		Modified iron oxide nanoparticles	
pH	Zeta potential (mV)	pH	Zeta potential (mV)
2.06	13.7	2.05	10.1
2.75	16.3	2.54	10.1
3.28	13.9	3.2	8.57
3.76	11.9	3.16	5.53
4.17	9.65	3.6	2.75
4.6	9.22	3.58	0.43
5.49	8.96	3.87	-1.05
5.68	3.88	3.87	-2.43
6.33	-1.89	4.37	-3.41
7.43	-9.3	5	-3.46
8.31	-18.3	5.2	-4.34
8.8	-21.9	5.41	-6.08
9	-24.8	5.88	-8.37
9.54	-26.3	6.33	-11.47
10.3	-30.2	6.82	-11.9
10.8	-28.7	7.45	-12.57
11.4	-27.5	7.79	-14.5
12	-31.2	8.51	-13.9
		8.85	-15
		9.24	-17.1
		9.76	-17.8
		10.3	-19.6
		10.8	-18.9

Table A3: Turbidity removal using magnetic iron oxide nanoparticles modified with *M. oleifera* seed proteins extracts at wavelengths 360, 450, 540 and 600 nm (Figure 5.13)

Dosage (g)	**Turbidity (100-%T)**			
	360 nm	450 nm	540 nm	600 nm
0.0	71.3	61.3	52.3	46.9
0.0071	56.7	45.6	36.7	31.8
0.0255	50.3	38.1	29.0	24.3
0.0448	44.6	34.4	26.9	22.9
0.0641	34.7	26.0	19.8	16.6
0.0850	30.2	22.0	16.2	13.4

Table A4: Turbidity removal using magnetic iron oxide nanoparticles unmodified with *M. oleifera* seed proteins extract at wavelengths 360, 450, 540 and 600

Dosage (g)	**Turbidity (100-%T)**			
	360 nm	450 nm	540 nm	600 nm
0.0	71.3	61.3	52.3	46.9
0.0075	71.6	59.4	48.9	42.8
0.0257	66.1	54.6	45.0	39.5
0.0475	64.6	51.9	41.7	36.1
0.0651	63.6	52.3	43.0	37.6
0.0833	57.2	45.8	36.9	32.0

Table A5: Turbidity removal using magnetic iron oxide nanoparticles unmodified with *M. oleifera* seed proteins extract at pH 2.5; 4.0; 7.0 and 9.5 (Figure 5.15)

Dosage (g)	%Turbidity removal at pH 2.5	%Turbidity removal at pH 4.0	%Turbidity removal at pH 7.0	%Turbidity removal at pH 9.5
0.0050	96.4	41.8	38	32.9
0.0250	95.1	28.3	35.8	16.7
0.0450	95.9	8.2	37.3	16.2
0.0650	97.7	5	28.6	9.8
0.0850	95.9	1.7	28.2	7.3

Table A6: Turbidity removal using magnetic iron oxide nanoparticles modified with *M. oleifera* seed proteins extract at pH 2.5; 4.0; 7.0 and 9.5 (Figure 5.15)

Dosage (g)	%Turbidity removal at pH 2.5	%Turbidity removal at pH 4.0	%Turbidity removal at pH 7.0	%Turbidity removal at pH 9.5
0.0050	97.3	45.2	40.9	36.3
0.0250	96.8	24.8	30.1	24.4
0.0450	96.0	21.2	24.7	21.9
0.0650	94.7	14.2	19.1	17.5
0.0850	82.3	6.9	13.3	14.6

Table A7: Concentrations in sample units of precious metal ions using 0.065g of unmodified iron oxide at pH 2.0 for palladium and 3.0 for both gold and platinum (Figure 5.16)

Sample Id	QC Status	Pt 265.945 (mg/L)	Pt 214.423 (mg/L)	Pt 299.797 (mg/L)	Pd 340.458 (mg/L)	Pd 363.470 (mg/L)	Au 267.595 (mg/L)	Au 242.795 (mg/L)
BLK	0.000	0.000	0.000	0.000	0.000	0.000	0.000	0.000
PGM 0.1	0.100	0.100	0.100	0.100	0.100	0.100	0.100	0.100
PGM 0.5	0.500	0.500	0.500	0.500	0.500	0.500	0.500	0.500
PGM 1.0	1.000	1.000	1.000	1.000	1.000	1.000	1.000	1.000
QC1	Passed	0.998	1.014	0.983	1.002	1.023	0.996	0.995
Pd control		-0.002	-0.002	0.008	79.216	80.710	0.002	0.001
Pd Fe_3O_4		-0.004	0.004	0.002	0.389	0.405	0.000	-0.002
Pt control		88.383	92.358		-0.017	-0.041	0.000	0.243
Pt Fe_3O_4		94.067	90.629	93.377	0.091	0.050	0.000	0.221
Au control		0.045	0.037	0.034	-0.016	0.043	104.742	103.743
Au Fe_3O_4		0.078	0.008	0.029	-0.011	-0.020	87.373	84.605
Pd control not shaken		0.006	-0.007	0.022	85.285	87.824	0.042	0.037
Pt control not shaken		86.428	92.978	91.766	-0.008	-0.023	0.014	0.256
Au control not shaken		0.049	0.021	0.043	0.012	-0.002	107.294	104.456

Table A8: Concentrations in sample units of precious metal ions using 0.065g of modified iron oxide at pH 2.0 for palladium and 3.0 for both gold and platinum (Figure 5.16)

Sample Id	**QC Status**	**Pt 265.945 (mg/L)**	**Pt 214.423 (mg/L)**	**Pt 299.797 (mg/L)**	**Pd 340.458 (mg/L)**	**Pd 363.470 (mg/L)**	**Au 267.595 (mg/L)**	**Au 242.795 (mg/L)**
BLK	0.000	0.000	0.000	0.000	0.000	0.000	0.000	0.000
PGM 0.1	0.100	0.100	0.100	0.100	0.100	0.100	0.100	0.100
PGM 0.5	0.500	0.500	0.500	0.500	0.500	0.500	0.500	0.500
PGM 1.0	1.000	1.000	1.000	1.000	1.000	1.000	1.000	1.000
QC1	Passed	0.998	1.014	0.983	1.002	1.023	0.996	0.995
Pd control		-0.002	-0.002	0.008	79.216	80.710	0.002	0.001
Pd Mo Fe_3O_4		0.004	-0.016	0.001	16.134	16.723	-0.001	-0.001
Pt control		88.383	92.358		-0.017	-0.041	0.000	0.243
Pt Mo Fe_3O_4		75.972	75.634	76.856	-0.027	-0.025	-0.001	0.189
Au control		0.045	0.037	0.034	-0.016	0.043	104.742	103.743
Au Mo Fe_3O_4		0.020	-0.009	0.019	0.048	0.074	44.256	43.886
Pd control not shaken		0.006	-0.007	0.022	85.285	87.824	0.042	0.037
Pt control not shaken		86.428	92.978	91.766	-0.008	-0.023	0.014	0.256
Au control not shaken		0.049	0.021	0.043	0.012	-0.002	107.294	104.456

Table A9: Analysis summary of precious metal ions at 100 mg/L using 0.065g of unmodified and modified iron oxide at pH 2.0 for palladium and 3.0 for both gold and platinum (Figure 5.16)

Parameter on QC1	**Pt 265.945**	**Pt 214.423**	**Pt 299.797**	**Pd 340.458**	**Pd 363.470**	**Au 267.595**	**Au 242.795**
RSD	***0.9%***	1.2%	0.9%	***1.4%***	9.7%	2.6%	***1.5%***
% Recovery	98.5	98	99.8	99.3	102.9	98.9	97.6
R^2	***0.9928***	0.9546	0.9381	***0.9999***	0.0009	98.9	***97.6***

Table A10: Recovery of precious metal ions at 100 mg/L using 0.065g of unmodified and modified iron oxide at pH 2.0 for palladium and 3.0 for both gold and platinum from their individual solutions (Figure 5.16)

Adsorbent	**%Recovery**		
	Palladium 340.458	**Platinum 265.945**	**Gold 242.795**
Unmodified nanoparticles	99.5	0	18.4
Modified nanoparticles	79.6	14.0	57.7

Table A11: Concentrations in sample units of precious metal ions using 0.065g of unmodified iron oxide at pH 2.7 (Figure 5.17)

Sample Id	**QC Status**	**Pt 265.945 (mg/L)**	**Pt 214.423 (mg/L)**	**Pt 299.797 (mg/L)**	**Pd 340.458 (mg/L)**	**Pd 363.470 (mg/L)**	**Au 267.595 (mg/L)**	**Au 242.795 (mg/L)**
BLK	0.000	0.000	0.000	0.000	0.000	0.000	0.000	0.000
PGM 0.1	0.100	0.100	0.100	0.100	0.100	0.100	0.100	0.100
PGM 0.5	0.500	0.500	0.500	0.500	0.500	0.500	0.500	0.500
PGM 1.0		0.985	0.980	0.998	0.993	1.029	0.989	0.976
QC1	Passed	0.001	-0.010	-0.003	0.001	-0.081	0.003	0.007
Pd control		-0.008	-0.006	-0.015	84.317	87.034	0.003	0.005
Pd Fe_3O_4		-0.007	0.008	-0.012	44.792	45.912	0.003	0.004
Pt control		88.293	89.947	93.353	-0.063	-0.107	0.002	0.235
Pt Fe_3O_4		42.035	43.069	46.219	-0.046	-0.143	0.001	0.117
Au control		0.035	0.038	0.022	-0.033	-0.045	114.310	111.197
Au Fe_3O_4		0.002	0.001	-0.006	-0.050	-0.101	58.014	57.906
Pd, Pt, Au mixture control		91.802	93.853	99.535	105.546	110.378	115.625	111.195
Pd, Pt, Au Fe_3O_4		58.186	60.295	63.522	104.825	107.473	72.572	70.995

Table A12: Concentrations in sample units of precious metal ions using 0.065g of modified iron oxide at pH 2.7 (Figure 5.18)

Sample Id	QC Status	Pt 265.945 (mg/L)	Pt 214.423 (mg/L)	Pt 299.797 (mg/L)	Pd 340.458 (mg/L)	Pd 363.470 (mg/L)	Au 267.595 (mg/L)	Au 242.795 (mg/L)
BLK	0.000	0.000	0.000	0.000	0.000	0.000	0.000	0.000
PGM 0.1	0.100	0.100	0.100	0.100	0.100	0.100	0.100	0.100
PGM 0.5	0.500	0.500	0.500	0.500	0.500	0.500	0.500	0.500
PGM 1.0		0.985	0.980	0.998	0.993	1.029	0.989	0.976
QC1	Passed	0.001	-0.010	-0.003	0.001	-0.081	0.003	0.007
Pd control		-0.008	-0.006	-0.015	84.317	87.034	0.003	0.005
Pd Mo Fe_3O_4		0.002	-0.006	-0.016	6.910	7.202	0.002	0.005
Pt control		88.293	89.947	93.353	-0.063	-0.107	0.002	0.235
Pt Mo Fe_3O_4		50.177	52.099	54.551	-0.026	-0.114	0.002	0.141
Au control		0.035	0.038	0.022	-0.033	-0.045	114.310	111.197
Au Mo Fe_3O_4		0.007	0.008	0.002	-0.032	-0.105	56.084	53.984
Pd, Pt, Au mixture control		91.802	93.853	99.535	105.546	110.378	115.625	111.195
Pd, Pt, Au Mo Fe_3O_4		60.661	61.707	66.652	83.916	85.835	64.628	63.977

Table A13: Recovery of precious metal ions using 0.065g of unmodified and modified iron oxide at pH 2.7 from their individual solutions

Adsorbent	**%Recovery**		
	Palladium 340.458	**Platinum 265.945**	**Gold 242.795**
Unmodified Fe_3O_4 nanoparticles	46.9	52.4	47.9
Modified Fe_3O_4 nanoparticles	91.8	43.2	51.5

Table A14: Recovery of precious metal ions using 0.065g of unmodified and modified iron oxide at pH 2.7 from a mixture (data for Figure 5.17 and 5.18)

Adsorbent	**%Recovery**		
	Palladium 340.458	**Platinum 265.945**	**Gold 242.795**
Unmodified Fe_3O_4 nanoparticles	0.7	36.6	36.2
Modified Fe_3O_4 nanoparticles	20.5	33.9	42.5

Table A15: Analysis summary of precious metal ions using 0.065g of unmodified and modified iron oxide at pH 2.7 (data for Figure 5.17 and 5.18)

Parameter on QC1	**Pt 265.945**	**Pt 214.423**	**Pt 299.797**	**Pd 340.458**	**Pd 363.470**	**Au 267.595**	**Au 242.795**
RSD	***0.9%***	1.2%	0.9%	***1.4%***	9.7%	2.6%	***1.5%***
% Recovery	98.5	98	99.8	99.3	102.9	98.9	97.6
R^2	***0.9928***	0.9546	0.9381	***0.9999***	0.0009	98.9	***97.6***

Table A16: Concentrations in sample units of precious metal ions using 0.065g of unmodified iron oxide at pH 1.5 (Figure 5.17)

Sample Id	**QC Status**	**Pt 265.945 (mg/L)**	**Pt 214.423 (mg/L)**	**Pt 299.797 (mg/L)**	**Pd 340.458 (mg/L)**	**Pd 363.470 (mg/L)**	**Au 267.595 (mg/L)**	**Au 242.795 (mg/L)**
BLK	0.000	0.000	0.000	0.000	0.000	0.000	0.000	0.000
PGM 0.1	0.100	0.100	0.100	0.100	0.100	0.100	0.100	0.100
PGM 0.5	0.500	0.500	0.500	0.500	0.500	0.500	0.500	0.500
PGM 1.0		0.985	0.980	0.998	0.993	1.029	0.989	0.976
QC1	Passed	0.994	1.006	1.007	1.004	1.045	1.002	0.991
Pd control		-0.005	0.000	0.003	102.022	101.263	0.037	0.033
Pd Fe_3O_4		0.076	0.000	-0.020	105.617	103.890	0.035	-0.100
Pt control		88.426	93.307	92.322	-0.029	-0.010	0.034	0.272
Pt Fe_3O_4		86.633	88.658	89.166	-0.084	0.066	0.043	0.139
Au control		0.056	0.032	0.059	-0.033	0.011	105.477	103.768
Au Fe_3O_4		0.085	0.002	-0.011	-0.033	0.113	81.939	79.624
Pd, Pt, Au mixture control		99.733	99.828	99.905	94.779	94.009	104.673	102.230
Pd, Pt, Au Fe_3O_4		95.980	98.098	100.407	96.036	96.630	85.433	83.619

Table A17: Concentrations in sample units of precious metal ions using 0.065g of modified iron oxide at pH 1.5 (Figure 5.18)

Sample Id	**QC Status**	**Pt 265.945 (mg/L)**	**Pt 214.423 (mg/L)**	**Pt 299.797 (mg/L)**	**Pd 340.458 (mg/L)**	**Pd 363.470 (mg/L)**	**Au 267.595 (mg/L)**	**Au 242.795 (mg/L)**
BLK	0.000	0.000	0.000	0.000	0.000	0.000	0.000	0.000
PGM 0.1	0.100	0.100	0.100	0.100	0.100	0.100	0.100	0.100
PGM 0.5	0.500	0.500	0.500	0.500	0.500	0.500	0.500	0.500
PGM 1.0		0.985	0.980	0.998	0.993	1.029	0.989	0.976
QC1	Passed	0.994	1.006	1.007	1.004	1.045	1.002	0.991
Pd control		-0.005	0.000	0.003	102.022	101.263	0.037	0.033
Pd $MoFe_3O_4$		0.088	-0.004	-0.038	99.216	98.677	0.037	-0.120
Pt control		88.426	93.307	92.322	-0.029	-0.010	0.034	0.272
Pt Mo Fe_3O_4		80.092	81.194	83.492	-0.057	0.078	0.040	0.072
Au control		0.056	0.032	0.059	-0.033	0.011	105.477	103.768
Au Mo Fe_3O_4		0.122	-0.004	-0.030	-0.071	0.133	74.412	72.935
Pd, Pt, Au control		99.733	99.828	99.905	94.779	94.009	104.673	102.230
Pd, Pt, Au Mo Fe_3O_4		94.092	96.773	98.209	93.893	92.440	74.800	73.216

Table A18: Recovery of precious metal ions using 0.065g of unmodified and modified iron oxide at pH 1.5 from their individual solutions

Adsorbent	**%Recovery**		
	Palladium 340.458	**Platinum 265.945**	**Gold 242.795**
Unmodified Fe_3O_4 nanoparticles	0	2.0	23.3
Modified Fe_3O_4 nanoparticles	2.8	9.4	29.7

Table A19: Recovery of precious metal ions using 0.065g of unmodified and modified iron oxide at pH 1.5 from a mixture (Figure 5.17 and 5.18)

Adsorbent	**%Recovery**		
	Palladium 340.458	**Platinum 265.945**	**Gold 242.795**
Unmodified Fe_3O_4 nanoparticles	0	3.8	2.1
Modified Fe_3O_4 nanoparticles	0.9	5.7	2.1

Table A20: Analysis summary of precious metal ions using 0.065g of unmodified and modified iron oxide at pH 2.7 (Figure 5.17 and 5.18)

Parameter on QC1	**Pt 265.945**	**Pt 214.423**	**Pt 299.797**	**Pd 340.458**	**Pd 363.470**	**Au 267.595**	**Au 242.795**
RSD	***0.6%***	0.1%	2.5%	***0.9%***	12.1%	2.0%	***1.1%***
% Recovery	99.4	100.6	100.7	100.4	104.5	100.2	99.1
R^2	***0.9917***	0.9499	0.9357	***0.9999***	0.0005	0.9935	***0.9985***

Table A21: Concentrations in sample units of precious metal ions using 0.065g of unmodified and modified iron oxide at pH 2.5 (Figure 5.17 and 5.18)

Sample Id	QC Status	Pt 265.945 (mg/L)	Pt 214.423 (mg/L)	Pt 299.797 (mg/L)	Pd 340.458 (mg/L)	Pd 363.470 (mg/L)	Au 267.595 (mg/L)	Au 242.795 (mg/L)
PGM 0.1		0.100	0.100	0.100	0.100	0.100	0.100	0.100
PGM 0.5		0.500	0.500	0.500	0.500	0.500	0.500	0.500
PGM 1.0		1.000	1.000	1.000	1.000	1.000	1.000	1.000
QC1	Passed	1.006	1.015	0.999	1.005	1.003	0.994	1.000
Pd control		0.003	0.002	0.000	9.817	9.256	0.001	-0.002
Pd Fe_3O_4		0.003	0.020	-0.002	2.095	1.990	0.000	0.001
Pd Mo Fe_3O_4		0.012	0.002	0.005	2.329	2.208	0.000	-0.011
Pt control		8.147	8.353	8.456	-0.017	-0.037	0.001	0.021
Pt Fe_3O_4		1.752	1.754	1.781	-0.018	-0.023	0.000	-0.004
Pt Mo Fe_3O_4		1.027	1.045	1.065	-0.010	-0.033	0.000	0.001
Au control		0.007	0.013	0.003	-0.014	-0.033	9.201	9.401
Au Fe_3O_4		0.005	-0.003	-0.003	-0.021	-0.025	0.031	0.029
Au Mo Fe_3O_4		0.001	-0.001	0.006	-0.013	-0.027	0.103	0.105
Pd, Pt, Au control		10.800	10.983	11.138	9.896	9.189	10.439	10.584
Pd, Pt, Au Fe_3O_4		2.121	2.136	2.171	4.767	4.542	0.016	0.020
Pd, Pt, Au Mo Fe_3O_4		2.460	2.504	2.592	1.129	1.042	0.020	0.025

Table A22: Recovery of precious metal ions using 0.065g of unmodified and modified iron oxide at pH 2.5 from their individual solutions

Adsorbent	**%Recovery**		
	Palladium 340.458	**Platinum 265.945**	**Gold 242.795**
Unmodified nanoparticles	78.7	79.0	99.7
Modified nanoparticles	76.3	87.7	98.9

Table A23: Recovery of precious metal ions using 0.065g of unmodified and modified iron oxide at pH 2.5 from a mixture (Figure 5.17 and 5.18)

Adsorbent	**%Recovery**		
	Palladium 340.458	**Platinum 265.945**	**Gold 242.795**
Unmodified nanoparticles	51.8	80.4	99.8
Modified nanoparticles	88.6	77.2	99.8

Table A24: Analysis summary of precious metal ions at using 0.065g of unmodified and modified iron oxide at pH 2.5 (Figure 5.17 and 5.18)

Parameter on QC1	**Pt 265.945**	**Pt 214.423**	**Pt 299.797**	**Pd 340.458**	**Pd 363.470**	**Au 267.595**	**Au 242.795**
RSD	***1.3%***	1.0%	0.7%	***0.9%***	7.7%	0.1%	***0.6%***
% Recovery	100.6	101.5	99.9	100.5	100.3	99.4	100
R^2	***0.9867***	0.9473	0.9223	***0.9998***	0.0035	0.9987	***0.9994***

Table A25: Concentrations in sample units of precious metal ions using different dosages (g) of unmodified iron oxide at 10 mg/L (Figure 5.19)

Sample Id	QC Status	Pt 265.945 (mg/L)	Pt 214.423 (mg/L)	Pt 299.797 (mg/L)	Pd 340.458 (mg/L)	Pd 363.470 (mg/L)	Au 267.595 (mg/L)	Au 242.795 (mg/L)
BLK	0.000	0.000	0.000	0.000	0.000	0.000	0.000	0.000
PGM 0.1	0.100	0.100	0.100	0.100	0.100	0.100	0.100	0.100
PGM 0.5	0.500	0.500	0.500	0.500	0.500	0.500	0.500	0.500
PGM 1.0		1.000	1.000	1.000	1.000	1.000	1.000	1.000
QC1	Passed	1.003	1.025	1.000	1.008	1.031	0.994	0.999
Pd, Pt, Au control		10.033	10.322	10.358	9.485	9.287	9.136	8.971
Pd, Pt, Au 5.9 Fe_3O_4		7.856	8.240	8.250	9.446	9.109	5.797	5.807
Pd, Pt, Au 25.0 Fe_3O_4		3.123	3.208	3.240	8.370	8.076	0.402	0.401
Pd, Pt, Au 45.5 Fe_3O_4		1.877	1.901	1.936	7.040	6.899	0.040	0.035
Pd, Pt, Au 65.2 Fe_3O_4		1.223	1.223	1.241	5.625	5.466	0.015	0.012
Pd, Pt, Au 85.7 Fe_3O_4		1.198	1.239	1.255	3.099	3.026	0.005	0.002

Table A26: Concentrations in sample units of precious metal ions using different dosages (g) of modified iron oxide at 10 mg/L (Figure 5.20)

Sample Id	**QC Status**	**Pt 265.945 (mg/L)**	**Pt 214.423 (mg/L)**	**Pt 299.797 (mg/L)**	**Pd 340.458 (mg/L)**	**Pd 363.470 (mg/L)**	**Au 267.595 (mg/L)**	**Au 242.795 (mg/L)**
BLK	0.000	0.000	0.000	0.000	0.000	0.000	0.000	0.000
PGM 0.1	0.100	0.100	0.100	0.100	0.100	0.100	0.100	0.100
PGM 0.5	0.500	0.500	0.500	0.500	0.500	0.500	0.500	0.500
PGM 1.0		1.000	1.000	1.000	1.000	1.000	1.000	1.000
QC1	Passed	1.003	1.025	1.000	1.008	1.031	0.994	0.999
Pd, Pt, Au control		10.033	10.322	10.358	9.485	9.287	9.136	8.971
Pd, Pt, Au 5.5 $MoFe_3O_4$		8.253	8.601	8.672	8.956	8.596	5.284	5.317
Pd, Pt, Au 25.1 $MoFe_3O_4$		2.801	2.873	2.906	5.378	5.303	0.021	0.022
Pd, Pt, Au 45.3 $MoFe_3O_4$		2.949	3.014	3.041	4.629	4.540	0.014	0.017
Pd, Pt, Au 65.8 $MoFe_3O_4$		1.233	1.260	1.290	2.586	2.526	0.022	0.020
Pd, Pt, Au 85.0 $MoFe_3O_4$		2.889	2.880	2.982	4.012	3.940	1.307	1.287

Table A27: Recovery of precious metal ions at 10 mg/L using different dosages of unmodified iron oxide nanoparticles (Figure 5.19)

Dosage (g)	Palladium	Platinum	Gold
0.0059	0.4	21.7	35.3
0.0250	11.8	68.9	95.5
0.0455	25.8	81.3	99.6
0.0652	40.7	87.8	99.9
0.0857	67.3	88.1	100

Table A28: Recovery of precious metal ions at 10 mg/L using different dosages of modified iron oxide nanoparticles (Figure 5.20)

Dosage (g)	Palladium	Platinum	Gold
0.0055	5.6	17.7	40.7
0.0251	43.3	72.1	99.8
0.0453	51.2	70.6	99.8
0.0658	72.7	87.7	99.8
0.0850	57.7	71.2	85.6

Table A29: Concentrations in sample units of precious metal ions at different agitation time (min) using unmodified iron oxide (Figure 5.21)

Sample Id	QC Status	Pt 265.945 (mg/L)	Pt 214.423 (mg/L)	Pt 299.797 (mg/L)	Pd 340.458 (mg/L)	Pd 363.470 (mg/L)	Au 267.595 (mg/L)	Au 242.795 (mg/L)
BLK	0.000	0.000	0.000	0.000	0.000	0.000	0.000	0.000
PGM 0.1	0.100	0.100	0.100	0.100	0.100	0.100	0.100	0.100
PGM 0.5	0.500	0.500	0.500	0.500	0.500	0.500	0.500	0.500
PGM 1.0		1.000	1.000	1.000	1.000	1.000	1.000	1.000
QC1	Passed	0.998	0.999	1.004	1.013	1.009	0.999	1.012
Pd, Pt, Au control		8.499	9.138	9.092	8.718	8.606	10.736	10.791
Pd, Pt, Au 30 min Fe_3O_4		8.096	8.033	8.253	0.868	0.901	4.560	4.550
Pd, Pt, Au 60 min Fe_3O_4		8.085	7.965	8.157	0.705	0.664	3.826	3.794
Pd, Pt, Au 120 min Fe_3O_4		8.148	8.008	8.167	0.752	0.765	4.283	4.295
Pd, Pt, Au 240 min Fe_3O_4		8.028	7.928	8.188	0.642	0.621	4.289	4.279

Table A30: Concentrations in sample units of precious metal ions at different agitation time (min) using modified iron oxide (Figure 5.22)

Sample Id	QC Status	Pt 265.945 (mg/L)	Pt 214.423 (mg/L)	Pt 299.797 (mg/L)	Pd 340.458 (mg/L)	Pd 363.470 (mg/L)	Au 267.595 (mg/L)	Au 242.795 (mg/L)
BLK	0.000	0.000	0.000	0.000	0.000	0.000	0.000	0.000
PGM 0.1	0.100	0.100	0.100	0.100	0.100	0.100	0.100	0.100
PGM 0.5	0.500	0.500	0.500	0.500	0.500	0.500	0.500	0.500
PGM 1.0		1.000	1.000	1.000	1.000	1.000	1.000	1.000
QC1	Passed	0.998	0.999	1.004	1.013	1.009	0.999	1.012
Pd, Pt, Au control		8.499	9.138	9.092	8.718	8.606	10.736	10.791
Pd, Pt, Au 30 min $MoFe_3O_4$		3.579	3.492	3.579	5.158	5.166	1.728	1.713
Pd, Pt, Au 60 min $MoFe_3O_4$		5.684	5.627	5.678	5.977	6.014	2.415	2.402
Pd, Pt, Au 120 min $MoFe_3O_4$		4.277	4.216	4.304	5.154	5.144	1.801	1.808
Pd, Pt, Au 240 min $MoFe_3O_4$		4.278	4.197	4.249	5.153	5.091	1.507	1.495

Table A31: Effect of time on recovery of precious metal ions using unmodified iron oxide nanoparticles (Figure 5.21)

Time(min)	Palladium	Platinum	Gold
0	0	0	0
30	90.0	4.7	57.8
60	91.9	4.9	64.8
120	91.4	4.1	30.2
240	92.6	5.5	60.3

Table A32: Effect of time on recovery of precious metal ions using unmodified iron oxide nanoparticles (Figure 5.22)

Time(min)	Palladium	Platinum	Gold
0	0	0	0
30	40.8	57.9	84.1
60	31.4	33.1	77.7
120	40.9	49.7	83.2
240	40.9	49.7	86.1

Table A33: Concentrations in sample units of precious metal ion at different initial concentration (mg/L) using unmodified iron oxide (Figure 5.23)

Sample Id	QC Status	Pt 265.945 (mg/L)	Pt 214.423 (mg/L)	Pt 299.797 (mg/L)	Pd 340.458 (mg/L)	Pd 363.470 (mg/L)	Au 267.595 (mg/L)	Au 242.795 (mg/L)
BLK	0.000	0.000	0.000	0.000	0.000	0.000	0.000	0.000
PGM 0.1	0.100	0.100	0.100	0.100	0.100	0.100	0.100	0.100
PGM 0.5	0.500	0.500	0.500	0.500	0.500	0.500	0.500	0.500
PGM 1.0		1.000	1.000	1.000	1.000	1.000	1.000	1.000
QC1	Passed	0.998	0.999	1.004	1.013	1.009	0.999	1.012
Metals control 10mg/L		8.499	9.138	9.092	8.718	8.606	10.736	10.791
Metals Fe_3O_4 10mg/L		8.148	8.008	8.167	0.752	0.765	4.283	4.295
Metals control 30mg/L		26.879	28.322	28.274	30.344	30.005	33.489	33.219
Metals Fe_3O_4 30mg/L		25.444	25.645	26.105	4.312	4.454	16.701	16.677
Metals control 50mg/L		41.918	44.118	44.423	48.508	47.355	52.083	50.815
Metals Fe_3O_4 50mg/L		39.948	39.907	40.756	0.128	0.156	25.220	24.834
Metals control 70mg/L		58.636	61.982	62.881	69.329	68.095	73.941	73.083
Metals Fe_3O_4 70mg/L		51.061	51.890	51.941	0.246	0.275	18.012	17.902
Metals control 100mg/L		98.737	103.666	103.735	103.395	101.870	102.385	99.703
Metals Fe_3O_4 100mg/L		72.321	74.812	75.789	38.992	39.065	57.368	56.490

Table A34: Concentrations in sample units of precious metal ion at different initial concentration (mg/L) using modified iron oxide (Figure 5.24)

Sample Id	QC Status	Pt 265.945 (mg/L)	Pt 214.423 (mg/L)	Pt 299.797 (mg/L)	Pd 340.458 (mg/L)	Pd 363.470 (mg/L)	Au 267.595 (mg/L)	Au 242.795 (mg/L)
BLK	0.000	0.000	0.000	0.000	0.000	0.000	0.000	0.000
PGM 0.1	0.100	0.100	0.100	0.100	0.100	0.100	0.100	0.100
PGM 0.5	0.500	0.500	0.500	0.500	0.500	0.500	0.500	0.500
PGM 1.0		1.000	1.000	1.000	1.000	1.000	1.000	1.000
QC1	Passed	0.998	0.999	1.004	1.013	1.009	0.999	1.012
Metals control 10mg/L		8.499	9.138	9.092	8.718	8.606	10.736	10.791
Metals Fe_3O_4 10mg/L		8.148	8.008	8.167	0.752	0.765	4.283	4.295
Metals control 30mg/L		26.879	28.322	28.274	30.344	30.005	33.489	33.219
Metals Fe_3O_4 30mg/L		14.780	14.938	15.002	9.837	9.841	5.917	5.986
Metals control 50mg/L		41.918	44.118	44.423	48.508	47.355	52.083	50.815
Metals Fe_3O_4 50mg/L		24.383	24.982	25.393	18.917	19.091	16.287	16.281
Metals control 70mg/L		58.636	61.982	62.881	69.329	68.095	73.941	73.083
Metals Fe_3O_4 70mg/L		43.373	44.887	45.474	48.450	49.189	45.374	44.302
Metals control 100mg/L		98.737	103.666	103.735	103.395	101.870	102.385	99.703
Metals Fe_3O_4 100mg/L		72.321	74.812	75.789	38.992	39.065	57.368	56.490

Table A35: Effect of initial concentration on the recovery of precious metal ions using unmodified iron oxide nanoparticles (Figure 5.23)

Concentration (mg/L)	Palladium	Platinum	Gold
10	91.4	4.1	10
30	85.8	5.3	30
50	99.7	4.7	50
70	99.6	12.9	70
100	62.4	26.8	100

Table A36: Effect of initial concentration on the recovery of precious metal ions using unmodified iron oxide nanoparticles (Figure 5.24)

Concentration (mg/L)	Palladium	Platinum	Gold
10	40.9	49.7	83.2
30	67.6	45	82
50	61.0	41.8	68
70	30.8	26	39.4
100	35.1	32	42.3

Table A37: Langmuir isotherm data for the adsorption of platinum (IV) on unmodified iron oxide nanoparticles

Dosage (g)	C_0 (mg/L)	C_f/C_e (mg/L)	C_e/q_e (g/L)	$1/C_e$ (L/mg)	$1/q_e$(g/mg)	q_e (mg/g)
0.0059	10.033	7.9	0.4	0.1273	0.05	18
0.0250	10.033	3.1	0.2	0.3202	0.07	14
0.0455	10.033	1.9	0.2	0.5328	0.11	9
0.0652	10.033	1.2	0.2	0.8177	0.15	7
0.0857	10.033	1.2	0.2	0.8347	0.19	5

Table A38: Langmuir isotherm data for the adsorption of platinum (IV) on modified iron oxide nanoparticles

Dosage (g)	C_0 (mg/L)	C_f/C_e (mg/L)	C_e/q_e (g/L)	$1/C_e$ (L/mg)	$1/q_e$(g/mg)	q_e (mg/g)
0.0055	10.033	8.3	0.5	0.12	0.06	16
0.0251	10.033	2.8	0.2	0.36	0.07	14
0.0453	10.033	2.9	0.4	0.34	0.13	8
0.0658	10.033	1.2	0.2	0.81	0.15	7
0.0850	10.033	2.9	0.7	0.35	0.24	4

Table A39: Langmuir isotherm data for the adsorption of palladium (II) on unmodified iron oxide nanoparticles

Dosage (g)	C_0 (mg/L)	C_f/C_e (mg/L)	C_e/q_e (g/L)	$1/C_e$ (L/mg)	$1/q_e$(g/mg)	q_e (mg/g)
0.0059	9.485	9.4	28.6	0.11	3.03	0
0.0250	9.485	8.4	3.8	0.12	0.45	2
0.0455	9.485	7.0	2.6	0.14	0.37	3
0.0652	9.485	5.6	1.9	0.18	0.34	3
0.0857	9.485	3.1	0.8	0.32	0.27	4

Table A40: Langmuir isotherm data for the adsorption of palladium (II) on modified iron oxide nanoparticles

Dosage (g)	C_0 (mg/L)	C_f/C_e (mg/L)	C_e/q_e (g/L)	$1/C_e$ (L/mg)	$1/q_e$(g/mg)	q_e (mg/g)
0.0055	9.485	9.0	1.9	0.11	0.21	5
0.0251	9.485	5.4	0.7	0.19	0.12	8
0.0453	9.485	4.6	0.9	0.22	0.19	5
0.0658	9.485	2.6	0.5	0.39	0.19	5
0.0850	9.485	4.0	1.2	0.25	0.31	3

Table A41: Langmuir isotherm data for the adsorption of gold (III) on unmodified iron oxide nanoparticles (Figure 5.25)

Dosage (g)	**C_0 (mg/L)**	**C_f/C_e (mg/L)**	**C_e/q_e (g/L)**	**$1/C_e$ (L/mg)**	**$1/q_e$(g/mg)**	**q_e (mg/g)**
0.0059	8.971	5.8	0.2	0.1722	0.04	27
0.0250	8.971	0.4	0.0	2.5	0.06	17
0.0455	8.971	0.0	0.0	28.6	0.10	10
0.0652	8.971	0.0	0.0	83.3	0.15	7
0.0857	8.971	0.0	0.0	500.0	0.19	5

Table A42: Langmuir isotherm data for the adsorption of gold (III) on modified iron oxide nanoparticles

Dosage (g)	**C_0 (mg/L)**	**C_f/C_e (mg/L)**	**C_e/q_e (g/L)**	**$1/C_e$ (L/mg)**	**$1/q_e$(g/mg)**	**q_e (mg/g)**
0.0055	8.971	5.3	0.2	0.1881	0.03	33
0.0251	8.971	0.0	0.0	45.5	0.06	18
0.0453	8.971	0.0	0.0	58.8	0.10	10
0.0658	8.971	0.0	0.0	50.0	0.15	7
0.0850	8.971	1.3	0.3	0.8	0.22	5

Table A43: Freundlich isotherm data for the adsorption of platinum (IV) on unmodified iron oxide nanoparticles

Dosage (g)	**C_0 (mg/L)**	**C_f/C_e (mg/L)**	**ln C_e**	**ln q_e**	**$1/C_e$**	**$1/q_e$**	**q_e (mg/g)**
0.0059	10.033	7.856	2.06	2.92	0.1273	0.05	18
0.0250	10.033	3.123	1.14	2.63	0.3202	0.07	14
0.0455	10.033	1.877	0.63	2.19	0.5328	0.11	9
0.0652	10.033	1.223	0.20	1.91	0.8177	0.15	7
0.0857	10.033	1.198	0.18	1.64	0.8347	0.19	5

Table A44: Freundlich isotherm data for the adsorption of platinum (IV) on modified iron oxide nanoparticles

Dosage (g)	C_0 (mg/L)	C_f/C_e (mg/L)	ln C_e	ln q_e	$1/C_e$	$1/q_e$	q_e (mg/g)
0.0055	10.033	8.253	2.11	2.78	0.12	0.06	16
0.0251	10.033	2.801	1.03	2.67	0.36	0.07	14
0.0453	10.033	2.949	1.08	2.06	0.34	0.13	8
0.0658	10.033	1.233	0.21	1.90	0.81	0.15	7
0.0850	10.033	2.889	1.06	1.44	0.35	0.24	4

Table A45: Freundlich isotherm data for the adsorption of palladium (II) on unmodified iron oxide nanoparticles

Dosage (g)	C_0 (mg/L)	C_f/C_e (mg/L)	ln C_e	ln q_e	$1/C_e$	$1/q_e$	q_e (mg/g)
0.0059	9.485	9.446	2.25	-1.11	0.11	3.03	0
0.0250	9.485	8.370	2.12	0.80	0.12	0.45	2
0.0455	9.485	7.040	1.95	0.99	0.14	0.37	3
0.0652	9.485	5.625	1.73	1.09	0.18	0.34	3
0.0857	9.485	3.099	1.13	1.32	0.32	0.27	4

Table A46: Freundlich isotherm data for the adsorption of palladium (II) on modified iron oxide nanoparticles

Dosage (g)	C_0 (mg/L)	C_f/C_e (mg/L)	ln C_e	ln q_e	$1/C_e$	$1/q_e$	q_e (mg/g)
0.0055	9.485	8.956	2.19	1.57	0.11	0.21	5
0.0251	9.485	5.378	1.68	2.10	0.19	0.12	8
0.0453	9.485	4.629	1.53	1.68	0.22	0.19	5
0.0658	9.485	2.586	0.95	1.66	0.39	0.19	5
0.0850	9.485	4.012	1.39	1.17	0.25	0.31	3

Table A47: Freundlich isotherm data for the adsorption of gold (III) on unmodified iron oxide nanoparticles (Figure 5.26)

Dosage (g)	**C_0 (mg/L)**	**C_f/C_e (mg/L)**	**ln C_e**	**ln q_e**	**1/C_e**	**1/q_e**	**q_e (mg/g)**
0.0059	8.971	5.807	1.76	3.29	0.1722	0.04	27
0.0250	8.971	0.401	-0.91	2.84	2.5	0.06	17
0.0455	8.971	0.035	-3.35	2.28	28.6	0.10	10
0.0652	8.971	0.012	-4.42	1.93	83.3	0.15	7
0.0857	8.971	0.002	-6.21	1.65	500.0	0.19	5

Table A48: Freundlich isotherm data for the adsorption of gold (III) on modified iron oxide nanoparticles

Dosage (g)	**C_0 (mg/L)**	**C_f/C_e (mg/L)**	**ln C_e**	**ln q_e**	**1/C_e**	**1/q_e**	**q_e (mg/g)**
0.0055	8.971	5.317	1.67	3.50	0.1881	0.03	33
0.0251	8.971	0.022	-3.82	2.88	45.5	0.06	18
0.0453	8.971	0.017	-4.07	2.29	58.8	0.10	10
0.0658	8.971	0.020	-3.91	1.92	50.0	0.15	7
0.0850	8.971	1.287	0.25	1.51	0.8	0.22	5